Reducing Costs of Tidal Energy Through a Comprehensive Characterization of Turbulence in Minas Passage

Project Lead: Richard Karsten

Project number: 300-210

Start date: 01 October 2017

Reporting period: Final Report

Submission date: September 21, 2020

Table of Contents

1 Executive summary

Turbulence is a significant issue at every site being considered for instream tidal energy development. The turbulence in strong tidal flow creates fluctuating forces that can degrade turbine performance and shortening turbine lifespan. Thus, properly characterizing turbulence is a critical step to designing durable devices and accelerating the pace of technology development. The three Work Packages of this project address the challenge of characterizing turbulence by: validating mobile methods of measuring the turbulence around an operating turbine, improving and validating a numerical models of turbulence and turbine operation in turbulent flow, and developing the data analysis methods to include turbulence analysis in resource and site assessment. The project examined sites in Grand Passage and Minas Passage, two locations where tidal turbines have or will be deployed in flows that display a variety of turbulent features.

Work Package 1 (WP1) used innovative mobile measurement devices to characterize the spatial variation of turbulence in Grand Passage. Two field experiments were conducted in the vicinity of Sustainable Marine Energy Canada (SME) PLAT-I turbine platform. For both field experiments, measurements of turbulent velocities were collected using stream-following surface drifters with a down-looking turbulence-resolving acoustic Doppler current profiler (ADCP). Data were collected over a range of flow conditions and when the turbines were and were not operating. Analysis of the data generated maps to describe the spatial and temporal variations of mean-flow velocities and turbulence parameters in the studied area. When turbines are operational, the wake is mapped out, identifying the maximum velocity deficit and how farther downstream the wake expands vertically, the velocity deficit decreases, and the wake begins to recover. WP1 demonstrated that surface drifters are an efficient and economical methods for mapping both mean-flow velocities and resolved turbulence in the vicinity of an operating tidal turbine.

Work package 2 (WP2) developed and validated a high-resolution numerical model of the Grand Passage. The numerical simulations were carried out using a GPU based CFD solver developed at the University of New Brunswick. The research team produced fine grid mesh for Grand Passage with 24 million control-volumes, an average horizontal resolution of $2\ \mathrm{m} \times 2\ \mathrm{m}$, and an innovative smooth transition between the main channel and the shoreline. The numerical simulations run on the mesh clearly illustrates the multi-dimensional, complicated flow structures of the strong tidal flow. The simulations were used to illustrate several important aspects of the PLAT-I project. Although the PLAT-I platform lies outside the wake of Peter's Island, locations near the deployment site experience periodic, low-velocity, unsteady flow structures. And, a location only 300 m north of the PLAT-I, where and ADCP was previously deployed, has significantly different velocity profiles and larger flow variations than those from locations near the PLAT-I

In the second part of the WP2, numerical models of turbines were embedded into these flow simulations. The researchers developed an innovative methodology based on the actuator line (AL) method and takes advantage of both CPU and GPU processing power to increase

computational efficiency. In the initial results, even though a very coarse grid has been used, the simulation successfully produces the wake of the turbine, which can be affected by unsteady tidal flows. The development of a fine resolution simulation with PLAT-I properly located in Grand Passage has been completed and initial testing has indicated a successful implementation of the many-to many technique. The final step of activate the AL method in the rotor block and simulated the turbine for sufficient time to obtain statistical convergence of the flow field variables and turbine performance is under way.

Finally, the third work package further developed data analysis methods and a regional numerical model. The Acadia regional numerical models, which were developed in previous projects, were used to generate years-long data set of 3D simulated tidal flow for all tidal passages in the Bay of Fundy. These data sets were used in both WP1 and WP2, but were also shared with other stakeholders. On the data analysis side, the research team worked with Luna Ocean to develop a data analysis tool, LunaTide, that can better predict tidal flow, using a wide range of measurements (ADCPs, drifters, X-band radar, etc.) and numerical simulation data. Working with FORCE, the numerical simulations and LunaTide were used to show how X-Band radar can be used to predict surface velocities and analyze wakes across the FORCE site. As well, the research team participated in pilot projects to images and videos from drones to collect bathymetry data and analyze tidal flow. When all the results are combined together, the project has produced data sets and data tools that can make maps and forecasts of tidal conditions in all the Bay of Fundy passages, at a unprecedented level of details and accuracy.

Given the short length of the project, the original project proposal was extremely ambitious, a complete mapping of the turbulence characteristics in tidal passage. As well, the project faced with the challenge of having to shift the entire project's focus from the OpenHydro turbine in Minas Passage to the SME PLAT-I in Grand Passage. Despite the challenges, the project has been successful in developing all the tools necessary to meet its goal: an efficient method to measure the spatial variation of flow around an operating turbine; a high-resolution model capable modelling in-situ tidal turbines in a realistic, fully turbulent flow; and the data analysis tools to combine these results (and others) with the long-term, regional, tidal flow data sets to produce the complete mapping of the flow characteristics. As we see new projects preparing for turbine deployments in the Bay of Fundy, we will start using these tools to provide project developers the information that they require.

2 Introduction and Objectives

2.1 Introduction

Turbulence is a significant issue at every site being considered for instream tidal energy development. As strong tidal flow passes over the rough sea bottom and past variations in the coastline, eddies and random fluctuations in tidal currents develop, generically known as turbulence. This turbulent flow, in turn, creates fluctuating forces on tidal turbine blades and support structures, degrading turbine performance and shortening turbine lifespan. Thus, properly characterizing turbulence is a critical step to designing durable devices and accelerating the pace of technology development. Furthermore, improving and validating

numerical models of turbulence and turbine operation in turbulent flow is necessary to better predict device operation and, thus, develop efficient and financially viable tidal energy projects.

This project examined the turbulent tidal flow in two tidal passages in the Bay of Fundy. The work is primarily focused on the flow in Grand Passage, where Sustainable Marine Energy Canada (SME) deployed PLAT-I was deployed in Grand Passage, Nova Scotia in September 2018. The PLAT-I is a three-hulled floating platform designed to support four 6.3 m diameter Schottel Hydro turbines, each rated at 70 kW. The work also completed some initial analysis on the flow in Minas Passage, as part of the long term goal of using the tools and techniques developed at the commercial berths that are part of Fundy Ocean Research Centre for Energy (FORCE) site. The project was divided into three Work Packages, each the focus of one university's team, Dalhousie, UNB and Acadia, respectively.

In the Work Package 1 (WP1), innovative mobile measurement devices were used to characterize the spatial variation of turbulence in Grand Passage, including the turbulence in PLAT-I turbine wakes. In the Work Package 2 (WP2), a high-resolution numerical model of Grand Passage was used to simulate the generation and dissipation of turbulence. Furthermore, numerical models of turbines were embedded into these simulations to determine the effect of turbulence on turbine performance and turbine wakes. Finally, In the Work Package 3 (WP3), a regional numerical model and innovative data analysis tools are used to both support WP1 and WP2, and to begin the process of combining all results into ocean forecasts for suitable for both short term planning of marine operations and long term project assessments.

In the sections below, the methodology and the progress of each work package is described in detail.

2.2 Project objectives

Listed below are the original Work Package objectives. Some of these objectives changed after OpenHydro ceased operations and the focus of the project shifted to Grand Passage and the SME PLAT-I.

2.2.1 Work Package 1: Quantify turbulence and characterize wakes using field measurements

The first objective will quantify the spatial and temporal variability of flow and turbulence in Grand Passage and Minas Passage. Mobile and stationary measurement systems will be deployed to achieve a comprehensive, validated, quasi-synoptic mapping of turbulence statistics and (large-eddy) flow variability within both passages, both under natural conditions, including the Black Rock wake in Minas Passage, and in the presence of turbines: i.e. the PLAT-I turbine in Grand Passage and, if possible, the Open Hydro turbine in Minas Passage.

2.2.2 Work Package 2: Simulate turbulence, simulate wakes, quantify impact on turbines

To quantify how turbulence and wakes impact turbines, the turbulent fluid flow in the vicinity and within a tidal turbine will be simulated using multi-resolution Computational Fluid Dynamic (CFD)

simulations. These simulations will be run on a state-of-the-art graphical processing unit (GPU) cluster using the powerful, world-class, CFD capability called EXN/Aero.

This objective was further sub-divided into the following tasks:
(i) Initial regional model testing; data at field locations compared to initial measurements.
(ii) Initial testing of (embedded) approximate and full rotor turbine models; initial wake predictions.
(iii) Validate turbulence generation in regional simulations; generate of maps of turbulence characteristics.
(iv) Analysis of turbine models under different turbulence conditions; classification of turbine performance and wakes.
(v) Validate wake modelling; refinement of turbine models; comparison of model wakes to measurements.
(vi) Complete analysis of all embedded turbine simulations, focusing on temporal/spatial variability of turbulence and turbine performance.

2.2.3 Work Package 3: Develop ocean forecasting system for Minas Passage

This part of the project will use a dedicated Advanced Research Computing (ARC) system to run regional-level simulations of the Bay of Fundy tides and tidal currents, and extra-high resolution environmental simulations to support specific turbine design and performance. The simulations will produce real-time forecasts of the sea conditions for use in planning the field campaigns. ARC resources will also be used to store and analyze all the data associated with the project. The data analysis will continue to use and develop PySeidon.

3 Work Package 1

3.1 Methodology

3.1.1 Fieldwork

The primary goal of fieldwork during the project was to map mean flow and turbulence in Grand Passage, a tidal channel in the southeast of Bay of Fundy. Data collection concentrated around PLAT-I, a floating tidal energy platform. PLAT-I is a three-hulled floating platform designed to support four horizontal-axis hydrokinetic turbines along its cross-deck, developed and operated by Sustainable Marine Energy Canada (SME). PLAT-I was deployed in Grand Passage, Nova Scotia in September 2018 to the north of Peter's Island (N 44.2639º W 66.3369º). PLAT-I supports four 6.3 m diameter Schottel Hydro turbines, each rated at 70 kW and designed for a maximum flow speed of 4 m s^{-1}.

Two field experiments were conducted in the vicinity of PLAT-I. The first occurred on November 19th and 20th 2018 before turbine blades were installed on the turbine rotors. Results from this first experiment are described in Guerra et al. (2019) and were summarized in the last interim report. A second experiment was conducted on May 17th and 18th 2019, while turbines were fully assembled and underwater. Turbines were operational for a brief period of time during peak ebb on May 17th, immediately prior to SME's permit expiring on May 24th 2019. The main objective

of the second experiment was to capture the turbine's wake while they were both operational and not operational.

Measurements of turbulent velocities were collected using stream-following surface drifters for both field experiments. An improved drifter design (smaller and lighter) was used in the second experiment. Each drifter consisted of a disk buoy, an HDPE body and fins, a down-looking turbulence-resolving Nortek Signature acoustic Doppler current profiler (ADCP) and a fast sampling GPS logger. For the May 2019 experiment, there were two drifters, one equipped with a 1000 kHz unit and a second equipped with a 500 kHz unit to prevent acoustic contamination between the two instruments. Columbus P1 GPS loggers, which recorded drifter position and drifting velocity at 10 Hz, were mounted on both drifters. These GPSs are also an improvement from the first experiment and allowed for a better measurement of the drifter trajectory and therefore flow speed at the sea-surface.

Each Nortek Signature was set to record single-ping along-beam turbulent velocities at different intervals through the water column at the fastest sampling frequency possible when using all five acoustic beams (4 Hz for the 500 kHz unit, and 8 Hz for the 1000 kHz unit).

Data were collected over a range of flow conditions on ebb and flood tides, with maximum surface currents above 2 m s^{-1}. There were 227 drifts in total, 149 on ebb and 78 on flood. Of the ebb drifts, 16 were at times when the turbines were operating (based on operational times provided by SME Canada).

In addition, controlled transects using a vessel-mounted RDI Workhorse 600 kHz ADCP were conducted both upstream and downstream of the platform during both field experiments. A Garmin 78s GPS receiver recorded vessel position at 1 Hz (synchronized with the ADCP). There were 66 flood transects and 34 ebb transects during this experiment, all while turbines were not operational.

As for the first experiment, a local coordinate system was defined for data organization purposes, with its origin at the PLAT-I center location. The y-axis corresponds to the along-channel principal direction of the currents at this site (18.8◦ CCW from north, positive northward), while the x-axis corresponds to the cross-channel principal direction of the flow (positive eastward). Figure 1 shows a map of Grand Passage together with a map of drift trajectories (colored by average drift velocity) and a map of all transects colored by subsurface velocity measured by the vessel mounted ADCP. All drifts occurred downstream of PLAT-I, thus all flood drifts flow in the positive *y* direction, while all ebb drifts flow in the negative *y* direction.

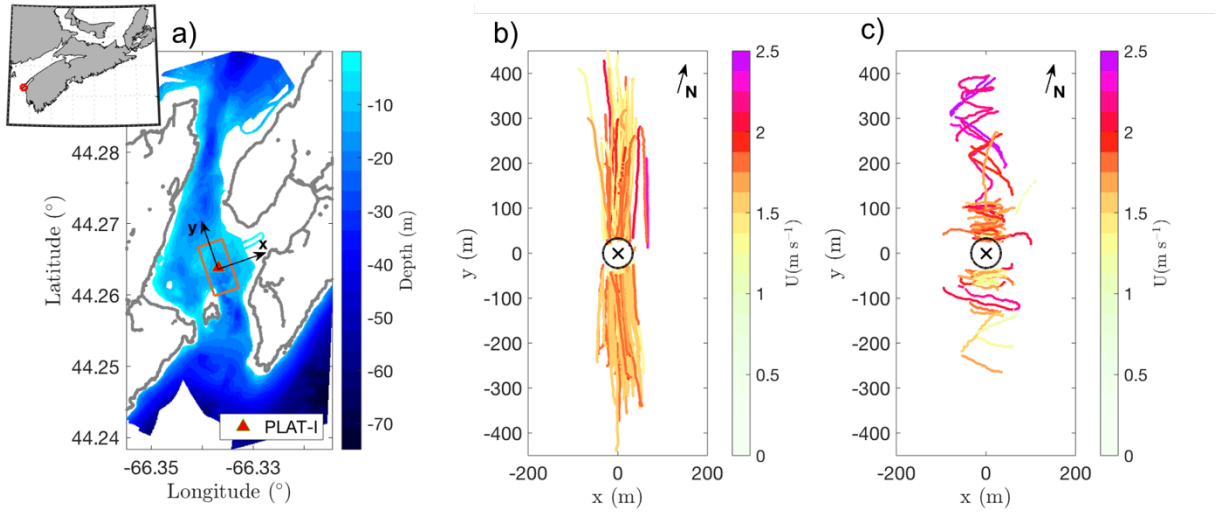

Figure 1: a) Grand Passage map colored by bathymetry. The triangle corresponds to PLAT-I location in Grand Passage. The orange rectangle corresponds to the measurement area, and the x-y represent the local coordinate system used on b). b) All drift trajectories colored by average drifting velocity. The X represents Plat-I location nominal location, and the circle represents the average turbine excursion.

3.1.2 Data Processing

3.1.2.1 Drifters

All drifter data were quality controlled and corrected for contamination induced by drifter motion at the sea-surface (surface motion due to large-eddy turbulence and or small surface gravity waves). Following quality control, ADCP measured beam velocities were converted to earth-coordinate velocities, which are later combined with GPS drifting velocities to obtain vertical profiles of horizontal Eulerian velocities. The vertical beam of the ADCPs provides a direct measurement of the vertical velocity through the water column. These velocities were then used to estimate turbulence parameters such as velocity variance (i.e. turbulent kinetic energy) and turbulent kinetic energy dissipation rates. The methodologies used to estimate these quantities are detailed in Guerra et al., (2019).

After examining data from each drift, drifts were organized by mean-flow condition using an undisturbed reference flow velocity. In the absence of a concurrent bottom ADCP deployment, a reference velocity at PLAT-I's nominal position was obtained from FVCOM numerical simulations of Grand Passage (O'Flaherty-Sproul, 2013). Drift data were organized into eleven 0.5 m s^{-1} along-channel velocity bins, ranging from -2.5 to 2.5 m s^{-1} (negative along-channel velocities correspond to ebb tide). Once drifts have been assigned to a velocity bin, data from each particular velocity bin were organized into a structured, regular grid in the local coordinate system. Then, quasi-synoptic tri-dimensional maps of mean-flow velocities and turbulence parameters were constructed for the area surrounding PLAT-I for different tidal flow conditions, expanding the method developed by Guerra and Thomson (2019) for steady-state flow conditions.

3.1.2.2 Transects

The vessel-mounted RDI Workhorse ADCP provides vertical profiles of horizontal velocity along each transect. Data from this ADCP were quality controlled, and later converted to true earth-coordinates velocities using bottom-track velocities to correct for vessel motion. Transects are also organized by mean-flow condition following the same procedure as for the drifter data. Only mean-flow velocities are obtained from this data set.

3.2 Results and Conclusions

3.2.1 Results

The following results are all based on drifter data, as transect data continues to be processed.

For each drift, the spatio-temporal distribution of along-channel and vertical velocities, and TKE dissipation rates along its trajectory were analyzed. Finally, drifter data were processed to evaluate the PLAT-I wake and to compare flow velocity and turbulence when turbines are operational and not operational. Main findings are summarized below.

Along most of the drifts, vertical velocities ranged between $\pm$ 0.5 m s^{-1}. Along different drift trajectories a wide range of scales are observed in the vertical velocities, with different patterns for ebb and flood. Figure 2a and 2b show the vertical and horizontal structure of vertical velocities (averaged to 1 s) along two particular ebb drifts. These drifts occurred 3 minutes apart at the same location within PLAT-I's wake (i.e. same reference velocity). The first drift (a) occurred when the turbines were not operational, while the second drift (b) occurred when the turbines were not operational. When the turbines are operational stronger and coherent vertical velocities are observed right downstream of the turbines. The stronger vertical velocities are observed in the region covered by the turbines' rotors (approximately between z = -4 and z = -10 m).

Figure 3a, shows vertical profiles of along-channel velocity averaged over the first 30 s of drifting for the same drifts shown in Figure 2 (marked with the vertical dashed line in Figures 2a and 2b). A decrease in along-channel velocity is observed in the region covered by the turbine rotors of about 0.3 m s^{-1} when the turbines are operational. Also, there is a small decrease in velocity (negative shear) in the same region for the not-operational drift.

TKE dissipation rates, ε, were estimated along each drift trajectory through the second-order structure function (Pope, 2000) for all drifts. A large dynamic range is observed in the TKE dissipation rates, illustrating that turbulence varies along each drift and between them. Although variable, temporal coherence is observed in the TKE dissipation rates along each drift. Observed values are within the range of previous estimates of TKE dissipation rate in Grand Passage using bottom-mounted ADCPs and direct measurements at mid-depth with shear probes (McMillan et al., 2016). The TKE dissipation rates also exhibit a log-normal probability distribution, as expected for turbulent flows, and as observed previously in Grand Passage using bottom-mounted ADCP data (McMillan and Hay, 2017).

Figure 2c and 2d show the corresponding TKE dissipation rates along the selected not-operational and the operational drifts. A region of strong TKE dissipation rates, indicative of stronger turbulence, is observed in the vicinity of the operational turbines. Vertical profiles of TKE dissipation rates estimated with first 30 s of drift data for each trajectory are shown in Figure 3b. Again, higher TKE dissipation rates are observed in the depth interval spanned by turbine rotor, consistent with the decrease in along-channel velocities.

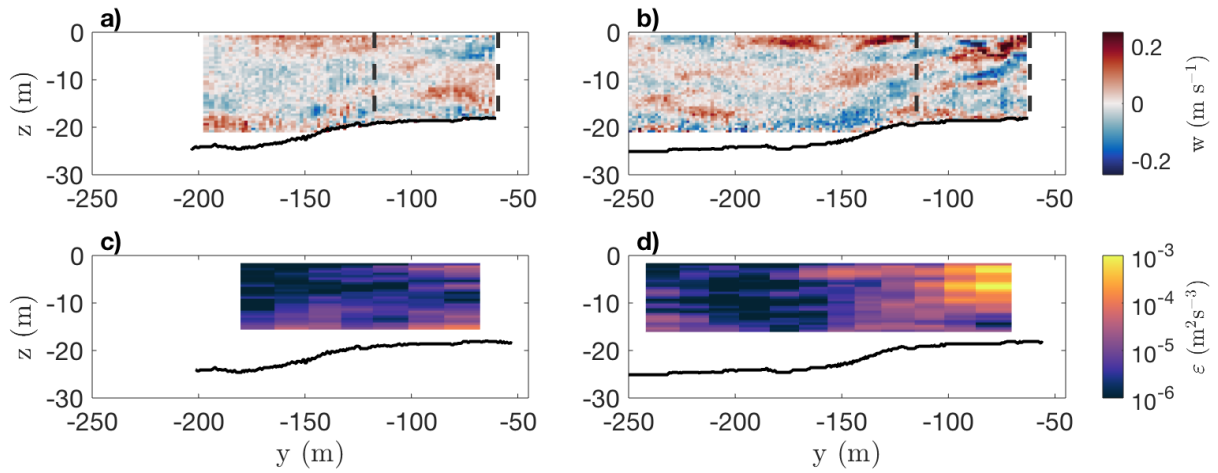

Figure 2: Vertical and horizontal structure of vertical velocity along two typical drifts a) while turbines are not-operational, and b) when turbines are operational. Both drifts occurred during ebb tide, at the same location, and 3 minutes apart. Black line represents the sea-bottom. Flow (drift) direction is from right to left. Plots c) and d) show the corresponding TKE dissipation rates.

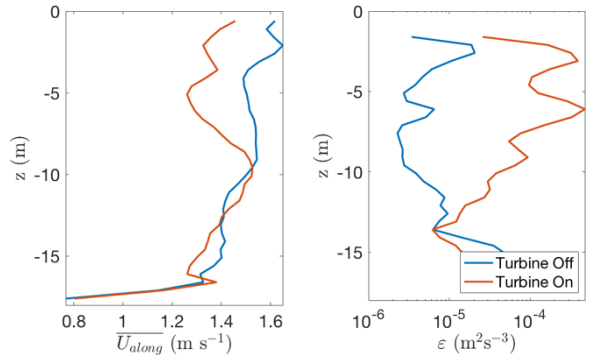

Figure 3: Averaged vertical profiles of along-channel velocity and standard deviation for a middle drift at a) flood tide, and b) ebb tide. Note that on these plots the vertical axis corresponds to distance from the bottom.

Tri-dimensional maps of mean-flow velocity, vertical velocity variance, and TKE dissipation rate are constructed for each velocity bin for not-operational and for operational turbines if data are available. These maps illustrate the time (tidal) and spatial variability of these flow parameters. Figure 4 and Figure 5 show examples of these maps for two of the most populated velocity bins for flood and ebb tide respectively for not operational turbines data. Spatial variability is observed in all maps. During flood, even if turbines are not operational, a region of slower velocities is observed downstream PLAT-I. Stronger vertical velocity variance are observed close to the platform and about x = 0 m, consistent with the region of stronger TKE dissipation rates.

Spatial variability is also observed in the ebb maps in Figure 5. However, the velocities do not exhibit a clear wake region for non-operational conditions, probably because it's effect on the flow is too small to distinguish. A sharp along-channel velocity gradient is observed beginning at y = 250 m. This gradient is thought to be naturally occurring due to changes in bathymetry upstream of Peter's Island, this same gradient is observed in FVCOM numerical results which do not include the platform's effects. However, during ebb a region of elevated vertical velocity variance and TKE dissipation rates is observed just downstream of the platform and about x = 0.

Similar maps were also constructed using data collected while the turbines were operational, however the data are too sparse to produce a tri-dimensional map. Instead, the data were collapsed along the x-axis to produce a single longitudinal profile of flow parameters. Figure 6 shows comparisons of the along-channel velocity longitudinal profile for non-operational and operational conditions when ambient along-channel velocity is on average -2 m s^{-1} (ebb, flow from right to left). When turbines are operational, a region of reduced velocities is observed downstream of the turbines, extending about 60-80 m downstream of the turbines (y = -100 m). A peak in the velocity deficit is observed about 30 m downstream of the turbines (y = -70 m), which might be related to lateral variability within the wake. Vertical profiles of along-channel velocity are shown in Figure 7 for both conditions at different distances from PLAT-I's nominal location. In these plots the wake evolution is observed. Close to the turbines, the region of reduced velocities (i.e. the wake) is concentrated at the depths spanned by the turbines' rotors. The maximum velocity deficit is ~0.5 m s^{-1}. Farther downstream the wake expands vertically, the velocity deficit decreases, and the wake begins to recover.

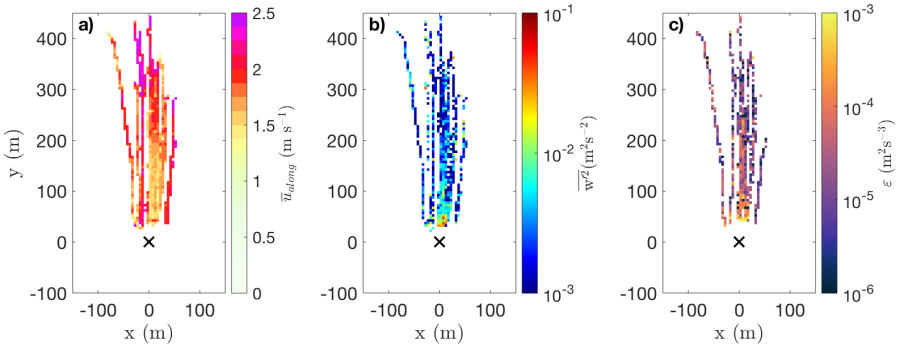

Figure 4: Maps of a) along-channel velocity, b) vertical velocity variance, and c) TKE dissipation rates at hub-depth (z=-4.5 m) for data collected during flood while ambient along-channel velocity (reference from FVCOM model) was between 1.75 and 2.25 m s^{-1}. The X symbol corresponds to the platform nominal location, and turbines are located around y = 40 m during flood.

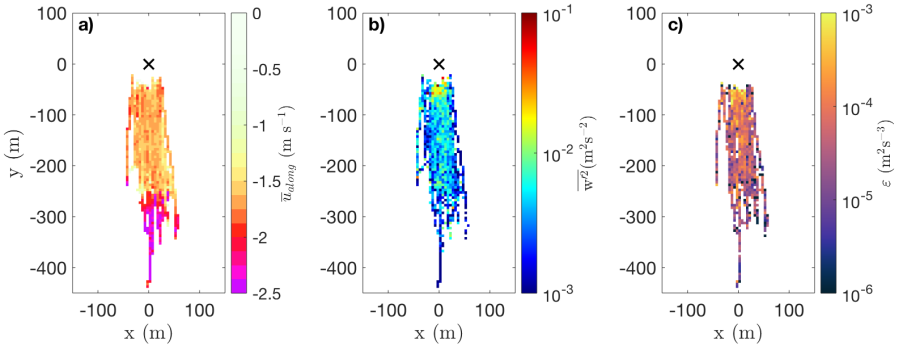

Figure 5: Maps of a) along-channel velocity, b) vertical velocity variance, and c) TKE dissipation rates at hub-depth (z=-4.5 m) for data collected during ebb while ambient along-channel velocity (reference from FVCOM model) was between -2.25 and -1.75 m s^{-1}. The X symbol corresponds to the platform nominal location, and turbines are located around y = -40 m during ebb.

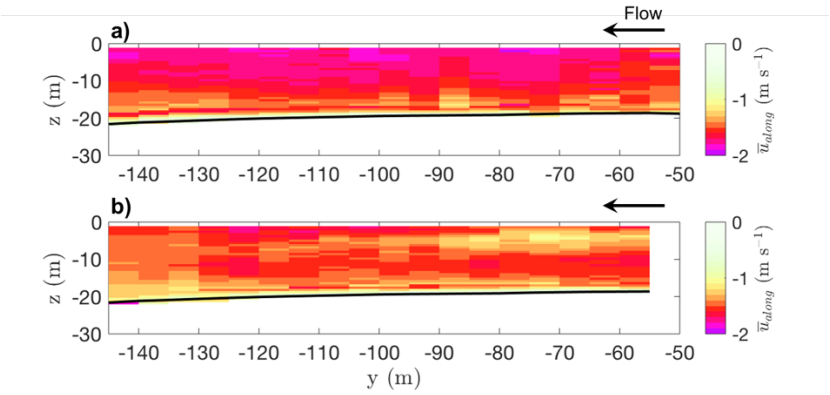

Figure 6: Longitudinal profile of along-channel velocity centered at x = 0 when while ambient along-channel velocity (from FVCOM model) was between -2.75 and -2.25 m s^{-1}. a) Not operational turbines, and b) Operational turbines.

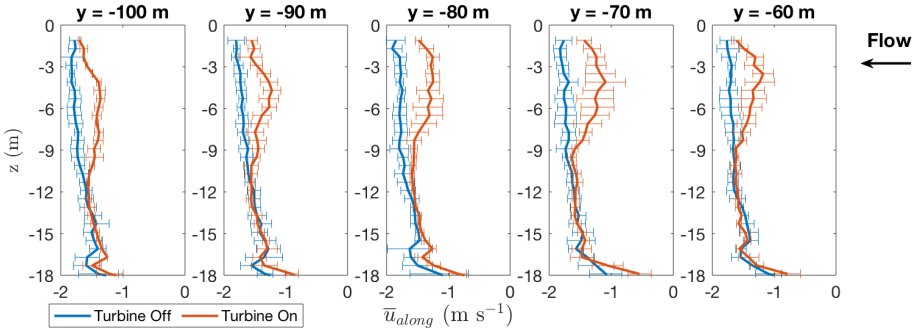

Figure 7: Vertical profiles of along-channel velocity at difference distances from PLAT-I's nominal location while ambient along-channel velocity (from FVCOM model) was between -2.75 and -2.25 m s^{-1}. Turbines are located around y = -40 m during ebb. Horizontal bars represent across wake variability.

3.2.2 Conclusions

3.2.2.1 Methods:

The employed field methods successfully captured both mean-flow velocities and turbulence parameters in Grand Passage. Drifter buoys followed surface streamlines, and turbulence was resolved as demonstrated by the TKE dissipation rate estimates. The combined use of validated numerical simulations, mobile platforms, and data processing techniques allowed for the construction of quasi-synoptic flow maps for different tidal flows. These maps successfully describe the spatial and temporal variations of mean-flow velocities and turbulence parameters in the studied area.

3.2.2.2 Wake:

The wake of PLAT-I was captured using the repeated drift method for the measured flow conditions while turbines were both not-operational and operational. The expected wake behavior of slower velocities and higher turbulence was observed for different tidal flows, including peak ebb and flood for the non-operational turbines case. The operational wake was detected for two ebb velocity bins. The operational turbine measurements suggest a vertically confined wake, and a partial recovery within the first 80 m downstream of the turbines (Figure

6). However, the number of drifts and their maximum downstream extent does not allow for the observation of a fully recovered wake (if any) for all stages of the tide.

Wake data are important to this particular turbine developer, policy makers, and local stakeholders. Information about the velocity decrease, turbulence increase, and wake extent is fundamental for the design of an array of platforms in this region. At the same time, results also provide key information for the evaluation the hydrodynamic impacts of tidal energy extraction in this area.

3.2.3 Dissemination activities

Through the project, on-going results from WP1 have been presented at three conferences:

- M. Guerra, A. E. Hay, R. A. Cheel, G. Trowse, and R. Karsten, "Turbulent flow mapping around a floating in-stream tidal energy platform". *13th European Wave and Tidal Energy Conference*, Naples, Italy, September 1-6, 2019. (Oral presentation by Dr. Guerra Paris)
- M. Guerra, A. E. Hay, R. Karsten, R. A. Cheel, and G. Trowse. "Field measurements of a floating tidal turbine wake". Pan American Marine Energy Conference, San José, Costa Rica, January 26-28, 2020. (Oral presentation by Dr. Richard Karsten)
- Guerra, M.., Hay, A.E., Cheel, R., Trowse, G. and Karsten, R. Mapping the wake of a full-scale floating tidal turbine platform, Ocean Sciences Meeting 2020, San Diego, CA, United States. (Poster presentation by Dr. Guerra Paris)

The project team was also part of the Data Science room at the Energy3 Conference (October 16-19 2019, Halifax, NS). At this conference examples of field results and numerical simulations were interactively presented to the public.

3.2.4 Future Work

A new MITACS Accelerate internship has been awarded to Dr. Guerra Paris for continuing the research conducted in this project. The new internship will focus on expanding the measurements of PLAT-I's wake for operational conditions.

A third field experiment is now planned for summer 2020. This experiment will focus on collecting a more extensive data set when PLAT-I's turbines are operating. In addition to the two drifters, a vertical microstructure profiler will be used to get high-resolution profiles of TKE dissipation rate at specific locations, which will be compared with estimates from the drifting ADCPs. It is expected that the new data set will allow the construction of 3D maps of mean-flow and turbulence parameters for all defined velocity bins while all four turbines are operational. There will also be opportunities to study the wake characteristics when 1 or more turbines are operating and how the wakes interact and combine. To date these questions have only been addressed at the laboratory scale and using hydrodynamic numerical models.

The continuation project also includes investigating about wave-turbulence-current interaction from bottom-mounted ADCP data at PLAT-I's location. Since PLAT-I is a floating platform, surface gravity wave motions impact both the floating platform and the turbines. It is important then to know how the local turbulence is affected by the presence of waves, and how PLAT-I and its

turbines perform under a wide range of wave-current conditions. Moreover, during the 2019 field experiments, it was found that waves play an important role in data collection and in data quality when using mobile platforms.

A research article, including the methods and up to date results from the two field experiments is being prepared for submission to *Renewable Energy*.

3.3 Bibliography

M. Guerra, A. E. Hay, R. A. Cheel, G. Trowse, and R. Karsten, "Turbulent flow mapping around a floating in-stream tidal energy platform", in *Proc. 13th European Wave and Tidal Energy Conference*, 2019.

P. Jeffcoate and N. Cresswell, "Field performance testing of a floating tidal energy platform. Part 2: Load performance," in *Proc. 4th Asian Wave and Tidal Energy Conference*, 2018.

S. B. Pope, *Turbulent Flows*. Cambridge University Press, 2000.

J. M. McMillan, A. E. Hay, R. G. Lueck, and F. Wolk, "Rates of dissipation of turbulent kinetic energy in a high Reynolds num- ber tidal channel," *Journal of Atmospheric and Oceanic Technology*, vol. 33, no. 4, pp. 817–837, 2016.

J. M. McMillan and A. E. Hay, "Spectral and structure function estimates of turbulence dissipation rates in a high-flow tidal channel using broadband ADCPs," *Journal of Atmospheric and Oceanic Technology*, vol. 34, no. 1, pp. 5–20, 2017.

M. Guerra and J. Thomson, "Wake measurements from a hydrokinetic river turbine," *Renewable Energy*, vol. 139, pp. 483– 495, 2019.

M. O'Flaherty-Sproul, "New high and low resolution numerical models of the tidal current through the Digby Neck passages," MSc. dissertation, Acadia University, 2013.

4 Work Package 2

4.1 Methodology

4.1.1 CFD Solver and Procedure

The simulations in this work have been carried out using EXN/Aero [1], a GPU based CFD solver being developed at the University of New Brunswick. This solver uses a collocated finite volume discretization method [2] and an implicit in time SIMPLEC approach for pressure-velocity coupling [3]. The solver also uses a second order transient discretization combined with an upwind biased

TVD (Van Leer) scheme for the advection term [4]. An algebraic multigrid [5] approach is employed to accelerate the solution in this solver.

4.1.2 CFD Domain and Boundary Conditions

Figure 8 shows a satellite view of the Grand Passage. In this passage, water moves from South to North during flood and in the opposite direction during ebb. Figure 9 shows the bathymetry of the Grand Passage that was used to create the ocean floor in the CFD domain by sampling at a $10\ \mathrm{m} \times 10\ \mathrm{m}$ resolution.

Figure 10 shows the top view of the grid generated over this bathymetry, which is $3.6\ \mathrm{km} \times 2.3\ \mathrm{km}$ in size. This grid topology is structured and, as illustrated in Figure 10, consists of 4 regions, representing the main channel (green), East shoreline (blue), West shoreline (red), and Peter's island (orange). In the main channel region, the bottom surface of the CFD domain was projected on the passage bathymetry shown in Figure 9 and a no-slip boundary condition was enforced. However, for the East and West shorelines and Peter's island, the immersed boundary method [6] was used to create the effect of the bathymetry. This was accomplished by extending the grid generated in these regions below the bathymetry level and the control-volumes that are located below the bathymetry surface have been block out by manipulating source terms in the CFD solution. This method results in better grid quality in areas where the water is shallow by avoiding highly skewed control volumes in these regions. Figure 11 shows the result of this hybrid approach, where one can see that there is a very smooth transition between the main channel region and the various shoreline regions.

Simulations were completed on both a coarse and fine grid. The coarse grid consisted of 12 control volumes in the vertical direction and a horizontal resolution the varied between 2.5 m and 5.5 m, producing a grid with 2.9 million control volumes. The fine grid consisted of 24 control volumes evenly distributed in the vertical direction and an average horizontal resolution of $2\ \mathrm{m} \times 2\ \mathrm{m}$, producing a grid with 24 million control-volumes.

North

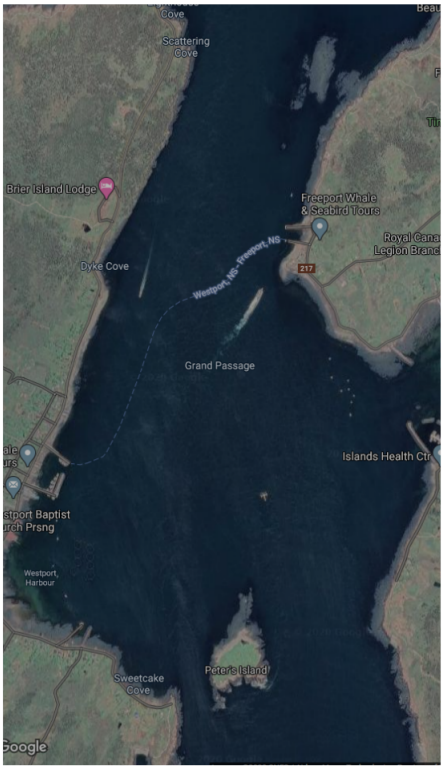

West East

South

Figure 8. Satellite view of Grand Passage

North

West East

South

Figure 9. Bathymetry of Grand Passage

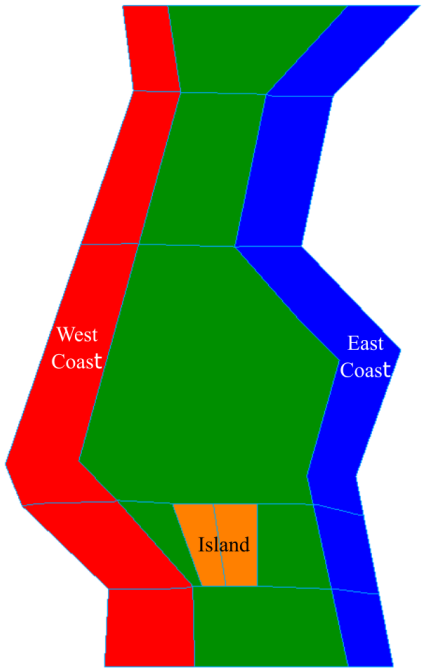

Figure 10. Top view of grid used for flood and ebb simulations

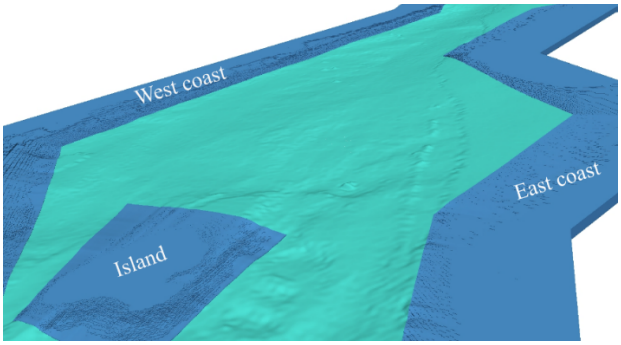

Figure 11. Bathymetry of Grand Passage generated by projecting grid over bathymetry database (light blue) and immersed boundary method (dark blue)

For flood simulations, the South boundary is an inlet with a prescribe velocity profile that was extracted from FVCOM simulations and the North boundary is an outlet with zero static pressure. On the other hand, for ebb simulations, the flow enters the domain from the North boundary and an inlet velocity profile is again specified using data extracted from FVCOM results, while the South boundary is assigned as the outlet with a zero static pressure. The exact time of the extracted FVCOM velocity profile is March 13, 2016 at 15:40 for flood and 21:20 for ebb, which are representative of peak energetic points in the tidal cycle. Velocity profiles extracted for the flood and ebb simulations are illustrated in Figure 12 and Figure 13, respectively. It should be noted, that once prescribed, these profiles remained fixed for the duration of the CFD simulation.

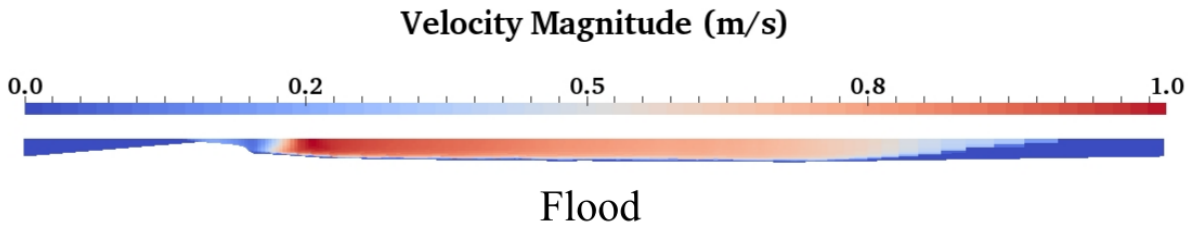

Figure 12. Velocity boundary condition applied to South boundary for flood simulations.

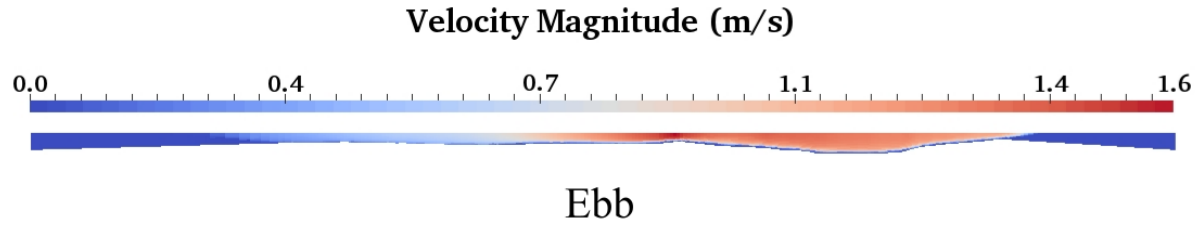

Figure 13. Velocity boundary condition applied to North boundary for Ebb simulations

Finally, the symmetry boundary condition has been employed for the water surface.

4.1.3 In-situ simulation of tidal turbine

As was discussed in the introduction, in-situ simulations of tidal turbines, as one of the objectives of this research, can play a crucial role in decreasing the risk associated with their operation and help tidal energy in becoming a mainstream source of renewable energy. The methodology used in this research for simulating the turbine, as discussed before, is the actuator line (AL) method. In this technique, the actual geometry of the rotor is not included in the simulation. Instead, the effects of the blades are produced through source term that are distributed around three lines that represent the three blades and rotate with the rotor's rotational speed. In the AL method, these source terms are calculated through three-dimensional projection of forces that in turn are estimated from the blade element theory.

Figure 14 shows the AL methods algorithm, which as shown in this figure, its computationally intensive parts have been implemented to be performed by GPUs. According to this figure, in the AL method, after determining the new location of the rotor, each blade is divided into a number of blade elements and flow velocity is interpolated at each blade element center. Axial and tangential components of the velocity and the angle of attack at the blade element centers are then calculated from u, v and w fluid velocity components. Next, using the spanwise location of each blade element and its angle of attack, the lift and drag coefficients are determined using a look-up table through linear interpolation. In the following step, utilizing the blade element theory, generated axial and tangential forces by each blade element are calculated. All of these steps are more suitable to be done by CPUs and therefore are assigned to them. Next, employing a Gaussian distribution function, the calculated force for each blade element is projected on the flow field around it. This step, due to its large size of computation, is performed on GPUs. In the final step, by dividing the axial and tangential components of the resulting force by the control-volume's volume, source terms in axial and tangential directions will be obtained.

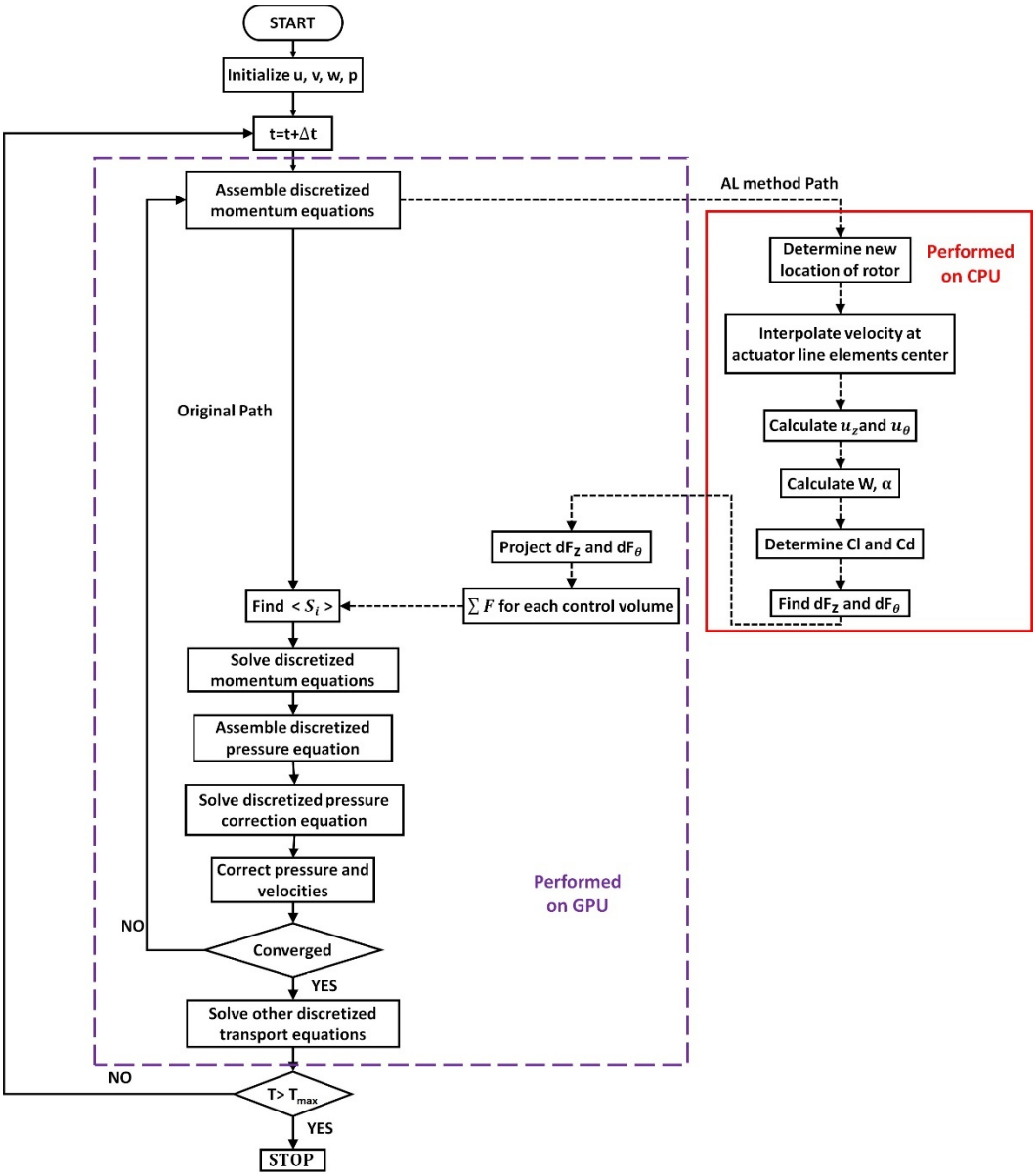

Figure 14. Actuator line method algorithm

4.2 Results and Conclusions

4.2.1 Coarse Tidal Flow Simulations of Grand Passage

For the coarse tidal flow simulations, the unsteady Detached Eddy Simulation (DES) turbulence model was used and a time step of $\Delta t = 1s$. Instantaneous velocity fields at 5 meters below the sea level are shown in Figure 15 and Figure 16, respectively, for flood and ebb flows. While due to the grid resolution and timestep size many of details of the flow have not been captured in this simulation, still these simulations provide a good insight into the flow pattern, velocity magnitudes, and potential locations in the passage for placing tidal turbines.

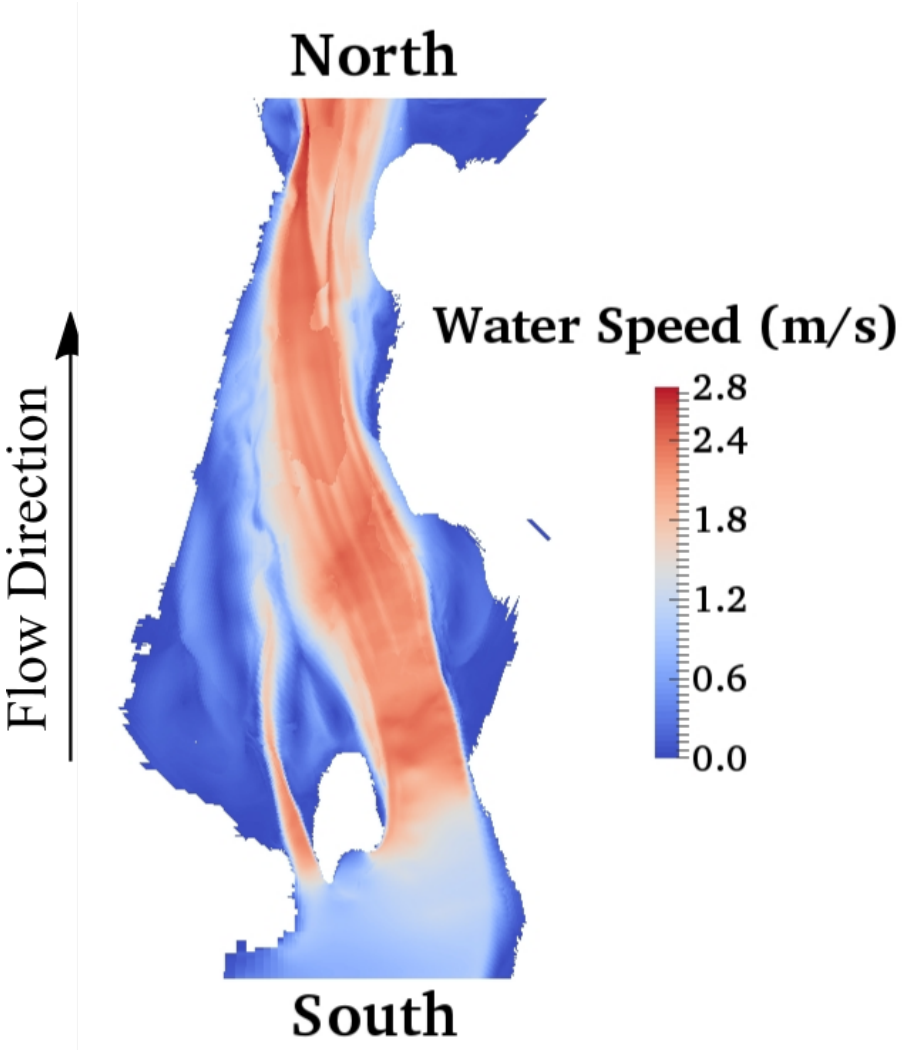

Figure 15. Instantaneous velocity field in flood flow at $\mathrm{z} = -5\ \mathrm{m}$

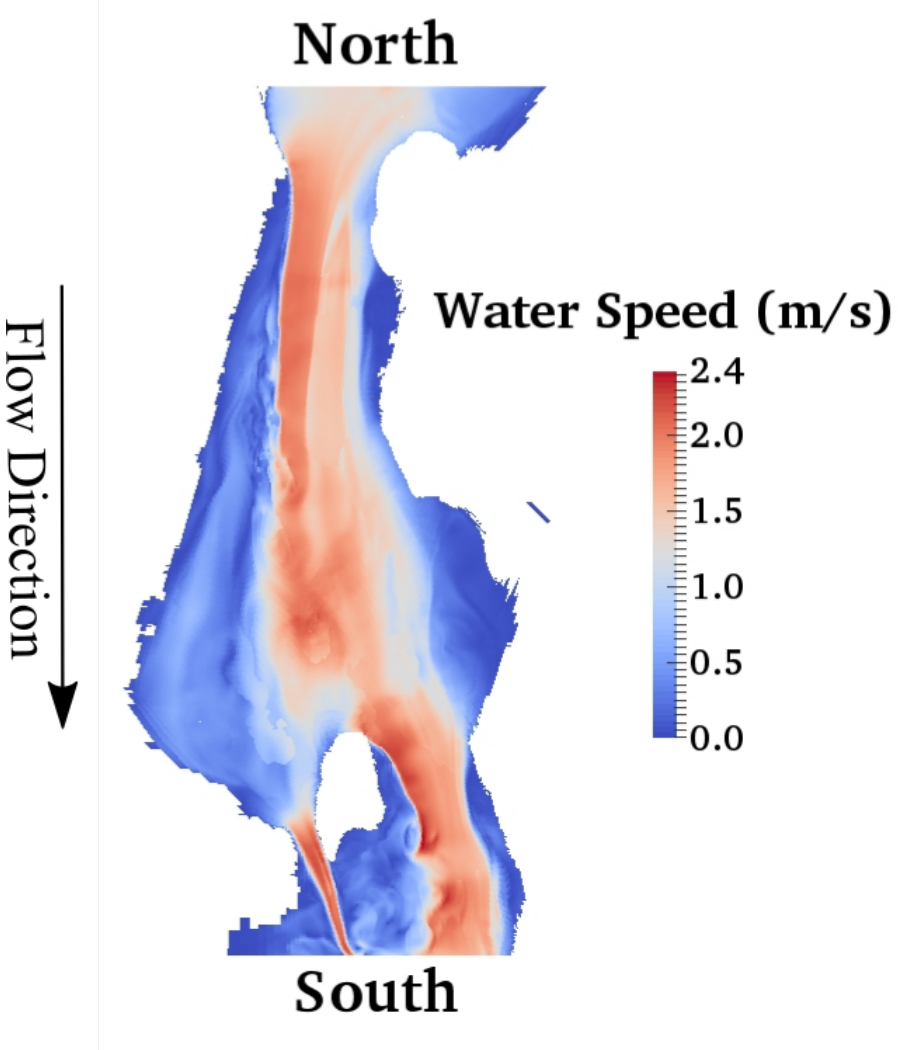

Figure 16. Instantaneous velocity field in ebb flow at $z = -5$ m

4.2.2 Fine Tidal Flow Simulations of Grand Passage

Similar to the coarse simulations, for the fine tidal flow simulations the DES turbulence model was employed. However, to capture unsteady features with higher frequencies, a timestep of $\Delta t = 0.1s$, which is 10 times smaller than the timestep in the coarse grid simulations. An extra feature included in the fine grid simulations of tidal currents is the monitoring points that have been included to provide high resolution time history of flow field variables. Analysis of such information can lead to tremendous insight into the interaction between tidal turbines and oceanic flows, which is the ultimate objective of this research.

The total number of monitoring points, included in this study is 1140, which has highlight in Table 1 are divide across 29 monitoring beams corresponding to locations where previous ADCPs were located and critical points around PLAT-I. Along every monitoring beam there is one monitoring point every 0.5 meters, which results in a different number of monitoring points on each beam

due to variations in ocean depth. Information on the ADCP locations were provided by Dr. Alex Hay's research team. The first ADCP (ECO SpraySig500) has 5 beams (4 slanted beams, 1 vertical) with a mean heading facing 170.68º true North. The angle of the slanted beams from the vertical line for this ADCP is 25º. Considering the small values of the mean pitch and mean roll for this ADCP (mean pitch: 2.04º, mean roll: 3.13º), these values have been approximated with zero. The second ADCP (ECO Spray RDI) has only the 4 slanted beams, which are 20º from the vertical line. The mean heading is 337.68º true North and the values of the mean pitch and mean roll are small (mean pitch: -6.88º, mean roll: 5.30º). Beams corresponding to these two ADCPs are shown in Figure 17.

For the rest of the monitoring beams listed in Table 1 there are no physical ADCPs in the passage and therefore, these monitoring beams are referred to as virtual ADCPs in this report. Flow variables at these points have been collected to provide some insight into the turbulence characteristics of the Grand Passage. These monitoring beams are distributed around the location of the PLAT-I, a tidal turbine platform that is operating in the Grand Passage.

The layout of monitoring beams corresponding to ECO Spray Sig500, ECO Spray RDI, and the virtual ADCPs located around the PLAT-I (1-20) is shown in Figure 18. The convention used for numbering the virtual ADCPs around PLAT-1 is illustrated in Figure 19.

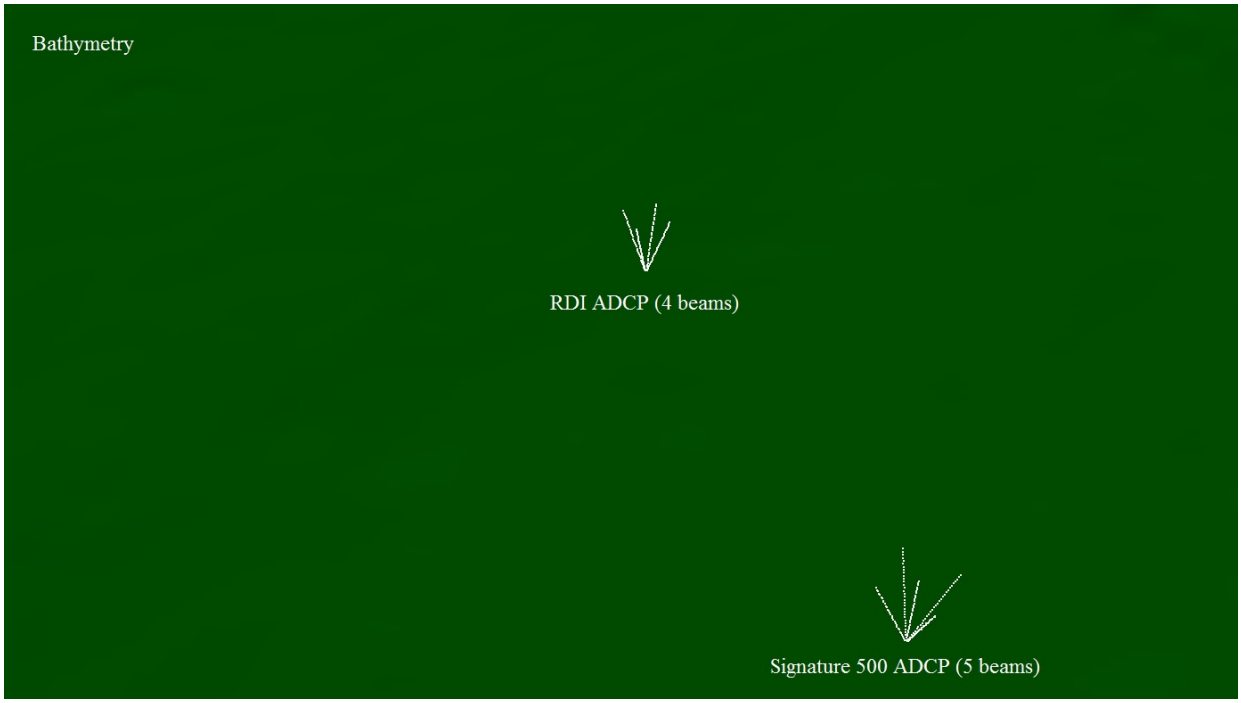

Figure 17. Signature 500 and RDI in-situ

Table 1. Monitoring beams specifications

Monitoring Beam	# of Beams	Number of monitoring points	Lat (º)	Lon (º)	Shifted UTM X (m)	Shifted UTM Y (m)	Depth Z (m)
ECO Spray Sig500	5	33	44.2669	-66.3371	2538.3185	4966.2133	-15.7414
ECO Spray RDI	4	33	44.2679	-66.3376	2494.8051	5075.9940	-15.9076
Around PLAT-I							
MB 1	1	43	44.2638	-66.3371	2546.1050	4619.5940	-20.7388
MB 2	1	41	44.2639	-66.3365	2593.0278	4637.2304	-19.8040
MB 3	1	41	44.2641	-66.3369	2560.7231	4651.7909	-19.8976
MB 4	1	41	44.2641	-66.3370	2558.9544	4656.4667	-19.8276
MB 5	1	41	44.2642	-66.3370	2557.1857	4661.1424	-19.6870
MB 6	1	41	44.2642	-66.3370	2555.4171	4665.8182	-19.6425
MB 7	1	41	44.2643	-66.3370	2551.8798	4675.1697	-19.6981
MB 8	1	41	44.2644	-66.3371	2548.3425	4684.5212	-19.9747
MB 9	1	42	44.2645	-66.3372	2541.2679	4703.2243	-20.0092
MB 10	1	41	44.2647	-66.3373	2534.1934	4721.9273	-19.5373
MB 11	1	36	44.2656	-66.3377	2498.8212	4815.4426	-17.2239
MB 12	1	42	44.2636	-66.3367	2578.4098	4605.0334	-20.2862
MB 13	1	42	44.2636	-66.3367	2580.1785	4600.3576	-20.2542
MB 14	1	42	44.2636	-66.3367	2581.9472	4595.6819	-20.2404
MB 15	1	42	44.2635	-66.3367	2583.7159	4591.0061	-20.2425
MB 16	1	42	44.2634	-66.3366	2587.2532	4581.6546	-20.2955
MB 17	1	42	44.2633	-66.3366	2590.7906	4572.3031	-20.2814
MB 18	1	43	44.2632	-66.3365	2597.8721	4553.3958	-20.9291
MB 19	1	44	44.2630	-66.3364	2604.9403	4534.8971	-21.2304
MB 20	1	55	44.2622	-66.3360	2640.3151	4441.3823	-26.8450

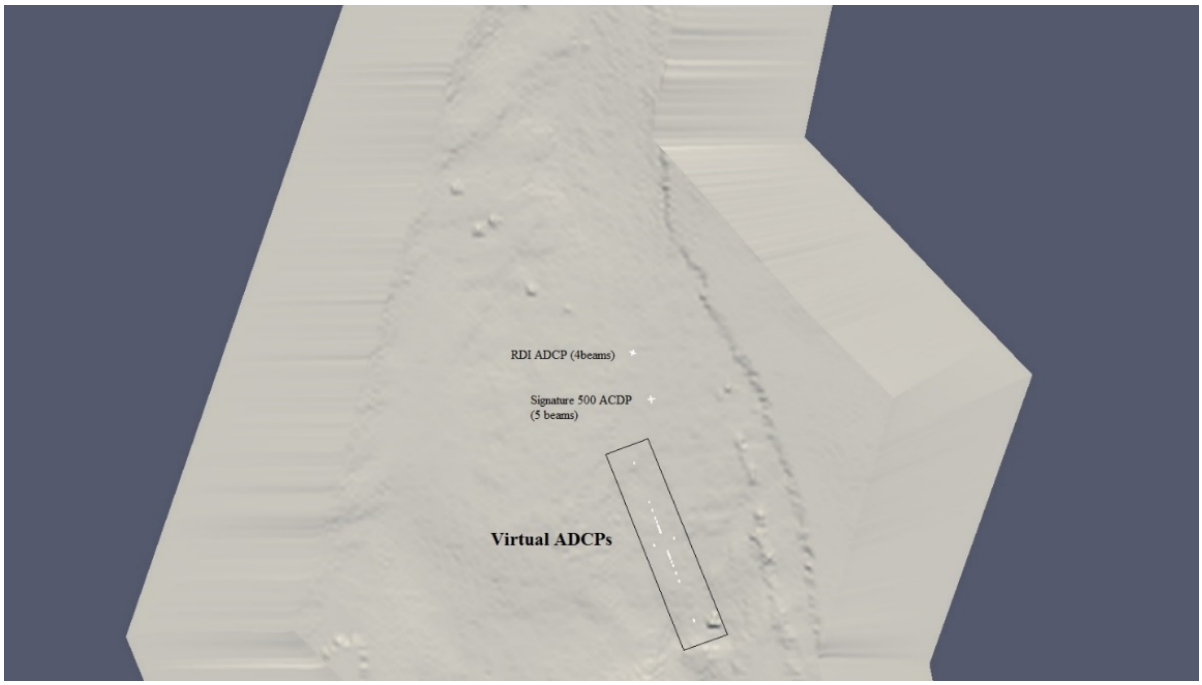

Figure 18. Top view of monitoring points

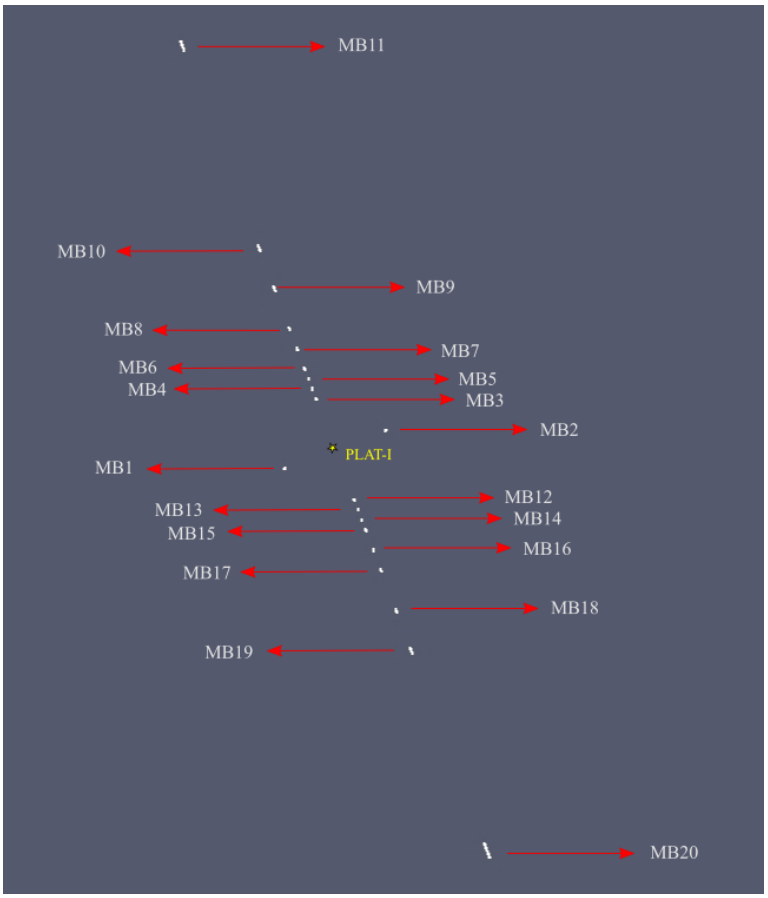

Figure 19. Monitoring beams located around PLAT-I

4.2.2.1 Flood Results:

Figure 20 shows the instantaneous velocity field obtained from the simulation of the flood flow using the fine grid. A closer view of this figure around the location of the PLAT-I is provided in Figure 21, which includes the location of the PLAT-I and monitoring beams as well. From this figure one can see that among the monitoring beams, MB 2 is exposed to periodic low velocity unsteady flow structures. Comparing this figure with Figure 15 , it can be seen that the high-resolution solution captures more flow details and smaller flow structures. Figure 20 and Figure 21 show the capability of CFD and the DES turbulence model in simulating complicated tidal flows which consist of flow structures of different sizes.

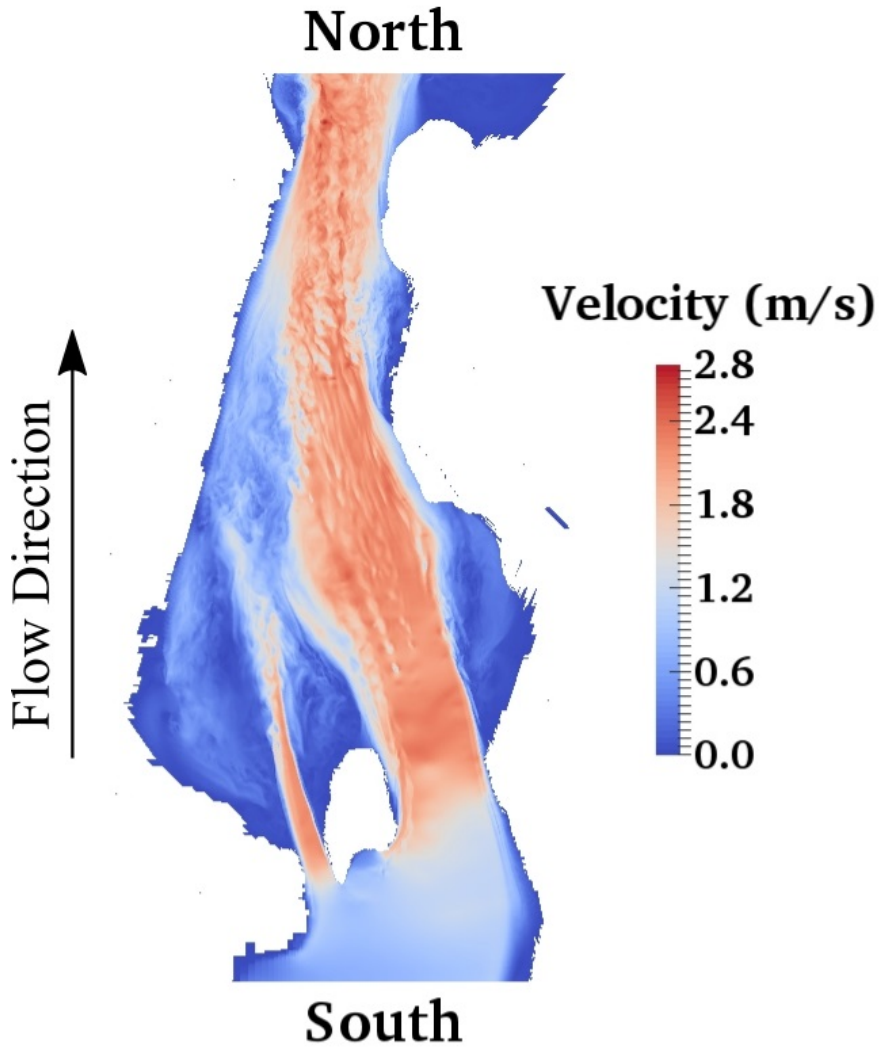

Figure 20 Instantaneous velocity field obtained from high-resolution simulation of flood ($z = -5$ m)

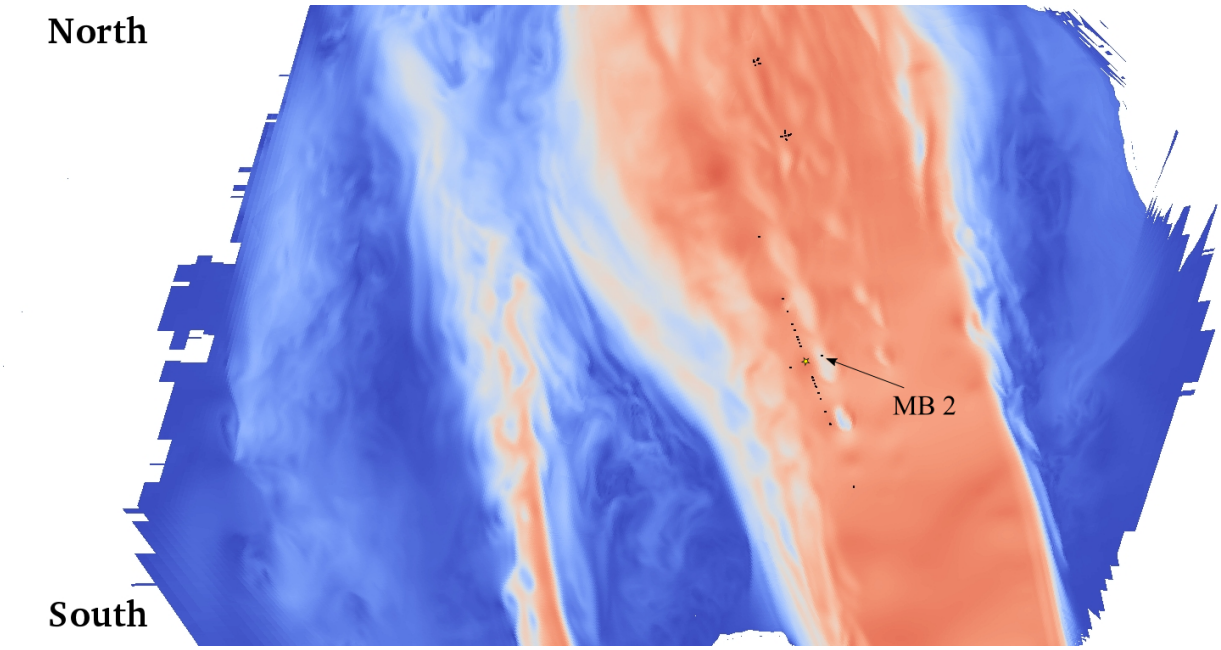

Figure 21 Closer view of instantaneous velocity field obtained from high-resolution simulation of flood ($z = -5$ m) with monitoring beams included

Figure 22 shows the mean velocity field at $z = -5$ m obtained for the flood flow and Figure 23 shows a closer view around the PLAT-I location and the monitoring beams. From this figure one can see that the turbine and all the monitoring beams, except MB 2, are exposed to high velocity flows. The lower mean velocity for MB 2, as was mentioned previously, is due to the unsteady and oscillating velocity at this point. It should be noted that considering the floating structure of the PLAT-I, depending on the time in the tidal cycle, the platform will be moved by tidal currents and can be at any location along the virtual ADCPs line, which is almost in the mean flow direction. Using the information provided by monitoring beams along the path of the platform, its operational condition at any point in a tidal cycle will be known. From Figure 23 it can be seen that the location of the platform has been chosen far enough from the wake of the Island. However, some other locations that merely based on the velocity magnitude, could be potential locations for this platform. For example, regions 1 and 2, identified on Figure 22 benefit from high velocity flows which happen due to narrow passages created at these points.

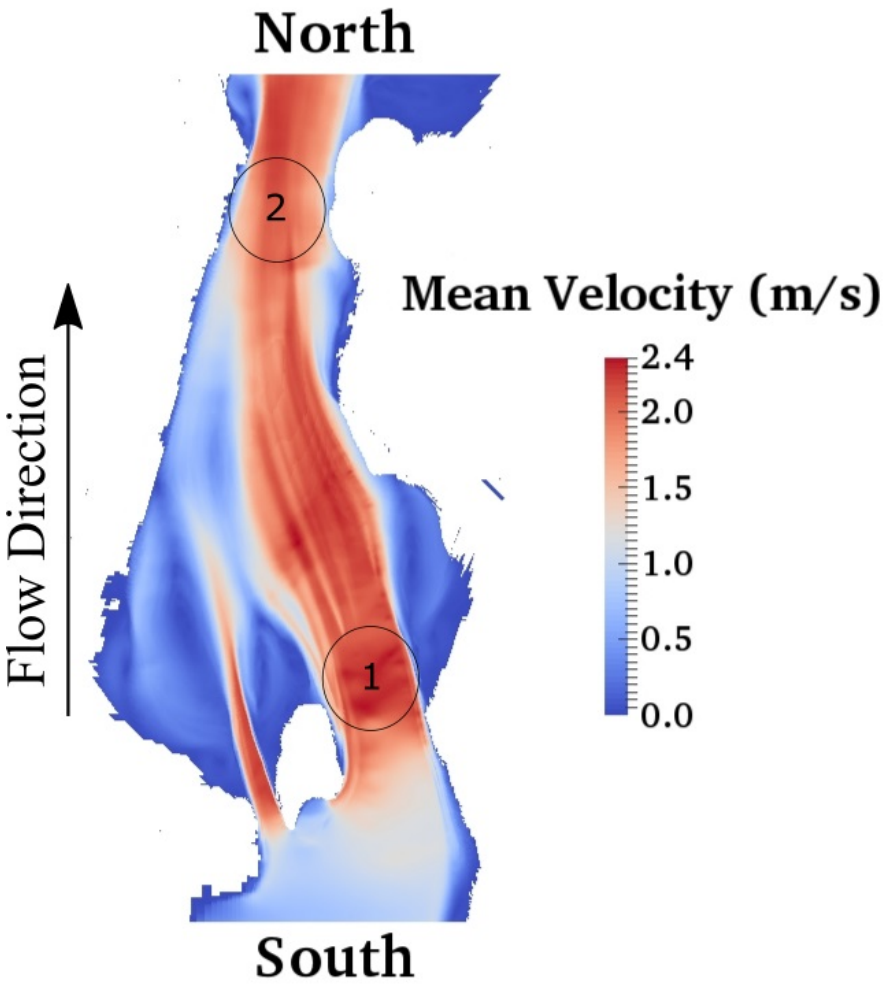

Figure 22 Mean velocity field obtained from high-resolution simulation of flood ($z = -5$ m)

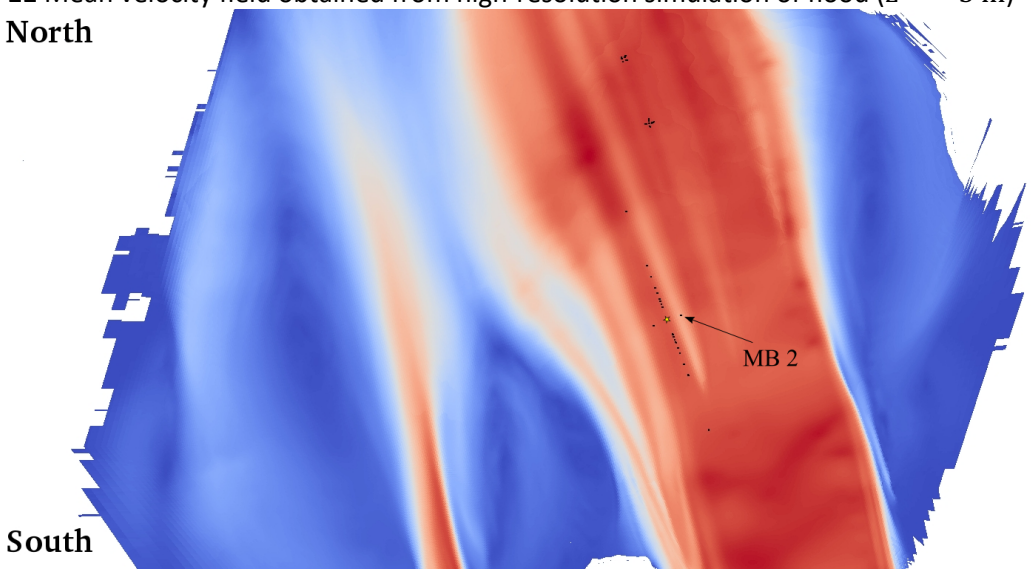

Figure 23 Closer view of mean velocity field obtained from high-resolution simulation of flood ($z = -5$ m) with monitoring beams included

As was mentioned, considering the floating design of the PLAT-I, gathering the flow information along its path can provide us with useful data necessary for predicting the platform efficiency or imposed forces on it. Performing this task in this research, the time-averaged profiles of x and y components of velocity for flood at the center beam of the Signature 500 ADCP and the 20 virtual monitoring beams around the PLAT-I are shown in Figure 24. A comparison between the velocity profiles shows that the mean velocity profiles recorded by monitoring beams from MB 3 to MB 20 along the virtual monitoring beams line, are very comparable. While for MB 1, the mean velocity profiles are still close to the pattern noticed for MB 3 to MB 20, the profiles recorded for MB 2, as discussed in Figure 23, are considerably different. Also, by comparing the velocity profile obtained for the center beam of the ECO Spray Sig500 and virtual monitoring beams from MB 3 to MB 20 one can see some differences between the two sets of profiles. This difference becomes more evident closer to the water surface, where the velocity profile obtained by the Signature 500 ADCP shows a higher gradient. One of the reasons contributing to the different velocity field at this point is the depth of ocean which is smaller at Sig500's location. This difference is more notable for the Y component of the velocity.

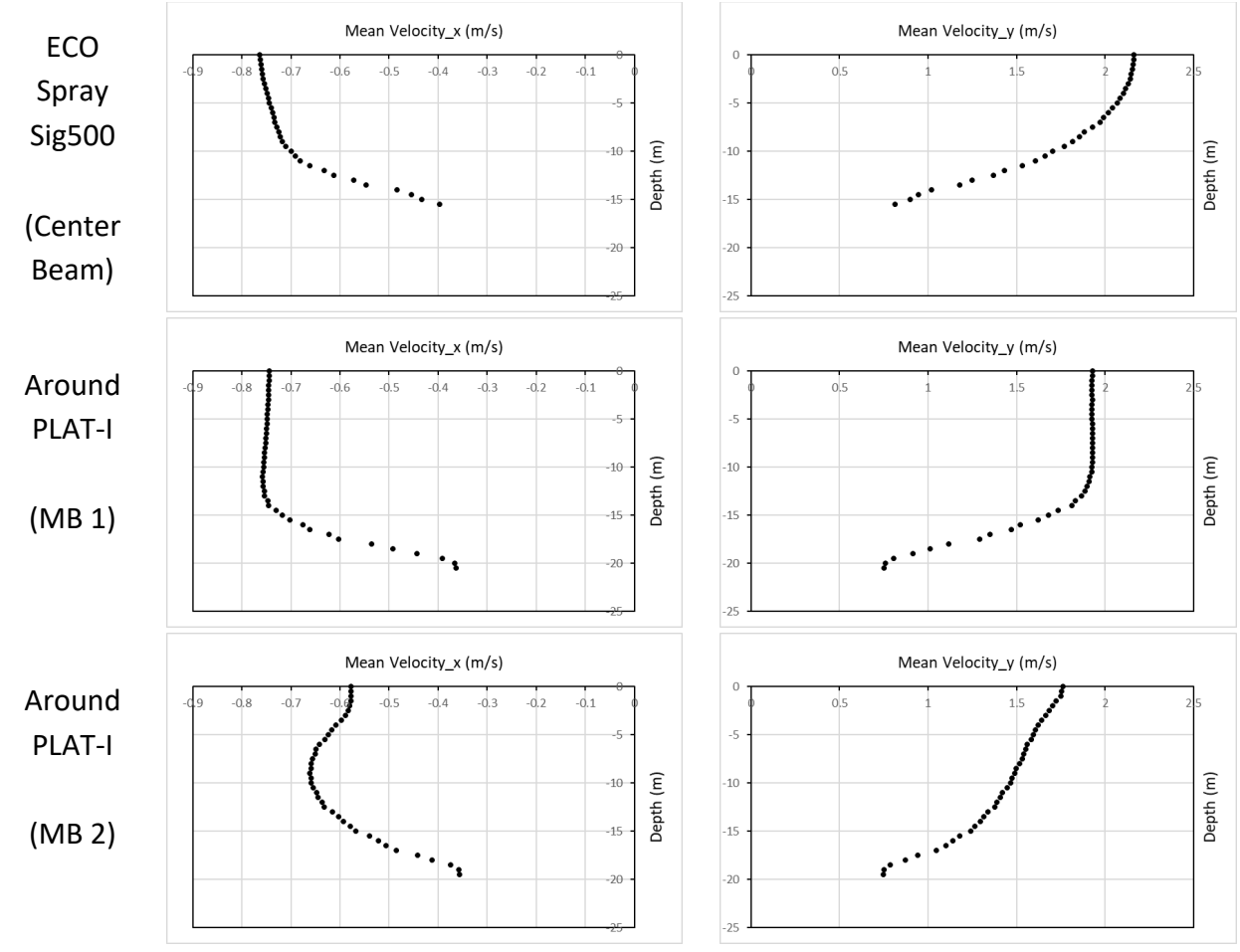

Around PLAT-I (MB 3)

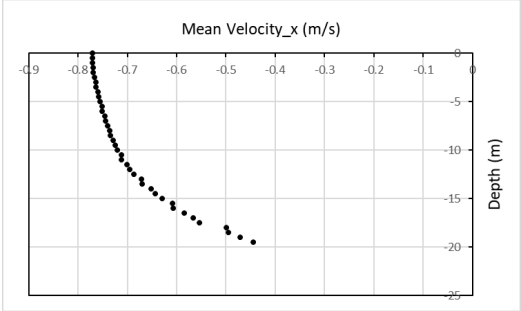

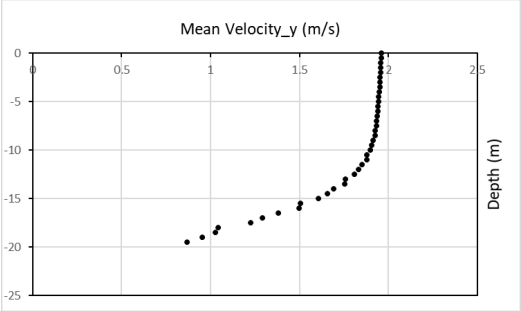

Around PLAT-I (MB 4)

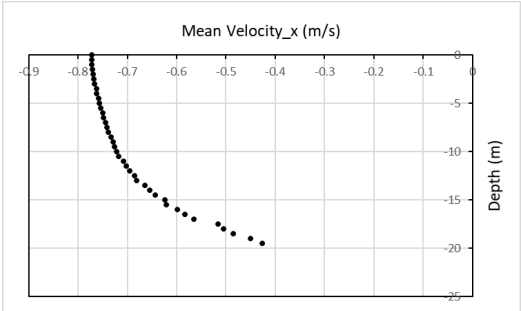

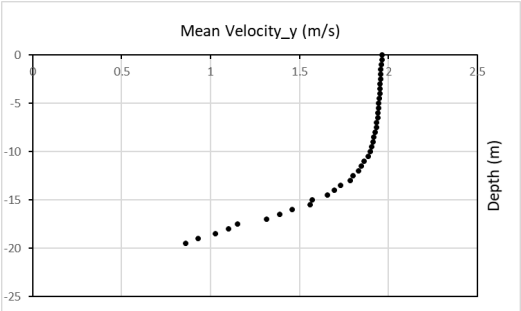

Around PLAT-I (MB 5)

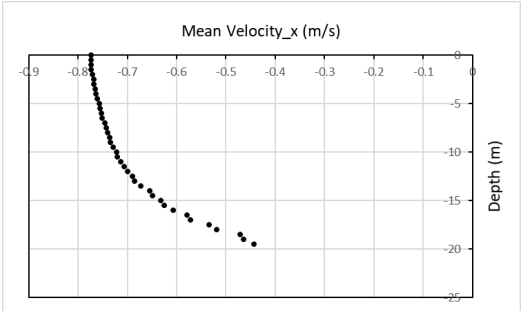

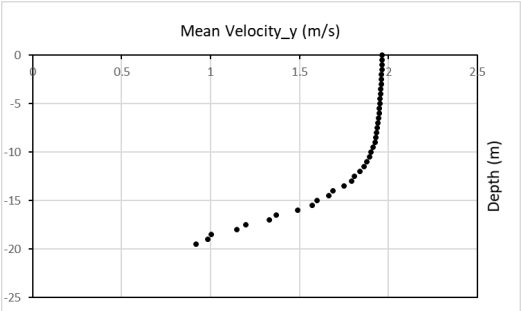

Around PLAT-I (MB 6)

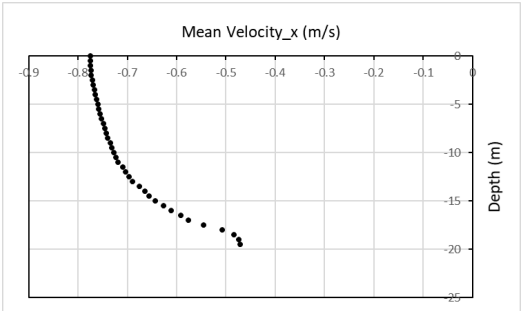

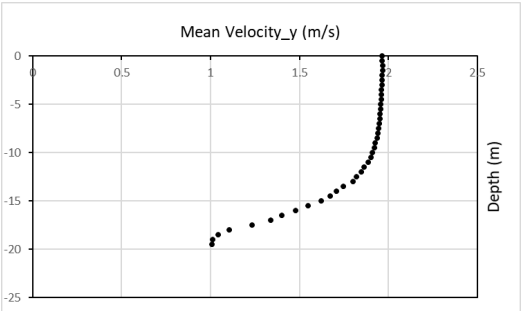

Around PLAT-I (MB 7)

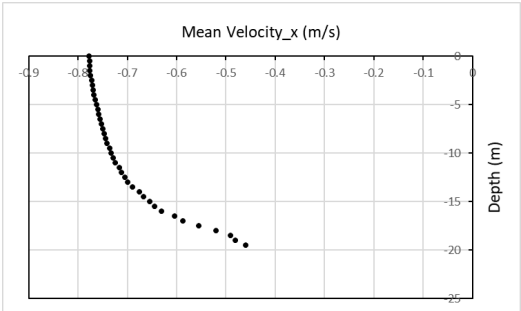

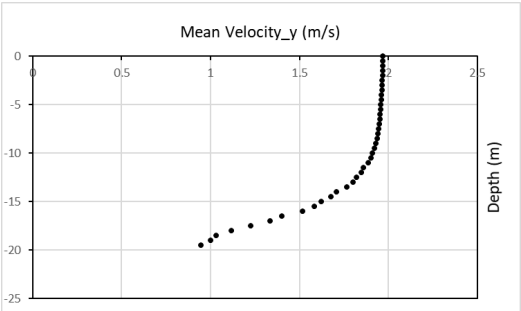

Around PLAT-I (MB 8)

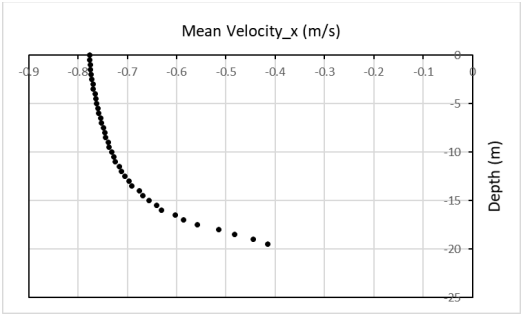

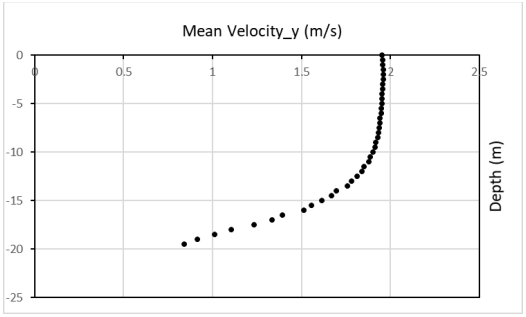

Around PLAT-I (MB 9)

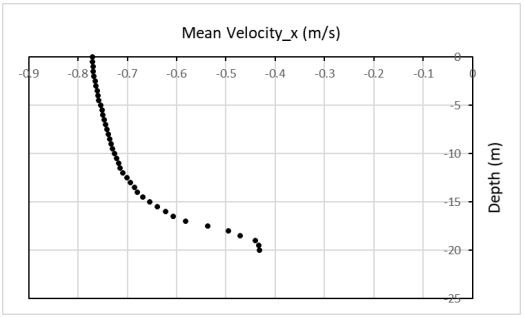

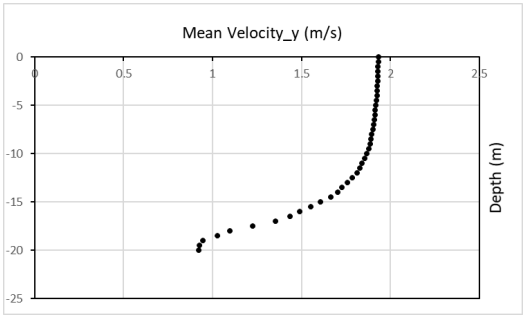

Around PLAT-I (MB 10)

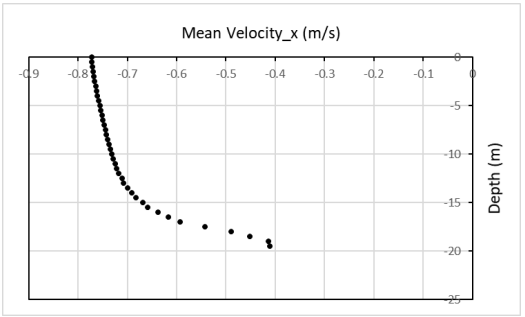

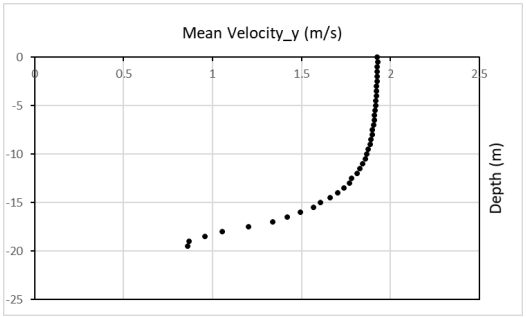

Around PLAT-I (MB 11)

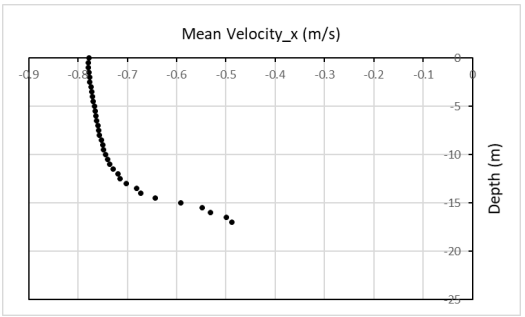

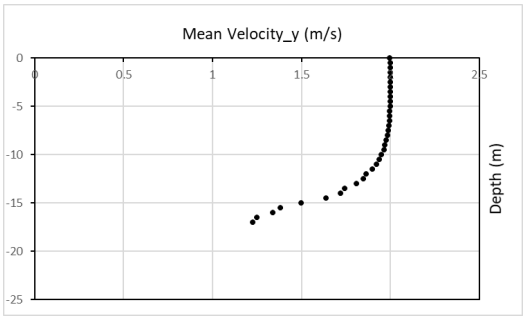

Around PLAT-I (MB 12)

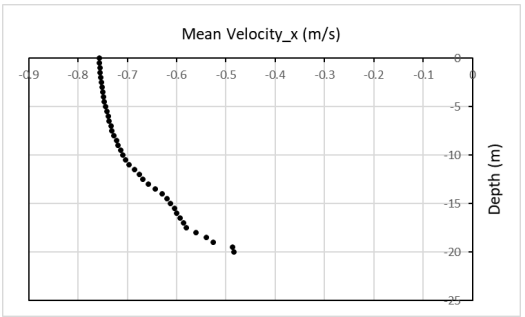

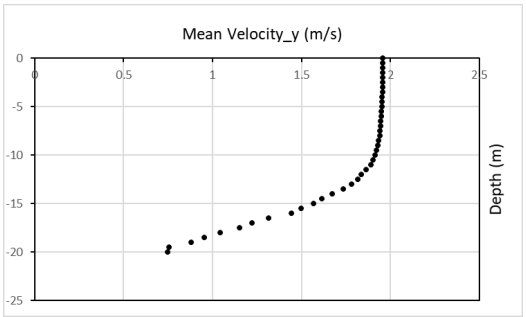

Around PLAT-I (MB 13)

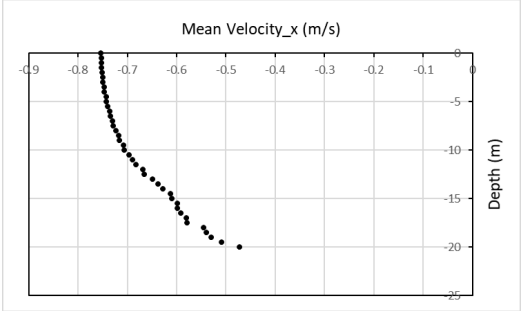

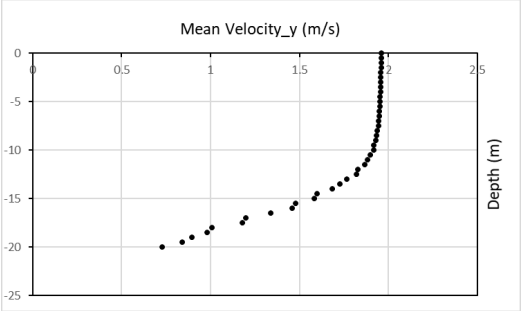

Around PLAT-I (MB 14)

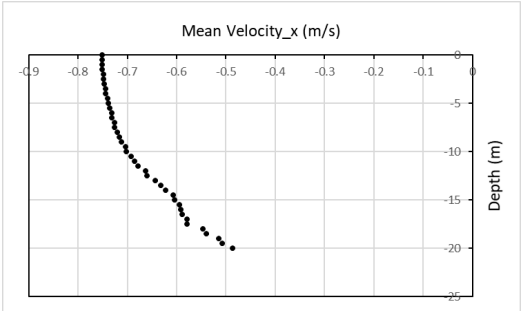

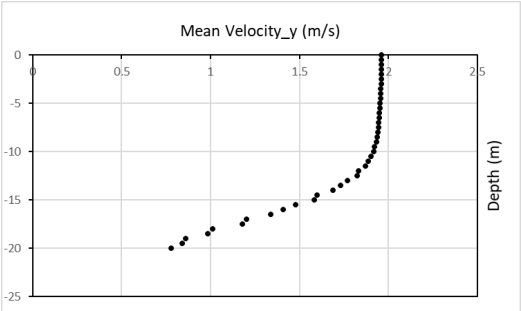

Around PLAT-I (MB 15)

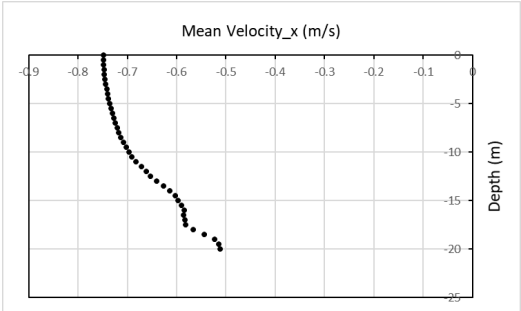

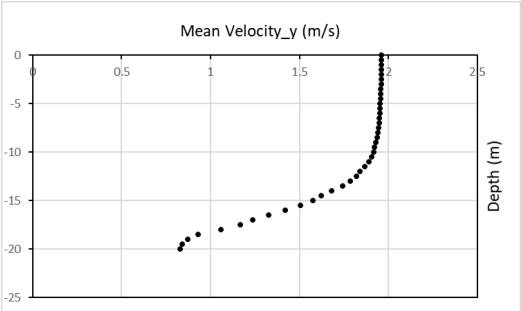

Around PLAT-I (MB 16)

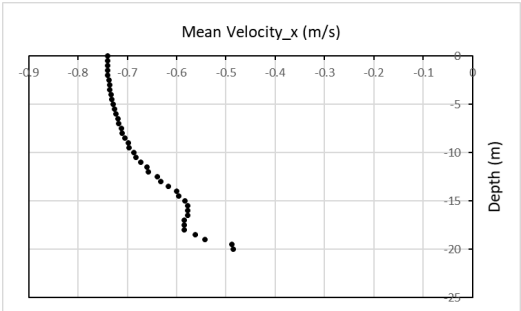

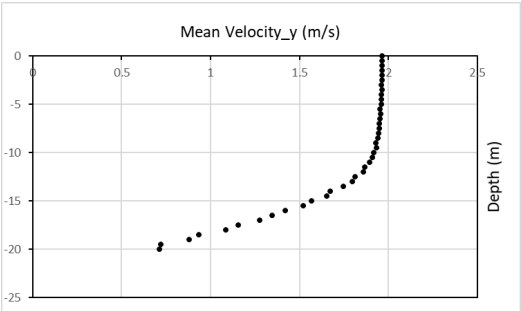

Around PLAT-I (MB 17)

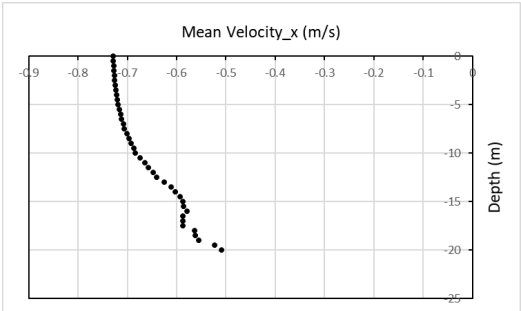

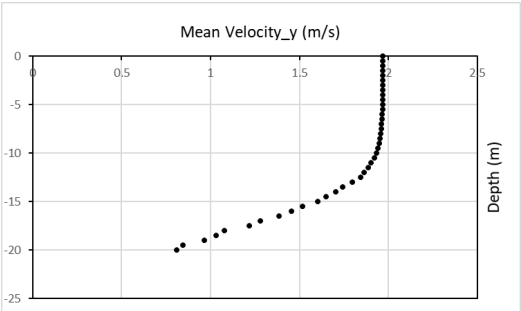

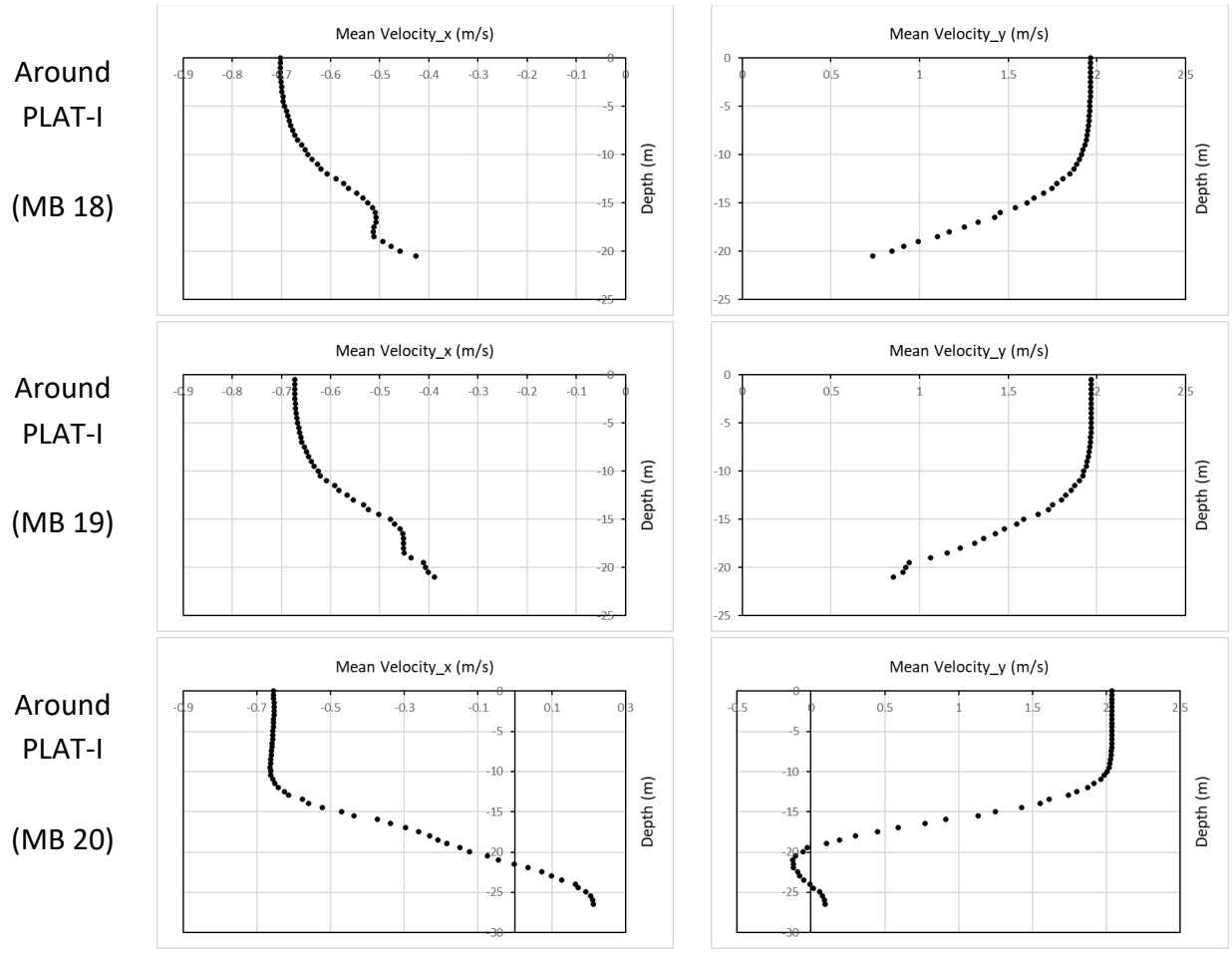

Figure 24. Time-averaged value of x and y components of velocity for flood for vertical monitoring beams

Figure 25 shows x and y components of the mean velocity for all the monitoring beams at $z = -5$ m. In this figure the horizontal axis is the number of monitoring beam and the vertical axis shows the x and y components of the mean velocity recorded by the monitoring beams at $z = -5$ m. Ecospary Sig500 ADCP has been shown as the zero (0) on the horizontal axis. From this figure, at $z = -5$ m, the velocity measured by this ADCP is in close agreement with the values obtained from the virtual monitoring beams and the difference in the recorded planar velocity by this ADCP when compared with the average of MB 3 to MB 20 is 5%. However, based on the observation made from Figure 24 by comparing the velocity profiles for the whole depth of water, for this ADCP, a location along the virtual monitoring beams could give a better prediction of velocity magnitude at different depths. An exception to all monitoring beams in Figure 24 is MB 2, which, as discussed, due to its location, experiences lower mean velocity when compared with other monitoring beams.

Figure 26 shows the time history of velocity components at $z = -5$ m on the center beam of the Signature 500 ADCP for one hour of the simulation. The first ~ 3 hours of the flow, which includes the initial transient part of the simulation, has been removed from this figure. From this figure one can see that there are significant fluctuations in the y component of velocity, which is almost aligned with the flow direction. While smaller, but still considerable amount of fluctuations can be seen in values recorded for velocity in the x direction. In the z direction (depth), fluctuations are smaller than x and y components. However, they are still noticeable, and their presence confirms that a 3D approach is necessary for tidal flows' studies.

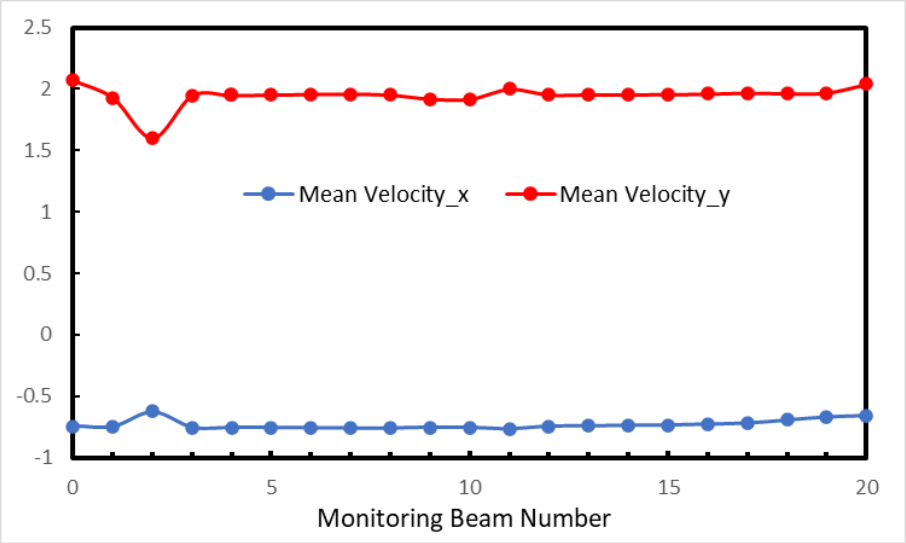

Figure 25. x and y components of mean velocity for all monitoring beams at $z = -5$ m

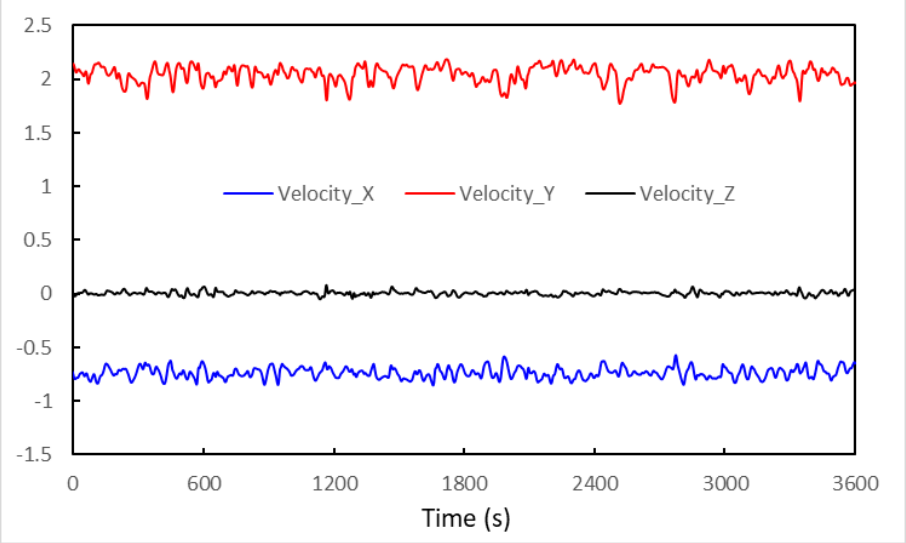

Figure 26. Time history of velocity components at $z = -5$ m on center beam of Signature 500 ADCP for flood

Figure 27 illustrates the time history of the planar velocity (combination of x and y component of velocity) and its fluctuations at $z = -5$ m on the center beam of the Signature 500 ADCP. The running mean of the velocity and the standard deviation of fluctuations are also shown in this figure. From this figure one can see that running mean of planar velocity and the standard deviation are not changing any more, indicating that the simulation has run long enough. The value of standard deviation of velocity fluctuations in the horizontal plan at this location is 8%.

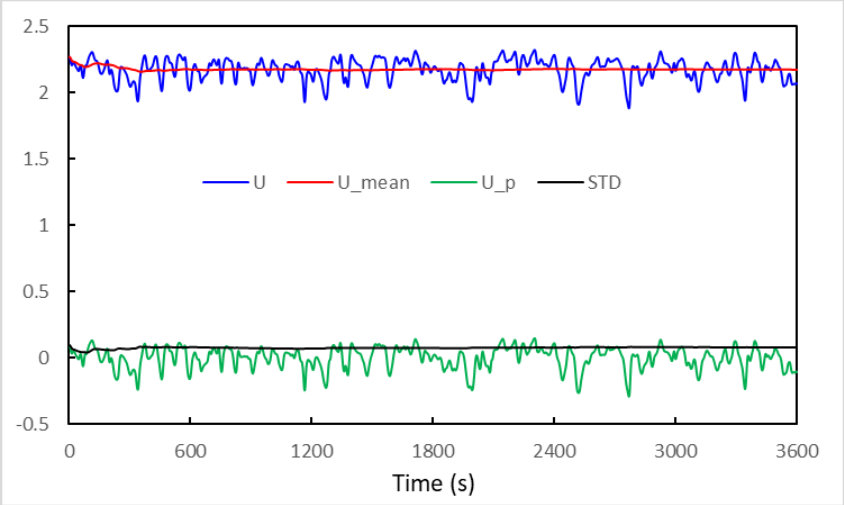

Figure 27. Magnitude, time-averaged, fluctuation, and standard deviation of horizontal velocity at $z = -5$ m on center beam of Signature 500 ADCP for flood

Figure 26 and Figure 27 can be compared, respectively, against Figure 28 and Figure 29, which show the same quantities at the same depth on MB 3. This comparison reveals visual differences between the two sets, indicating larger oscillations in the case of the Signature 500 ADCP. This is confirmed when comparing the standard deviation of oscillations in the two case, which is 5% for MB 3 against the 8% for the ADCP. From here it can be inferred that the ADCP will be over predicting the turbulence level encountered by the turbine.

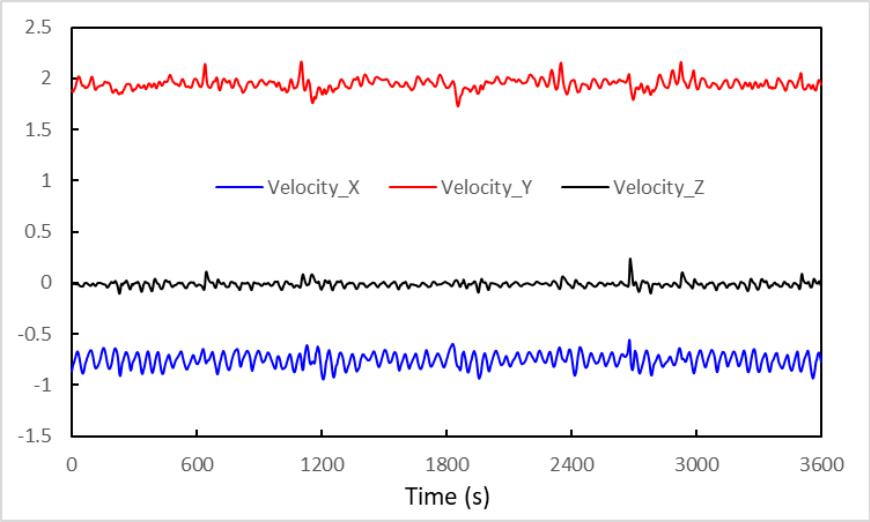

Figure 28. Time history of velocity components at monitoring point located at $z = -5$ m on MB 3 for flood

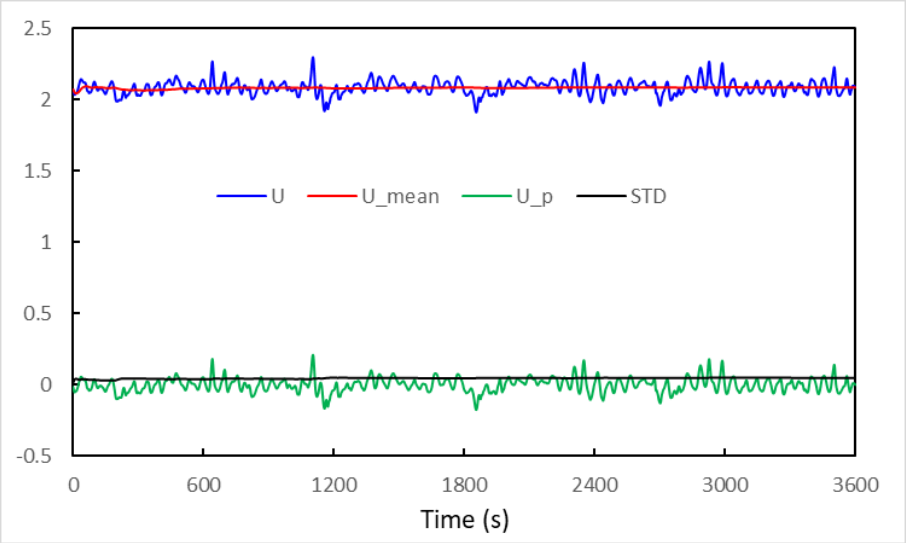

Figure 29. Magnitude, time-averaged, fluctuation, and standard deviation of horizontal velocity at $z = -5$ m on MB 3 for flood

4.2.2.2 Ebb Results:

Figure 30 shows the instantaneous velocity field obtained from the high-resolution simulation of ebb in the Grand Passage. Similar to the case of the flood, it can be seen that the high-resolution simulation reveals smaller flow structures when compared with Figure 16, which was obtained from the coarse grid simulation.

The mean velocity field, obtained for the ebb, is presented in Figure 31. From Figure 31 and the corresponding figure for flood (Figure 22), one can see that the two marked locations in this figure experience high velocity flows in both flood and ebb and therefore are suitable locations for tidal turbines. Therefore, while the current location for the PLAT-I is exposed to high velocity

flows, if moved approximately half a kilometer along the virtual monitoring beams line toward South, it will receive flows with higher velocities.

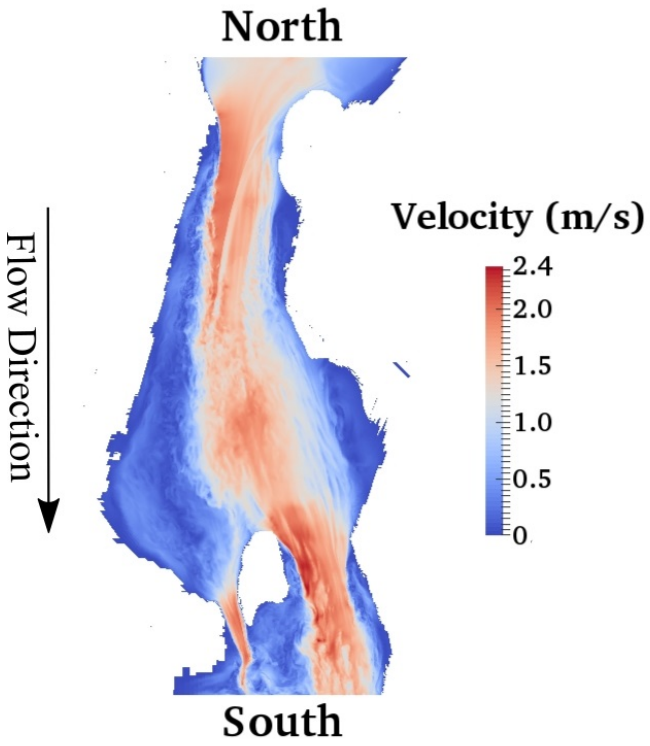

Figure 30. Instantaneous velocity field obtained from high-resolution simulation of ebb ($z = -5$ m)

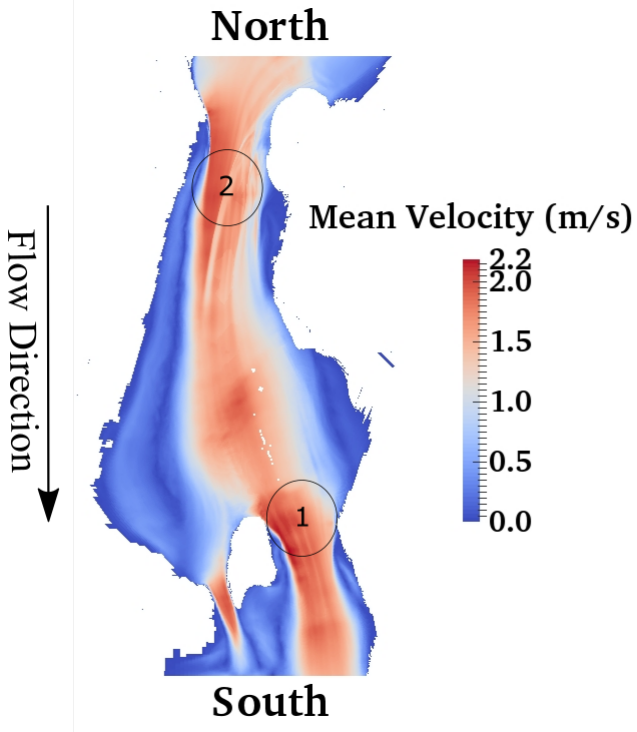

Figure 31. Mean velocity field obtained from high-resolution simulation of ebb ($z = -5$ m)

Using the velocity values recorded by the monitoring points, the mean velocity profiles for each of the vertical monitoring beams listed in Table 1 is shown in Figure 32. From this figure, one can see that similar to the case of the flood simulation, the velocity profiles obtained by the Signature 500 ADCP are different from the rest of the monitoring beams.

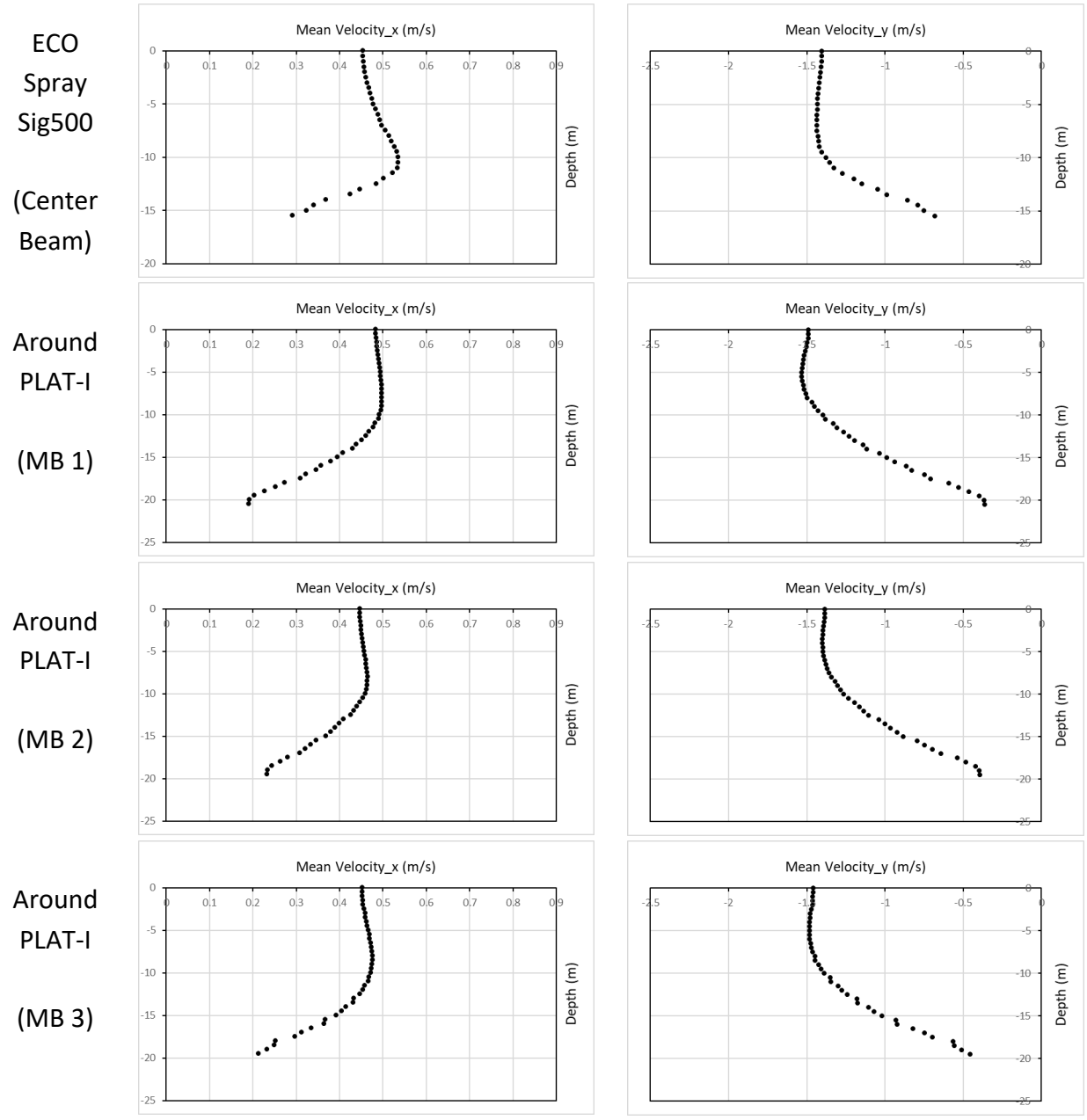

Around PLAT-I (MB 4)

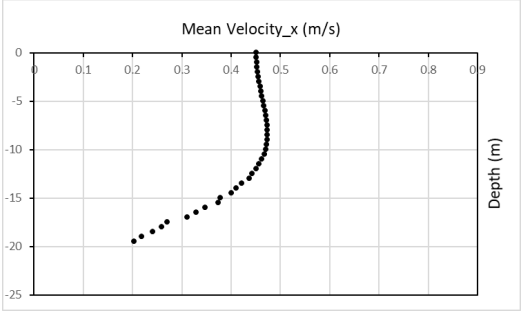

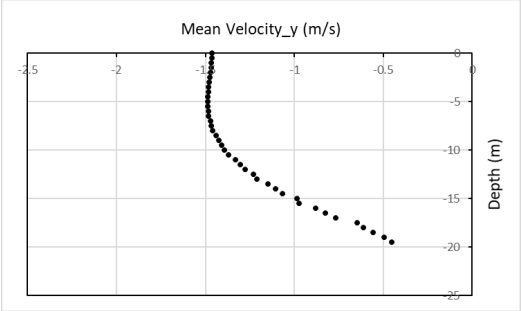

Around PLAT-I (MB 5)

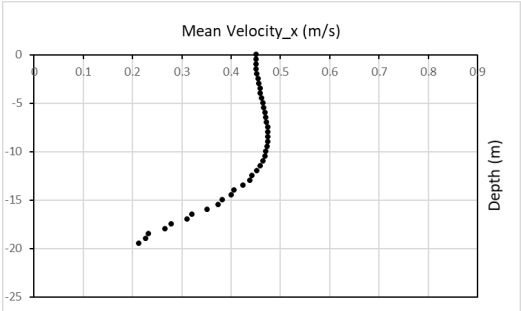

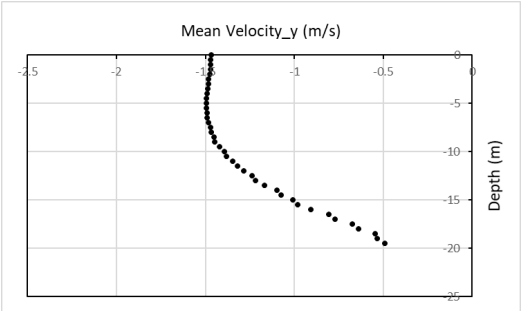

Around PLAT-I (MB 6)

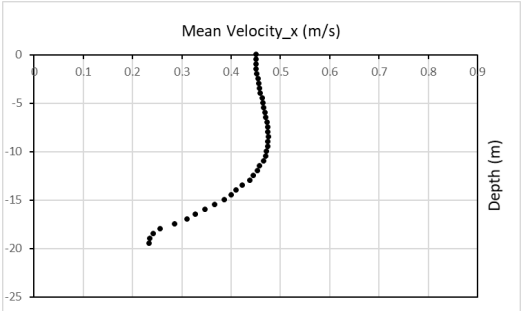

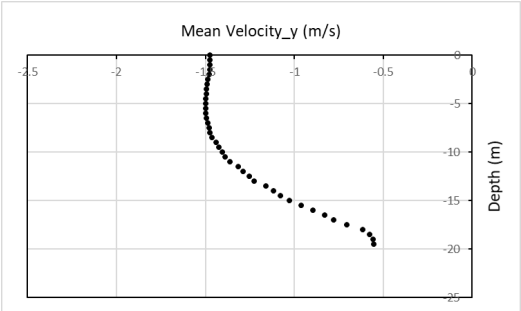

Around PLAT-I (MB 7)

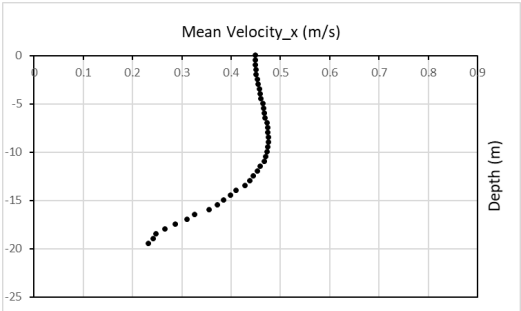

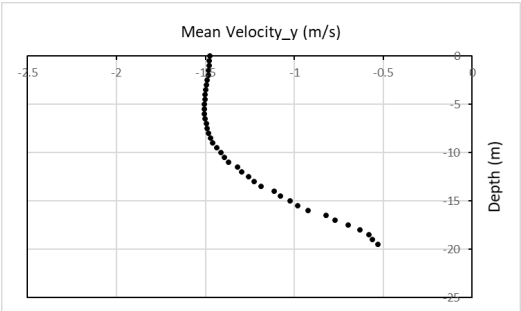

Around PLAT-I (MB 8)

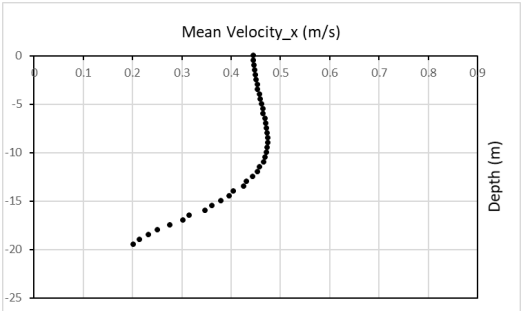

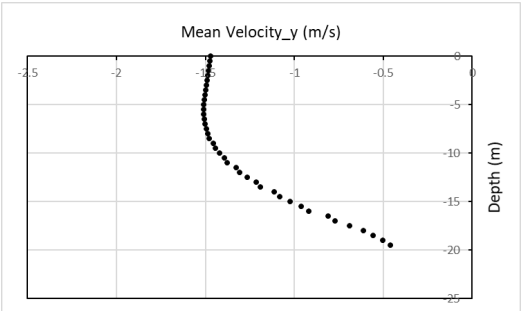

Around PLAT-I

(MB 9)

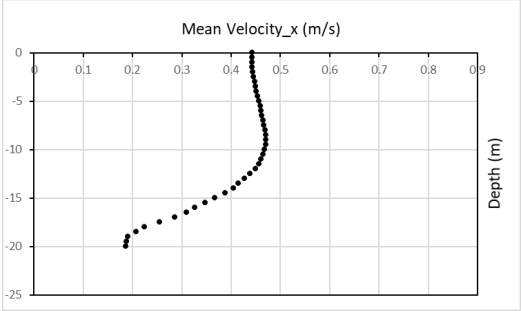

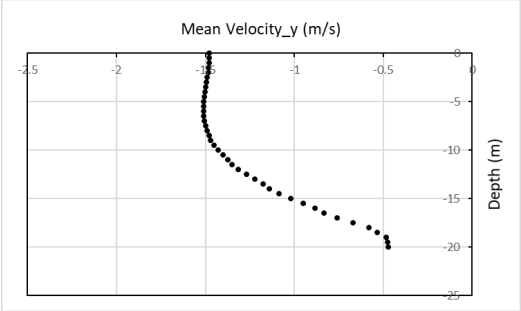

Around PLAT-I

(MB 10)

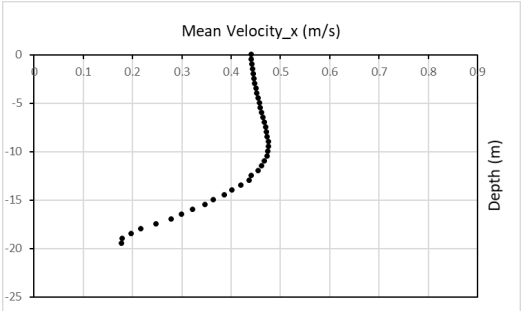

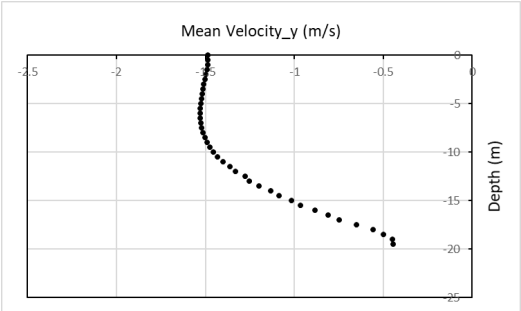

Around PLAT-I

(MB 11)

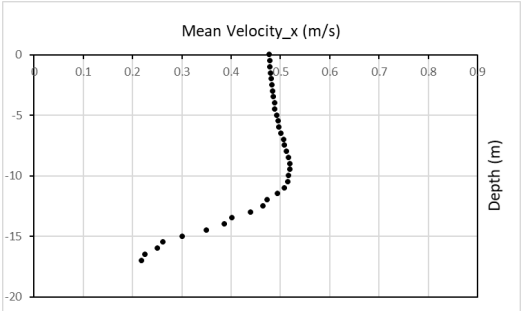

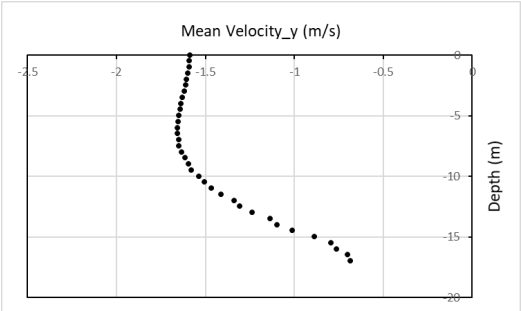

Around PLAT-I

(MB 12)

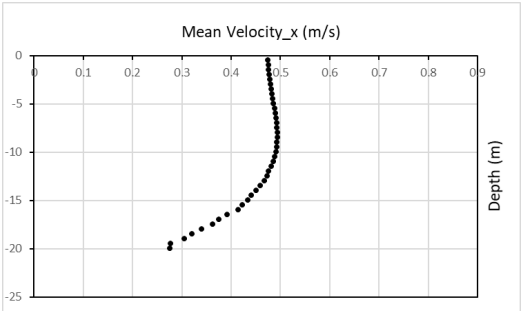

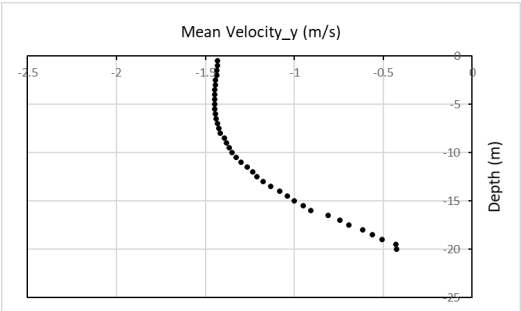

Around PLAT-I

(MB 13)

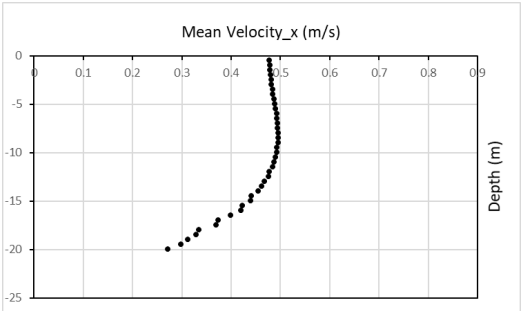

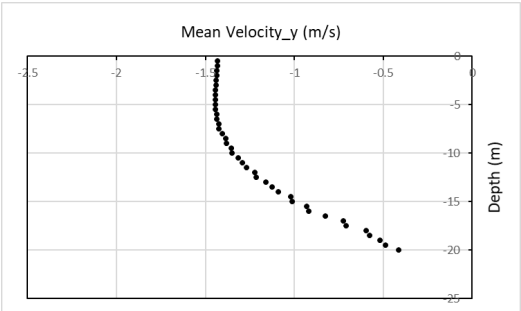

Around PLAT-I (MB 14)

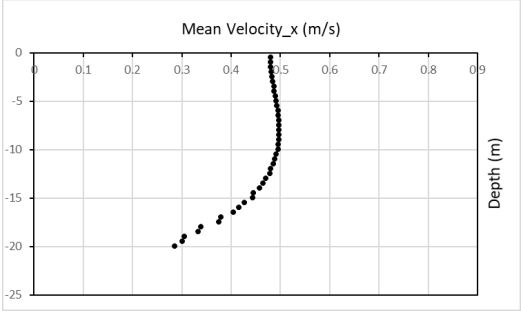

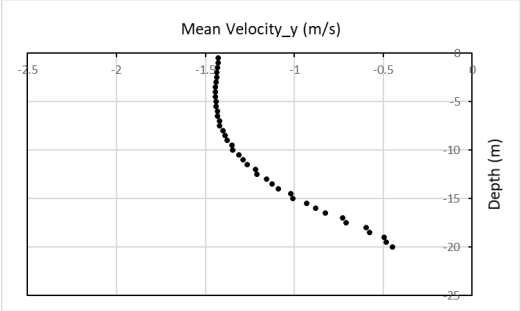

Around PLAT-I (MB 15)

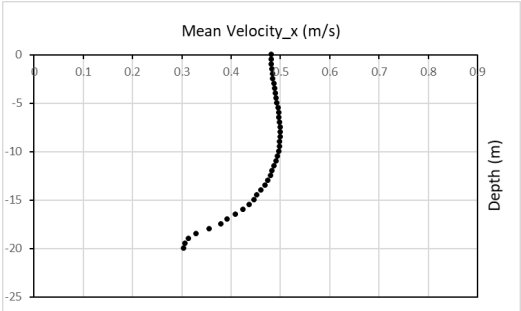

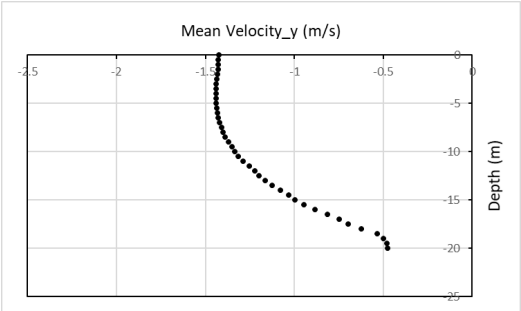

Around PLAT-I (MB 16)

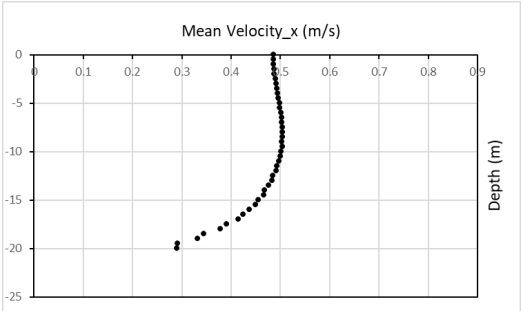

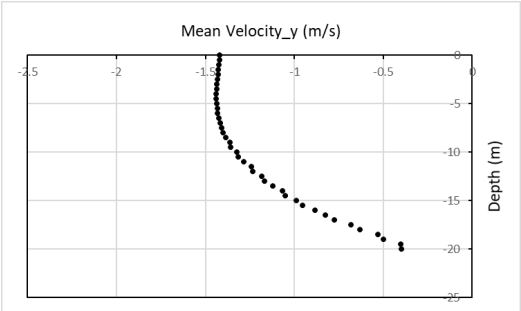

Around PLAT-I (MB 17)

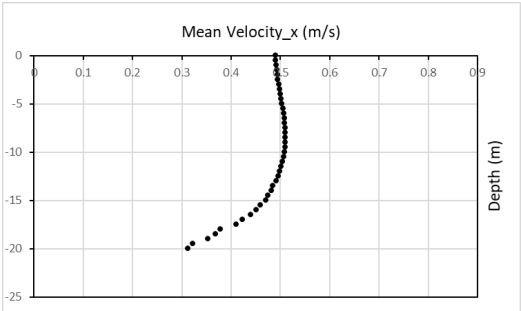

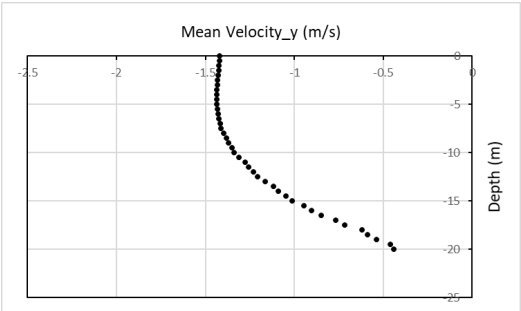

Around PLAT-I (MB 18)

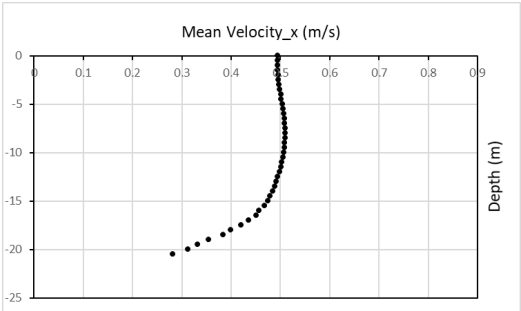

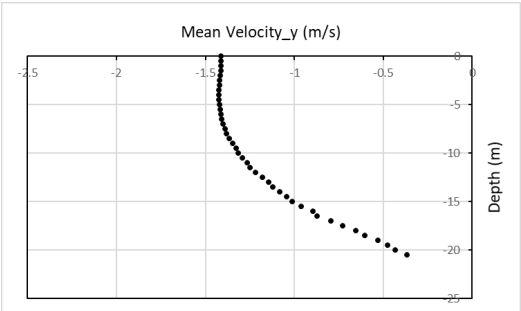

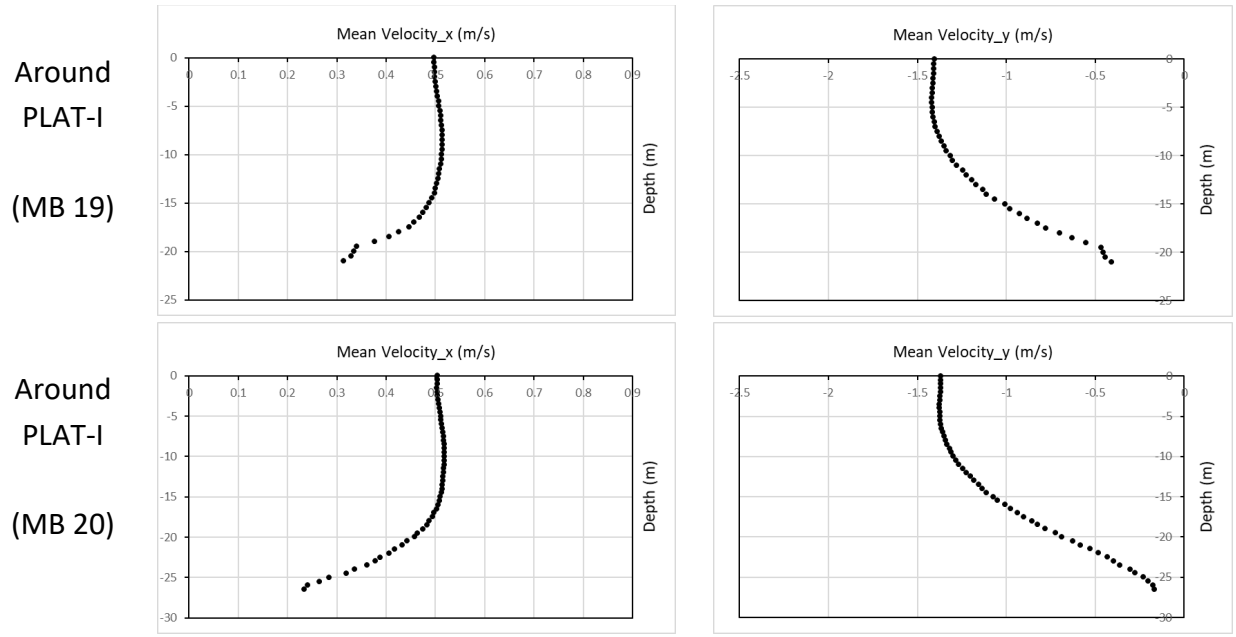

Figure 32. Time-averaged value of x and y components of velocity for ebb for vertical monitoring beam

Similar to the case of the flood flow, the time history of velocity components and the magnitude of horizontal velocity and its fluctuations at $z = -5$ m on the center beam of the Signature 500 ADCP for one hour of the simulation have been shown respectively in Figure 33 and Figure 34. The first ~ 3 hours of the flow results, which includes the initial transient part of the simulation, has been removed from these figures. Comparable with the corresponding figures obtained for the flood flow, large oscillations in the velocity components indicate turbulence in the flow which its turbulence intensity, based on the standard deviation of the oscillations in U (planar velocity), is 6%.

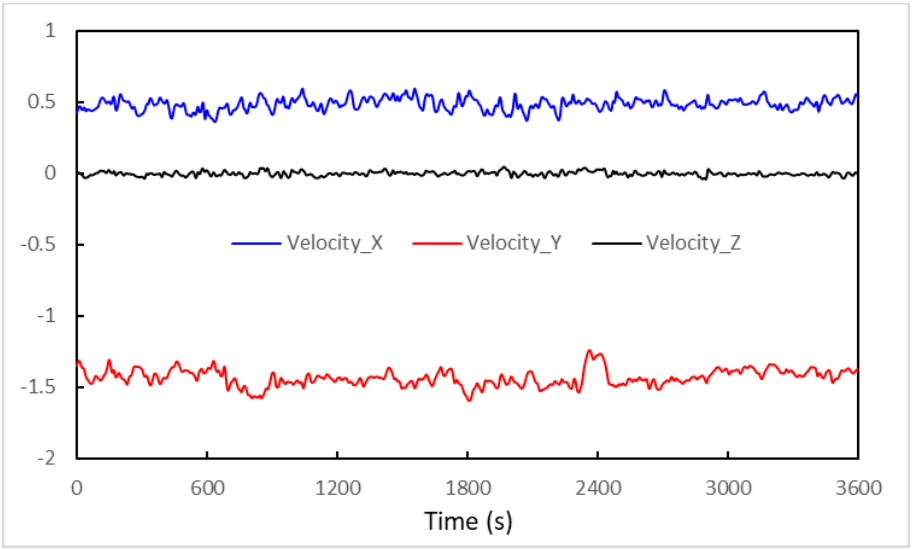

Figure 33. Time history of velocity components at $z = -5$ m on center beam of Signature 500 ADCP for ebb

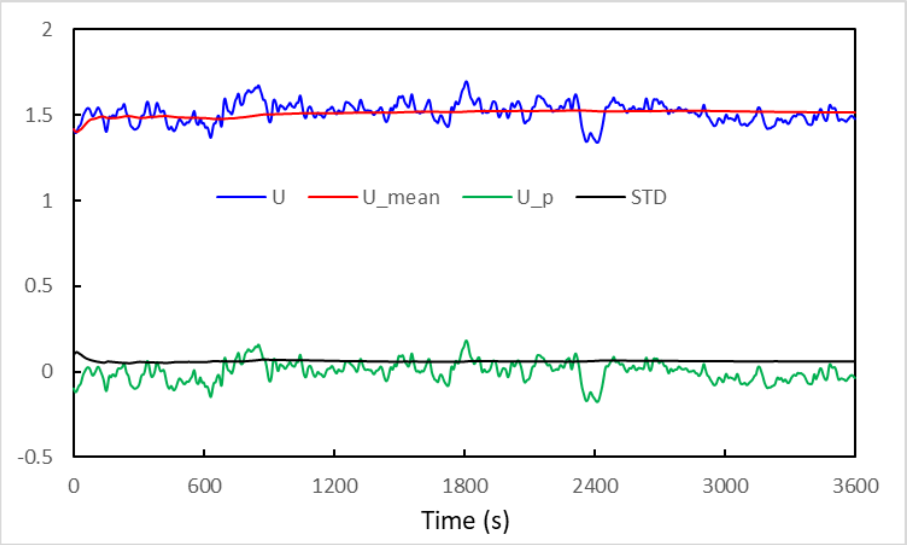

Figure 34. Magnitude, time-averaged, fluctuation, and standard deviation of horizontal velocity at $z = -5$ m on center beam of Signature 500 ADCP for ebb

By repeating the process for the monitoring point located at $z = -5$ m on MB 3, the following graphs are obtained. The turbulence intensity measured at this point is 7%.

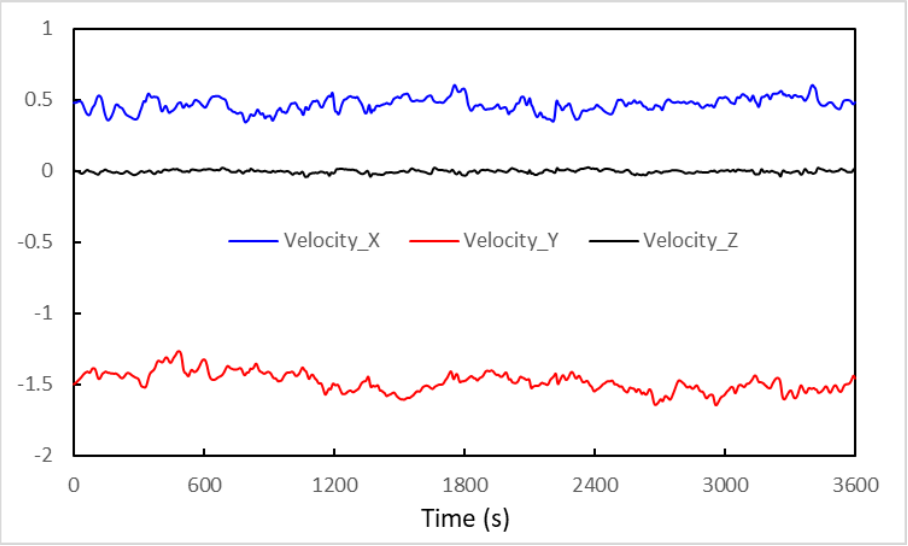

Figure 35. Time history of velocity components at $z = -5$ m on MB 3 for ebb

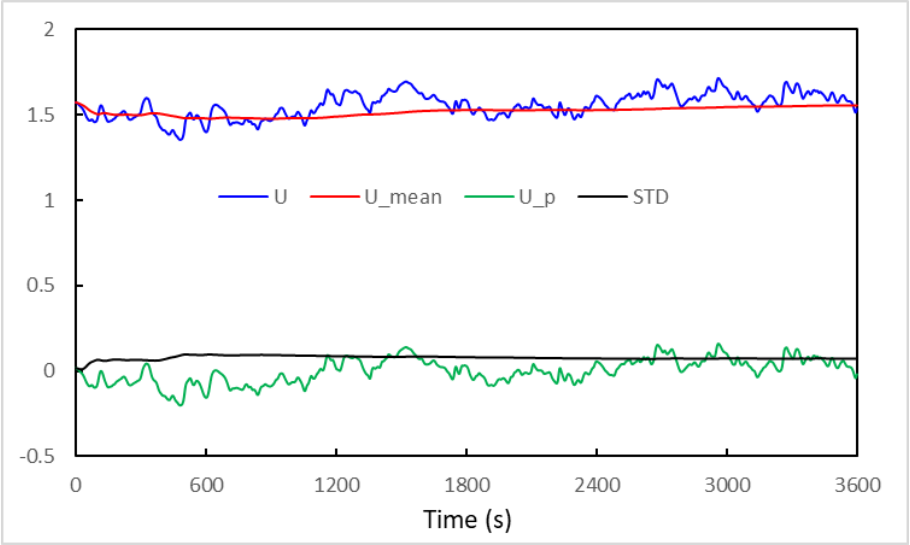

Figure 36. Magnitude, time-averaged, fluctuation, and standard deviation of horizontal velocity at $z = -5$ m on MB 3 for ebb

4.2.3 Coarse In-situ Simulations

The long-term goal of this research tidal installations, such as PLAT-I, in-situ. As proof-of-concept initial in-situ simulations were performed in this work using a coarse grid. For these simulations the tidal turbine experimentally studied by Bahaj et al. [33] and previously simulated using the AL method in EXN/Aero by Baratchi et al. [13] was chosen. After scaling up the turbine to a 5-meter diameter rotor, an angular velocity of 10 rad/s was prescribed representing nominal operations. The turbine was located in region 2 identified in Figure 31 and the rotor hub was placed 14 m below the water surface.

When using the AL method for simulating an isolated turbine an equidistant fine grid encapsulating the rotor and near wake region are used to properly capture the near region flow and unsteady structures behind the turbine. By using a $0.2\ \mathrm{m} \times 0.2\ \mathrm{m}$ resolution for the equidistant region in this case, if we consider the coarse grid that was used for the simulation of tidal flow (its resolution can be as high as $5\ \mathrm{m} \times 5\ \mathrm{m}$), there will be a significant difference between the two resolutions. Therefore, to bridge the gap between this multi-scale resolution, the many-to-many technique, which interpolated between grids without requiring a 1-to-1 connection was used. This approach allows different grid resolutions to be used for different regions of the domain. The grid developed for the coarse in-situ turbine simulation is shown in Figure 37.

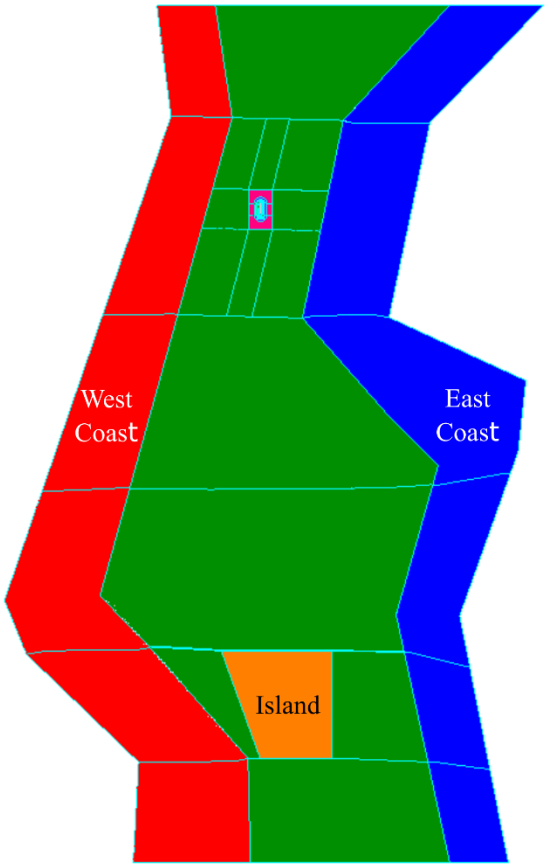

Figure 37. Generated grid for in-situ simulation of a tidal turbine

A closer view of the grid around the turbine is shown in Figure 38. In this figure the turbine block, where the source terms are distributed, is shown as a red square. Also, as shown in this figure and better illustrated in Figure 39, to smoothly transition from the near field resolution (Level 1) to the far field resolution (Level 5), three intermittent grid resolutions have been used. This was done to avoid abrupt changes in the resolution at interfaces which can result in non-physical effects, visible as non-smooth transition at the interfaces, which can affect the accuracy of the solution. The outer grid outer grid in the passage is structured with 3.9 million control-volumes, which like the grid used for the coarse simulations of tidal flows consists of 12 elements in the vertical direction.

All the boundary conditions for this problem are similar to those used for the coarse flood tidal flow simulation. For the timestep, according to the guidelines for the AL method, it should be chosen such that the blade tip moves one control-volume during one timestep. With a $0.2\ \mathrm{m} \times 0.2\ \mathrm{m}$ resolution in the rotor block and $\omega = 10\ rad/s$ as the rotational speed of the blades, the ideal timestep for this simulation is 0.004 s. However, to achieve more acceptable simulation times, a timestep of 0.1s was used for this initial simulation. Figure 40 shows the

instantaneous flow field for this case around the turbine. From this figure one can see that, even though a very coarse grid has been used, the simulation successfully produces the wake of the turbine, which can be affected by unsteady tidal flows. This simulation demonstrates the capability of the AL method for in-situ simulation of tidal turbines.

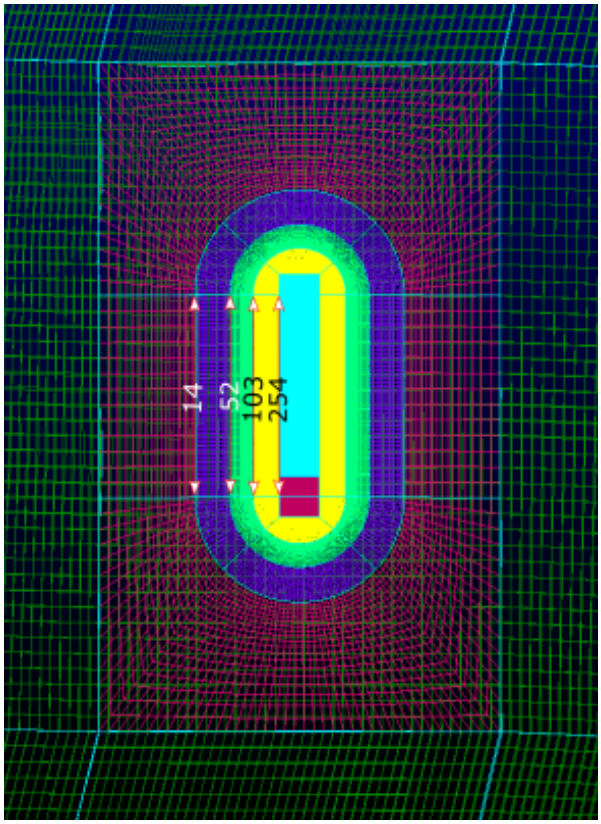

Figure 38. Closed-up view of the near field grid around the turbine

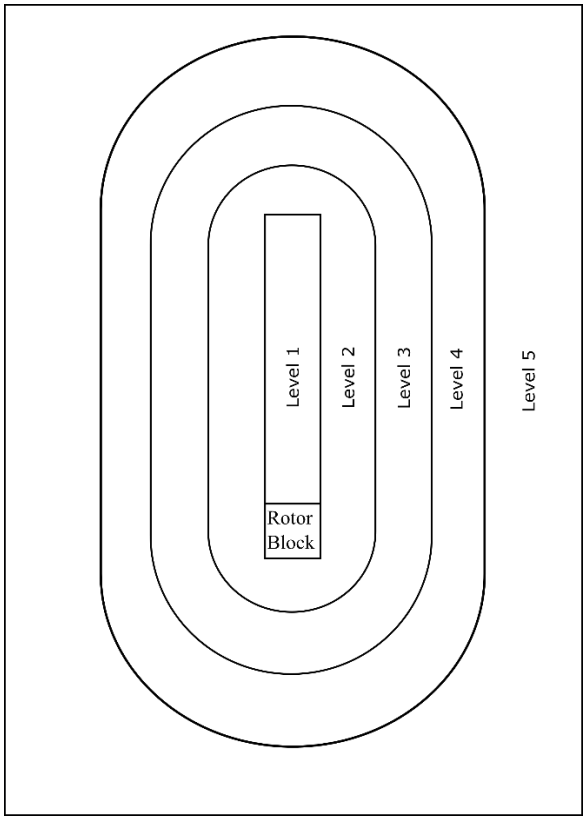

Figure 39. Schematic of grid levels in many-to-many method

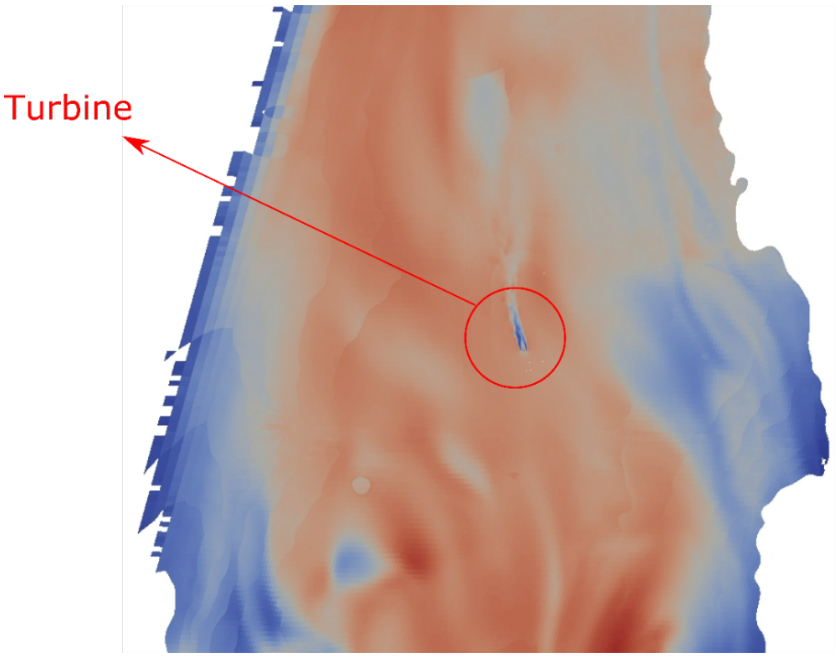

Figure 40. Velocity field around turbine in flood flow

4.2.4 Fine Resolution In-situ Simulations:

Initial development was completed for a fine resolution simulation with PLAT-I properly located in GP. A critical step was the proper development of the structured grid shown in Figure 41. . For this grid, the number of control-volumes is 36.4 million and the block that will include the turbine, as shown in Figure 42, has a 20^{o} angle with the CFD domain y-axis. This angle has been decided based on the mean flow direction in the flood. Obviously for simulating the turbine's operation in ebb, a different grid that the above-mentioned block has been oriented based on the mean velocity in ebb is necessary. In the tidal passage away from the turbine, the grid has 24 elements evenly distributed in the vertical direction and the average horizontal spacing is less than $2\ \mathrm{m} \times 2\ \mathrm{m}$.

Figure 43 shows the block that will enclose the rotor when the AL method has been activated. The resolution of the mesh in this block has been chosen based on the recommended of Troldborg et al. [8], that there be at least 30 control volumes along the rotor blades. Given the 2.5 m span rotor blade, this results in inner resolution of 0.084 m. This represents a 23x reduction in the resolution compared to the outer tidal passage region. Therefore, the many-to-many technique was again implemented, and consisted of with 5 layers of intermittent grids as illustrated in Figure 44.

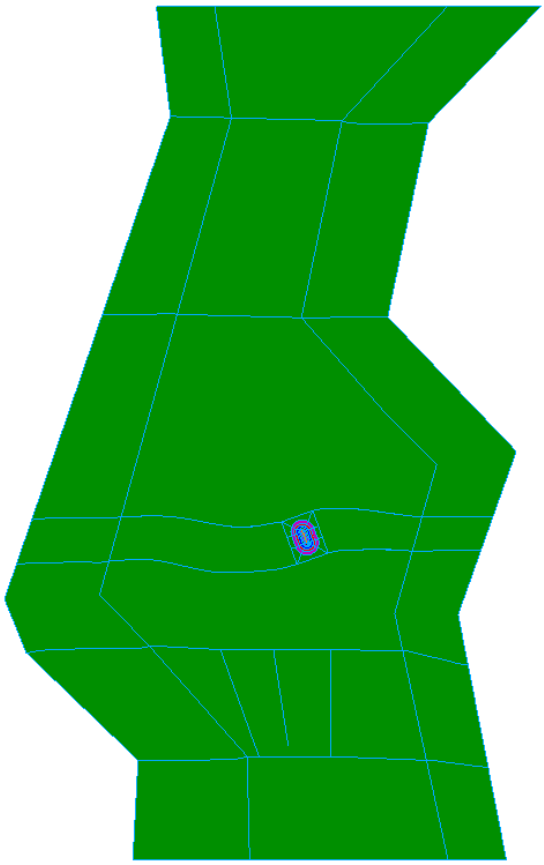

Figure 41. Fine grid for in-situ simulation of turbine

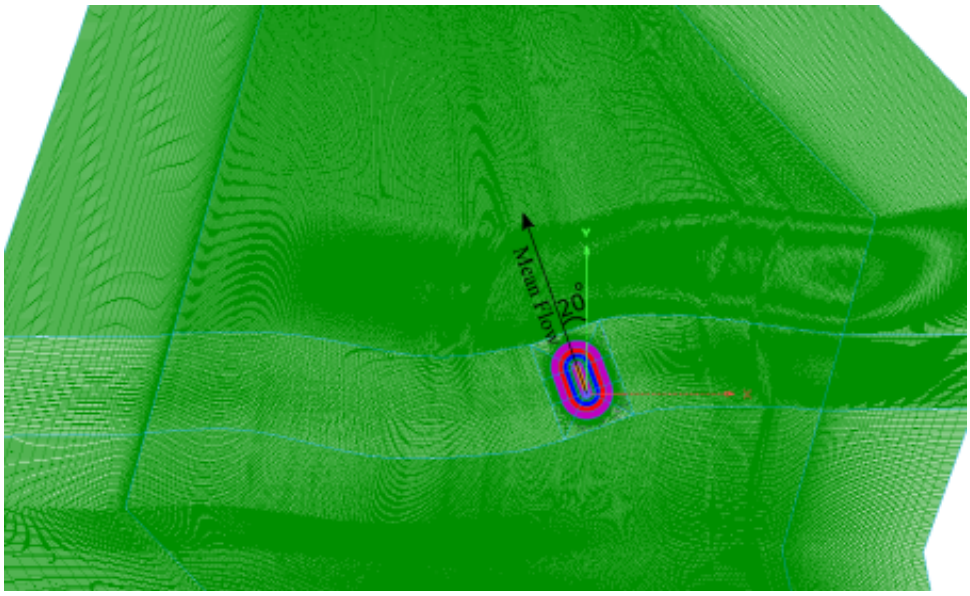

Figure 42. Direction of turbine block in fine grid for in-situ simulation of turbine in flood

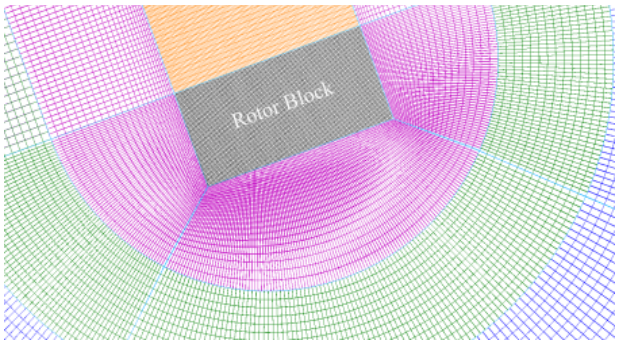

Figure 43. Rotor block

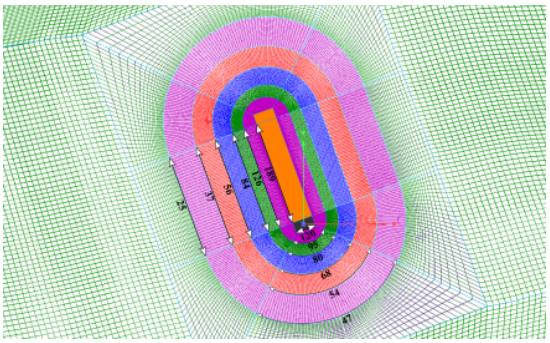

Figure 44. Transition in grid resolution in many-to-many method

Given the significant variation in scales, the implementation of the various layers with many-to-many connections was not trivial and significantly effort was placed on ensuring the accuracy of the results. To ensure proper implementation, a flood simulation was completed without the AL activated. As shown in Figure 45 the velocity field is smooth at the intersection of the various layers, indicating a successful implementation of the many-to many technique. The remaining step of this research, which has been tested for the coarse grid, is to activate the AL method in the rotor block and simulated the turbine for sufficient time to obtain statistical convergence of the flow field variables and turbine performance.

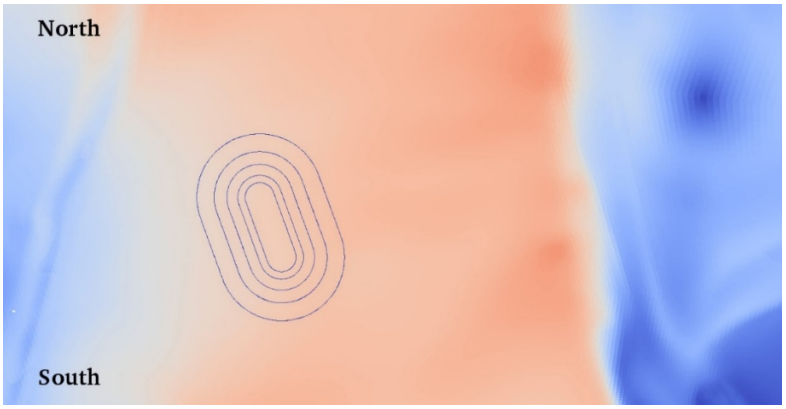

Figure 45. Smooth transition of velocity magnitude between different many-to-many layers.

4.2.5 Conclusions

Work Package 2 of the original proposal is admittedly behind schedule, with significant progress being made / or completed for objectives (i) - (iii). The original proposal was extremely ambitious given the two-year time constraint and the following choices / unexpected issues significantly slowed progress:

(i) It was decided early in the project to change the focus site from the FORCE region to Grand Passage. The was largely based on the bankruptcy of OpenHydro, the owner of the sole turbine

installed in the FORCE test site, while Sustainable Marine Energy was in the process of installing turbines in Grand Passage, and thus was the correct decision. However, additional complexities with simulating GP, such as including east and west shorelines in the CFD domain and having less experience previously simulating this site, significantly slowed progress on objectives (i) and (iii) due to complexities with simulation GP. Additionally, for these multi-scale simulations that integrate a variety of software tools and datasets, the initial setup of a new test site is extremely labour intensive. This process includes manually integrating available bathymetry, identifying shoreline locations, extracting FVCOM boundary conditions, and post-processing thousands of monitoring points. For this reason, a post-doctoral fellow in our research laboratory is developing a data manager that allows the various software tools (EXN-Aero, FVCOM, Paraview, Pointwise) necessary to setup and simulate a new tidal energy extraction site, to automatically communicate and exchange data. This data manager can also be used for the forecasting model described in WP3.

(ii) There was a software bug introduced into the latest versions of EXN/Aero that increased the wall-time of a simulation by a factor of 4 compared to previous simulations. This meant that previous simulations which took 1 month to complete on our GPU server increase to 4+ months. It is important to note that the introduction and resolution of this issue was out of control of our research laboratory. This issue is currently in the process of being correct by Envenio Inc., the industrial partner that owner the IP and maintains EXN/Aero

(iii) It was anticipated that the simulations for this project would be complete on a new GPU server that would be purchased and installed at UNB using funding from the successful CFI Innovation Fund, “Environmental Monitoring, Modelling and Forecasting Infrastructure for Instream Tidal Energy.” The procurement and installation of this server took significantly longer than anticipated and it only recently came online. Therefore, all simulations had to be completed on our older, slower, GPU server, and had to compete for resources with other projects.

In light of these delay, Dr. Jeans is committed to training a new MScE student that will focus on completing the in-situ AL simulations. A potential student has already been identified with an anticipated start date of January 2021. Funding for this student will be provided by the NSERC Discovery Grant of Dr. Jeans and no additional funds will be requested from OERA or Mitacs for the completion of this work. It is hoped that this commitment might initiate a new partnership between UNB and SME for future research.

4.3 Bibliography

[1] A. Gerber, K. Wicox, J. Zhang, "Benchmarking of a massively parallel hy brid CFD solver for ocean applications," in *, in: Proceeding of the ASME 32 International Conference on Ocean, Offshore and Arctic Engineering*, Nantes, France, 2013.

[2] C. Rhie, W. Chow, "A numerical study of the turbulent flow past an isolated airfoil with trailing edge separation," *AIAA,* vol. 21, p. 1525–1532, 1983.

[3] L. Careto, A. Gosman, S. Patankar, D. Spalding, "Two calculation procedures for steady, three-dimensional flow with reciculation, in:," in *Proceeding of the 3rd International Conference on Numerical Methods in Fluid Dynamics*, Paris, 1972.

[4] M. Darwish, F. Moukalled, "Tvd schemes for unstructured grids," *International Journal of Heat and Mass Transfer,* vol. 46, p. 599–611, 2003.

[5] B. Hutchinson, G. Raithby, "A multigrid method based on the additive correction strategy," *Numerical Heat Transfer,* vol. 9, p. 511–537, 1986.

[6] Khadra, K., Angot, P., Parneix, S., Caltagirone, J.P., "Fictitious domain approach for numerical modeling of Navier-Stokes equations," *International Journal of Numerical Methods in Fluids,* vol. 34, pp. 651-684, 2000.

[7] Bahaj, A., Molland, A., Chaplin, J., Batten, W., "Power and thrust measurements of marine current turbines under various hydrodynamic flow conditions in a cavitation tunnel and a towing tank," *Renewable Energy,* vol. 32, no. 3, pp. 407-426, 2007.

[8] N. Troldborg, J. SØrensen, R. Mikkelsen, "Actuator line simulation of wake of wind turbine operating in turbulent inflow," *Journal of Physics: Conference Series,* vol. 75, p. 1–15, 2007.

5 Work Package 3

5.1 Methodology

In Work Package 3 we used Advanced Research Computing (ARC) system to run regional-level simulations of the Bay of Fundy tides and tidal currents. The ARC resources were also used to store and analyze all the data associated with the project.

5.1.1 Numerical Simulations

The project continued to develop and use the regional oceanographic numerical models developed at Acadia University over the past decade. The numerical simulations uses the Finite Volume Community Ocean Model (FVCOM) as its numerical solvers, and numerical grids that have been developed in a series of related research projects (for example see [1] and [2]). All grids simulate the entire Bay of Fundy, with the tides forced on an open boundary beyond the continental shelf in the Atlantic Ocean. The different grids have regions of high resolution in the passages of interest. The model is run in hydrostatic mode, and therefore cannot simulate three-dimensional, small-scale turbulence. The horizontal resolution of the model is similar to the water depth in the areas of the most energetic flows, 15-30 m, which allows the model to capture large-scale eddies that extend through the water column. The model generates a reasonably accurate vertical profile of the flow by modelling 10 layers of flow.

In this project, the analysis focusses on the refinement and the use of two grids:

- Acadia Digby Neck numerical model: This model has high resolution in the three Digby Neck passages (15-20 m resolution) sufficient to resolve the details of the flow in the passages, but not to resolve flow characteristics on the scale of the turbine device. In

this project, these simulations were used to produce flow data for Grand Passage for the other Work Packages. For WP1, the simulation data was used for planning field campaigns and was compared to the gathered field data. For WP2, the simulation data was used to force the tides and flow on the boundary of the CFD simulations and was also compared to the CFD results.

- Acadia-Force Minas Passage Grid: This mode has high resolution in FORCE CLA region (20 -25m resolution). The simulation data was used in the analysis of X-Band radar data. Comparing the simulated data to the radar data was part of determining how the radar data could be used for resource assessment and spatially mapping flow variations like the wake behind Black Rock.

One goal of the project was to generate long-term data sets of simulated flow for both the Digby Passages and Minas Passage. Such data sets can be used for many purposes but in particular allow for several important research initiatives: the examination of long-term trends in tidal flow that are driven by long-term tidal variations; the validation of data analysis methods for long term predictions, and; the generation of robust data sets for comparison to field measurements and other models and for use as boundary and initial conditions for high-resolution numerical simulations.

During this project, we developed streamlined methods to generate these long-term data sets, where simulations could be run continuously (provided computing resources were available). The time to generate simulated data was reduced substantially, e.g. 1 year of two-dimensional data can be generated in as little as 36 hours, while 1 month of three-dimensional data can be generated in 2 to 4 days. As a result, the resource restriction on the simulations is moving from the computation time to data storage and analysis. For example, a 2D simulation generates over 120 GB of data and the 3D data generates over 2 TB of data for each simulated year (for these data sets, 10-minute averaged data is stored). During the project we have generated three data sets:

- For Grand Passage (and the other Digby Passages), two years of 3D data covering 2019 and 2020.
- For Minas Passage, a 4 year, 2D data set from 2018 through to the end of 2021 and a 3-year, 3D data set from April 2018 through March 2021

Finally, Acadia now has the capability to generate on-demand forecasts of tidal conditions in the tidal passages of the Bay of Fundy. And, if required, we can run additional simulation to generate forecast of the tidal conditions with the high-frequency output needed to analyse flow variations. Such simulations were run for the comparison to drifter data in WP1 and for the analysis of the Black Rock wake described below.

5.1.2 Data Analysis

A significant part of WP3 was the continuing development of data analysis tools. The focus of the project was to develop tools that can analyse the spatial variation in the flow from field measurements, i.e. drifters, transects and X-band radar (see *Figure 46*).

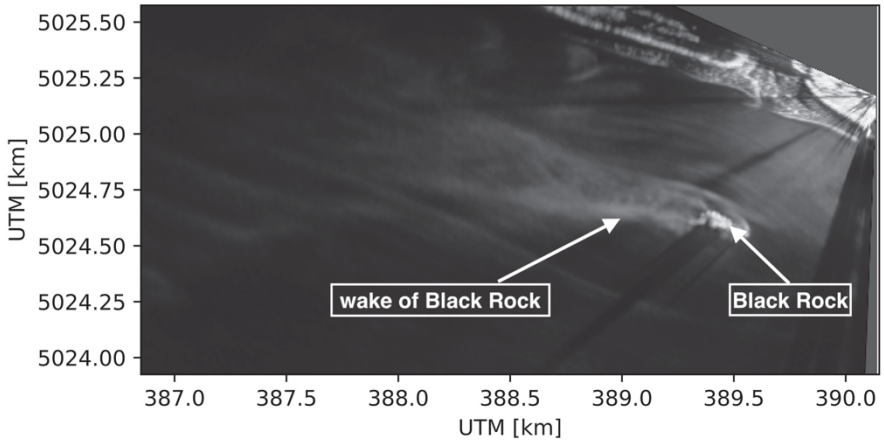

Figure 46: An image of radar backscatter averaged over a five-minute interval, that highlights the presence the wake behind Black Rock Island on the ebb tide. The data from such devices covers large spatial areas but can be limited in time or quality.

While these devices provide measurements over a wide spatial area, they often provide measurements over very limited times. Additionally, the flow being measured is often very turbulent, has a strong flood-ebb tidal asymmetry and is strongly influenced by surrounding bathymetry.

Predictions of tidal conditions are often made using harmonic analysis, for example we use the software package U-tide. Given a sufficiently long and accurate measurement of tidal heights, this package can generate accurate predictions of the tide. However, as mentioned above, at high energy sites where the tidal flow is often more variable in time (and space), harmonic analysis does not produce accurate predictions. Thus, our work on producing forecasts has focussed on the development and validation of forecasts using LunaTide. LunaTide's phase-learning methodology builds on the accuracy of u-tide to predict tidal heights to produce accurate predictions of tidal currents. Furthermore, since it uses machine learning techniques, it can be used to optimally combine measurements and numerical simulations to produce accurate forecasts that combine many different forms of information into a forecast. In this project,

we have worked with Greg Trowse and Dr. Aidan Bharath from Luna Oceans to further develop their software LunaTide. While Luna Oceans has focussed on making LunaTide more widely available, we focused on developing LunaTide as a research tool in the following steps:

- Developing the mathematical theory to support LunaTide's methodology
- Refining and validating the LunaTide phase-learning methods
- LunaTide code was translated into Python and intergated with Acadia's data analysis tools. Incorporating LunaTide into our data analysis tools will allow us to use LunaTide to analyse all of the project's observational and numerical data using our ARC resources.

In addition to the development of LunaTide, the project worked with other partners (FORCE, CoGS) to further develop and/or apply examine other types of data analysis methods, including:

- Deriving velocity data from X-band radar data

- Determining wake characteristics from X-band radar backscatter
- Determining flow speed from videos of drifters
- Extracting bathymetry data from drone images of intertidal zones.

5.1.3 Forecasts

Finally, a goal of the project as to develop tools to forecast the marine conditions in tidal passages. The primary goal is to predict the tidal currents, including the variability of the currents. The longer-term goal is to include these currents with forecasts of other marine conditions (wind, waves, etc.).

5.2 Results and Conclusions

5.2.1 Results

5.2.1.1 Generation of Data for other components of project

We continue to use the numerical model to inform field work plans and to assist in the analysis of the gathered field data. The best example of this is the from the work completed in Grand Passage as part of Work Package 1 (see above). The numerical model was used to simulate the flow for the periods of deployment of drifters around the PLAT-I structure. The resulting flow featured were used in the analysis of the results presented in [3]. A comparison of the simulated flows and the data from transects is shown in *Figure 47*. Once again, this comparison shows much greater variation in the observed flow than in the simulated flow. Although this discrepancy was not unexpected, the level of variation in the observed flow is higher than expected. It should be noted that the UNB model results also show a higher level of flow variation (see above in Work Package 2). We used the Acadia model to generate boundary conditions for the UNB model, so that UNB can simulate the tides at the same time that field observations were made (see discussion in WP2).

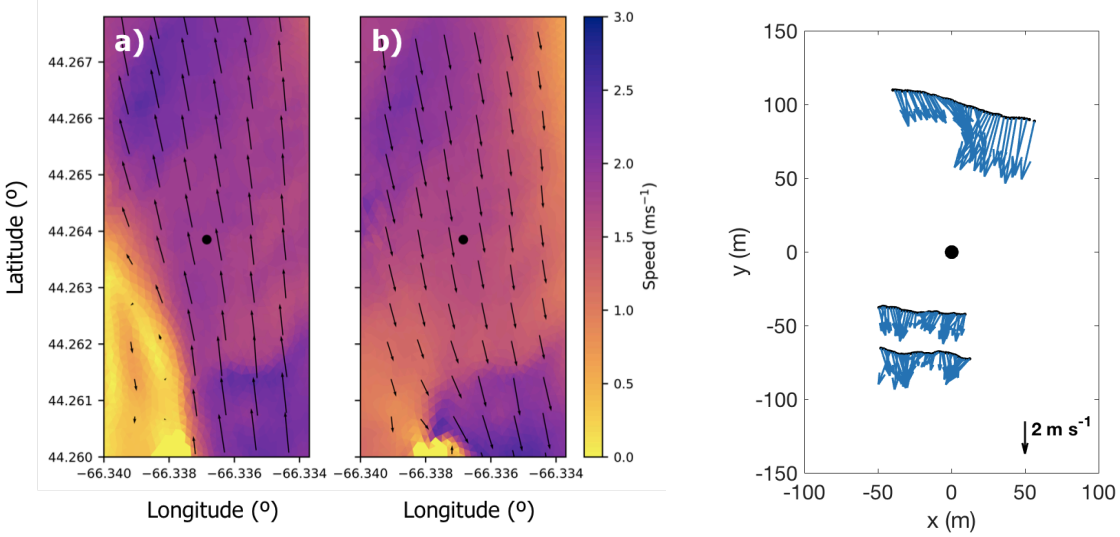

Figure 47: (Left) Model-predicted speed and velocity direction in the area surrounding PLAT-I. a) Peak flood on November 19th and b) peak ebb on November 20th, 2018. Arrows are plotted every 75 m. Note model resolution is ≈20 m. (Right) Velocity direction at selected transects 6.6

m below the free surface during an ebb tide. In both figures, the black dot shows the average PLAT-I location. (Figures from [3]).

5.2.1.2 Generation and comparison of ocean forecasts to field data

During the project, we have made significant progress on the use of LunaTide for the project's data analysis, including:

- Continued development and validation of LunaTide's methodology through comparison to historic ADCP data. Through refinement of LunaTide, we have established that it can produce accurate predictions based on short time series of field data (see *Figure 48*).

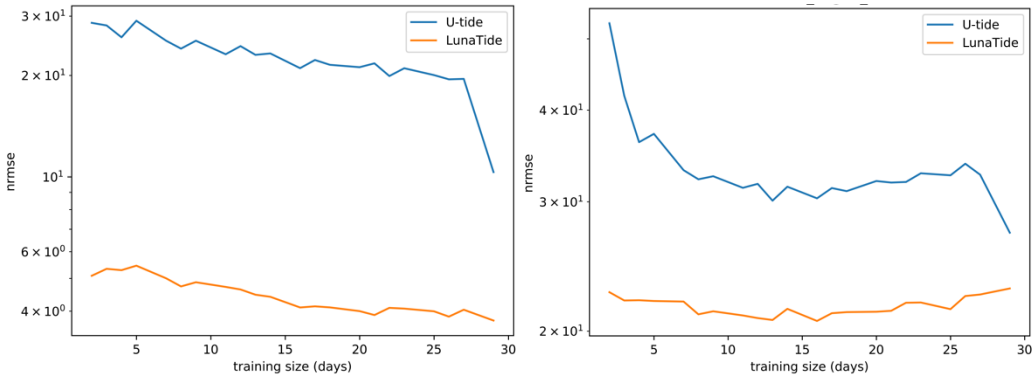

Figure 48: Results from comparing LunaTide and U-tide predictions to ADCP data with various lengths of training data. The Normalized Root Mean Square Error (nrmse) is plotted as a percentage on the y axis using a logarithmic scale. Both data sets are from Grand Passage. The one on the left is from a site with strong tidal flow and shows that LunaTide errors (4 to 5%) are significantly less than U-tide results (20 to 30%) for as little as 2 days of training data. The data on the left is taken from an ADCP that was located in the turbulent wake of Peter's Island. While LunaTide still produces more accurate results, this figure illustrates that predicting "instantaneous" 10-minute-average velocities in turbulent flow is much more challenging. (from presentation given at European Geophysical Union annual meeting in Vienna in April 2019)

- Dr. Bharath used LunaTide to combine the large amount of drifter data gathered by Greg Trowse with the Acadia numerical simulation data (see *Figure 49*). The combination of the data is now being used to calibrate/validate the model simuations.

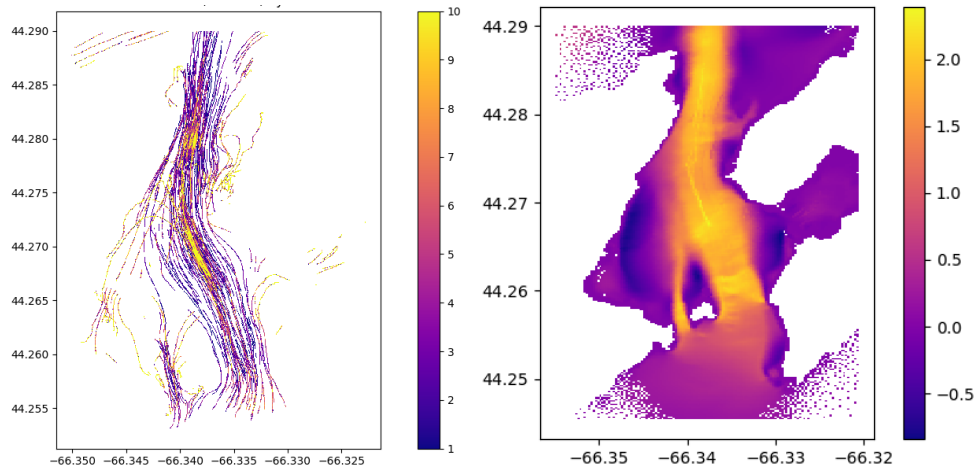

Figure 49: (Left) A plot of the number of drifter observation at each location during flood tide. (Right) A plot of signed flow speed in Grand Passage during a particular peak flood tide; positive is northward, units are m/s. The plot is a combination of drifter data and numerical model data. The paths of individual drifters can be seen as streaks in the image, indicating that there is still an important discrepancy between the measured and simulated flow for some drifts.

5.2.1.3 Analysis of X-Band Radar Data

A promising observational tool for mapping the eddy field is remote sensing by land-based radar, in particular X-band marine radar. As part of the project, Acadia researchers collaborated with FORCE researchers to examine two ways that radar data can be used in tidal site characterization. An X-band marine radar has been installed at the FORCE vistor centre on the norter shore of Minas Passage since 2015, see *Figure 50*.

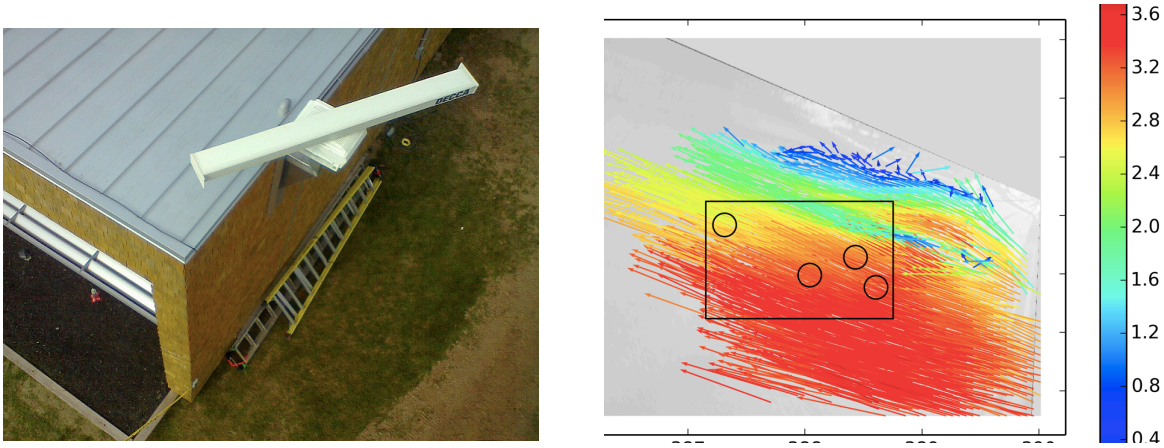

Figure 50: (left) X-band Radar at FORCE visitor centre. (right) A map of surface velocities calculated using radar backscatter. The black box is the FORCE crown lease area, the circles are the berths. Colours are speeds in m/s.

First, as documented in Jeremy Locke's MSc thesis [4], we used the data analysis techniques developed by [5], to construct the 2D near-surface velocity field from radar backscatter. The analsysis produced a map of the surface velocity, with a relatively course resolution of 50 m to

75 m, see *Figure 50*. The analysis requires the presence of waves, as it calculates the velocities from the observed speed of the surface gravity waves. But Minas Passage is realtively sheltered from the open ocean and often has low wave activity. Our work focused on overcoming the resulting challenge of having too little data to effectively use this technique.

The Locke research project produced several key results. First, by comparing the radar derived velocities to an ADCP measurements, we determined that even during the windy and wavey winter season, accurate velocities can be calcualted less than 10% of the time. Second, it was determined that the quality of the calculated velocities measurements could be determined, with useful precision. Most importantly, and encouragingly, is that when LunaTide was used to analyse the data, it was possible to make acurate predictions of the flow even given the limited amount of accurate data. *Figure 51* illustrates the results by comparing a time series of flow speed generated by LunaTide based on radar data to the measured flow speed by ADCP. The excellent agreement gives us confidence that, even in Minas Passage, X-band radar can be used to produce maps of surface velocities.

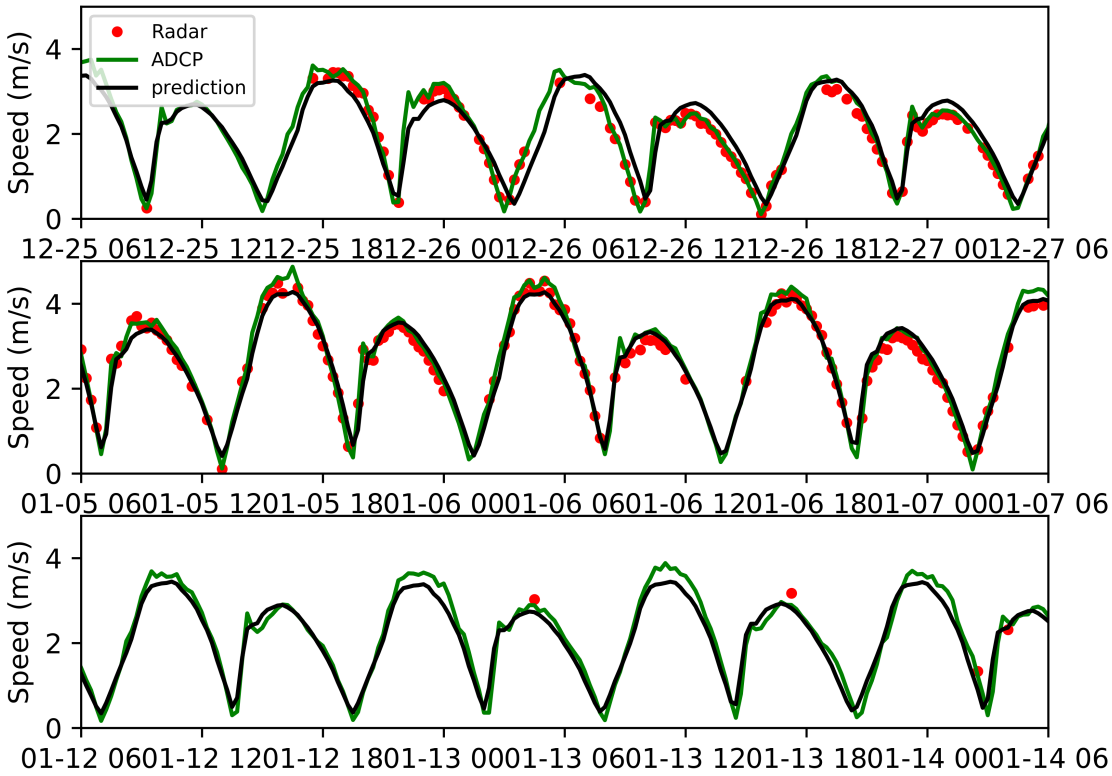

Figure 51: Results of analysis of X-band radar using LunaTide to analyse. The green line is the ADCP measured near- surface velocity at a location in Monas Passage. The red dots are the limited number of high-quality radar measurements at the location. The black line is the LunaTide prediction of the flow based on the radar data. Each graph is for a given 4-day period during the ADCP deployment. The bottom plot illustrates that even when there are few radar

measurements, the time series generated by LunaTide agrees with the ADCP measurements extremely well. (From[4])

5.2.1.4 Analysing turbulence

The analysis of turbulence using drifters is discussed in WP1 and using CFD models in WP2. Here we examine how the X-band radar data also gives an additional mechanism for mapping turbulent regions of flow. In work completed in colbaoration with Dr Joel Culina from FORCE [6], the radar data was used to examine the wake of Black Rock during the ebb tide, and the results compared to Acadia-FORCE numerical model simulations of the wake. The data analysis used proper orthogonal decomposition (POD) to analyse both the radar and model data. The results of such analysis are shown in *Figure 52* which plots the first two PODs for both the radar and model velocities in the wake of Black Rock. A comparison of the two results confirm two important results: analysis of the radar data can produce information of the structure of the flow variations, and; the numerical model simulates a wake behind black rick that has structures similar to measurements.

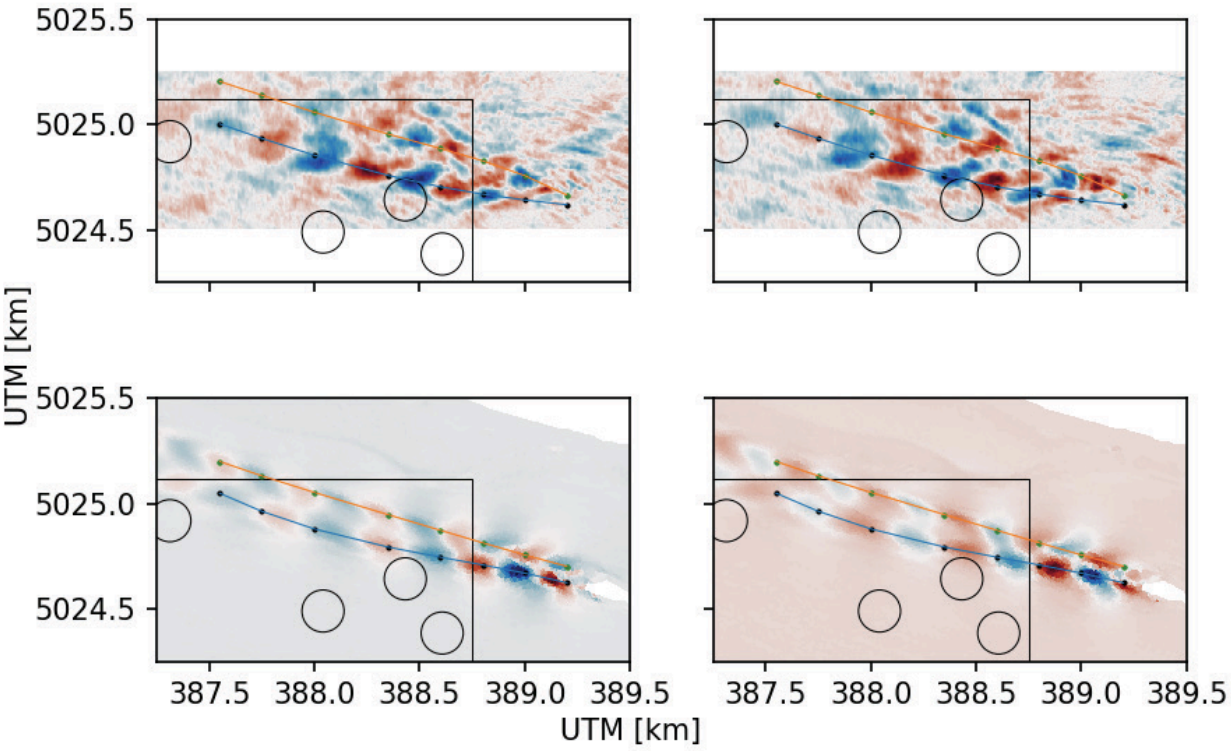

Figure 52: Spatial components of the first POD mode (left) and second POD mode (right), for radar backscatter (top) and modelled speed (bottom). From [6].

Further analysis examined the differences between the wake as seen in the radar backscater and simulated by the model, see [6] for all details. Examples of the results are shown in *Figure 53*; the figures illustrates that the wake seen in the analysis of the radar backscatter and Acadia-FORCE model are quite similar. The result both validates the data analysis technique and suggests that X-band radar can be a power tool for mapping regions of high turbulence. As expected, the Acadia model doesn't reproduce the detailed structure of the wake accurately,

but it does a sufficiently good job for initial site assessment. Modelling wakes accurately is a critical step if the model is to be used to simulate turbines' impact on the flow, and requires the more detailed modelling discussed in Work Package 2.

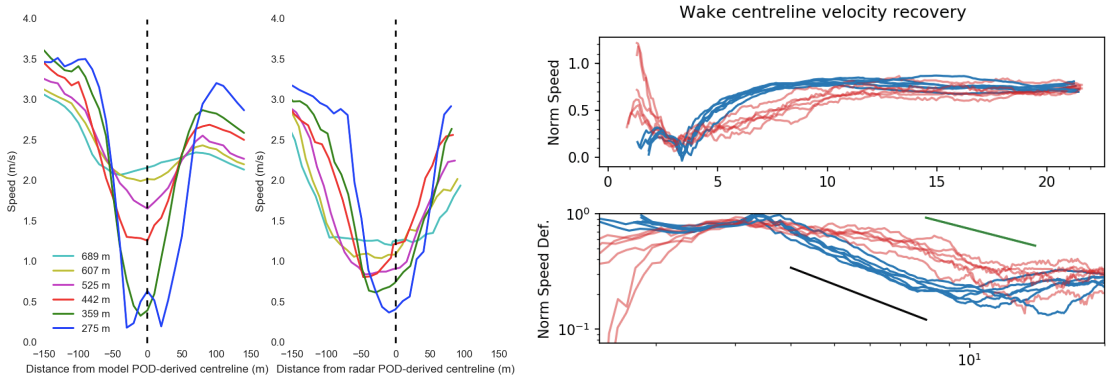

Figure 53: (left) Cross-stream velocity distributions at several downstream distances from Black Rock, for model (left) and radar (right) on January 5, 2018 at 21:45 UTC. Although there is rough agreement, the wake observed by the radar is both wider and longer than the modelled wake. This suggests that the numerical model's representation of the turbulence mixing in the wake is inaccurate and requires further calibration. (right) Normalized speed and normalized speed deficit [dimensionless] against normalized downstream distance [dimensionless], for model (blue) and radar (red). The bottom plot has a log-log scale, with the black line having a slope of -1.5 and the green line a slope of -1. (From [6])

5.2.1.5 Use of numerical simulation data sets

As described in the methodology, we have produced years-long data sets for the flow in the Bay of Fundy. These data sets have been used in the analysis described above, but also have proven useful for collaborations outside this project. For example, we have continued our collaboration with Dynamic Systems Analysis (DSA) in a couple of projects. For an aquaculture project, we provided year-long time series of the flow in a region of St. Mary's Bay that is dominated by the strong tidal through Petit Passage. In a second project, we provided the long-time series of flow in Minas Passage that was used to assist the design of a tidal energy converter. We continue to work with DSA to streamline the collaboration process.

5.2.1.6 Analysis of Drone Images and Video

Finally, we examined data from images and video of tidal flow gathered using drones. This work was primarily done as part of Coleman Hooper's cooperative work term, working in collaboration with Luna Oceans. Drones were used to gather high resolution images and video of the flow around Peter's Island in Grand Passage. The strong tidal flow around the island creates interesting flow features, and the goal of the project was to determine if these features could be analysed using the drone images. During some of the flights, passive drifters were placed in the flow. Data was gathered over 3 days, using several drones with different cameras. This initial pilot project produced several interesting results:

- It was difficult to quantify flow characteristics in videos without any drifters. The Particle Image Velocimetry (PIV) method used only works well if the video can easily

isolate the tidal currents. However, the videos had motion in multiple directions from the waves, moving clouds, and tidal currents, which made PIV infeasible.

- Analysing the motion of drifters in videos was more promising. The software could track individual drifters with reasonable accuracy. To improve the data collection, more drifters are needed, and they must be more easily distinguished from the water, especially the white foam generated by turbulent flow.
- The high-resolution images from the drone can be used to generate high-resolution 2D and 3D maps of the region (see *Figure 54*). By creating these images at high and low tide, a detailed map of the intertidal zone can be produced. And, further analysis of the data can produce a topographic map of the intertidal zone.

Figure 54: A two-dimensional, high resolution map of Peter's Island and the Brier Island coastline at high tide, composed from several hundred individual images. The full image has a very high resolution of roughly 25 pixels per metre.

5.2.2 Conclusions

Our goal in WP3 was to make better use of Acadia's numerical modelling and data analysis expertise; to move beyond developing these tools to using them in collaboration with other researchers and industry partners. As described above, we had many successes:

- Generation of years long data sets of tidal flow for the Digby passages and Minas Passage.
- Further development and validation of LunaTide.
- Success in using LunaTide to analyse field data and make forecasts.
- Generation of data for use in WP1 and WP2
- Analysis of FORCE's X band radar data to calculate velocities and wake characteristics
- Initial analysis of drone images and video.

Using the results, we have the ability to make forecasts of tidal conditions in the Bay of Fundy passages using numerical simulations and/or LunaTide. These forecasts can include input from a variety of field measurements (ADCPs, drifters, X-band radar, etc.) and be produced in real time. These forecasts can be provided through research collaborations with Acadia (as DSA has done) or through Luna Ocean's web app.

5.2.3 Future Work

As with most research projects, our worked resulted in as many new areas for future work.

5.2.3.1 Generate turbulence intensity maps

One of the goals of the project, was to generate of maps of turbulence intensity in tidal flow in the tidal passage of the Bay of Fundy. Generating maps of turbulence intensity is challenging since it requires information on turbulence, which occurs at the small-time scale of seconds and on spatial scales of cm to be mapped onto regional resource assessment maps, which include information on the time scales of years and spatial scales of 10s of km. As shown above, when the regional-scale simulations were compared to drifter and X-band radar data work, the Acadia model did capture some features of turbulence on the larger scales and but did not resolve small-scale turbulence. Therefore, while the Acadia model can be used to identify areas of flow that are highly variable-for example in the wake of islands, it should not be used to calculate turbulent statistics like turbulent intensity or turbulent kinetic energy.

Although this was not unexpected, since the model resolution is too coarse to accurately simulate the smaller-scale turbulence, the discrepancy was larger than expected. Furthermore, as discussed in [7], in order to accurately characterize turbulence for tidal energy sites, one must calculate higher-order turbulence statistics that will be even more poorly resolved in a regional model.

Overcoming this shortcoming of the regional model is being addressed using several approaches:

- First, we use higher resolution models like the UNB CFD model discussed above in Work Package 2. The CFD model will be able to provide spatial maps of turbulence at given flow conditions. In order to bridge the resolution gap between the UNB and Acadia models, we also worked with Dr. Angus Creech of Hariot Watts University. Dr. Creech has created a Large Eddy Simulation model of Grand Passage. The model is similar in

scope to the UNB model but since it is a coarser resolution, it can be run for full tidal cycles though at considerable computational expense. In an ongoing experiment, all three models will simulate the flow conditions during the during the time period of the field operation. The field data and data from the different modes will be compared to further calibrate/validate the models. The final results will be used to generate maps of turbulence characteristics for Grand Passage.

- Second, we have started using observations and simulated data to correlate turbulence characteristics to the tidal regime – the phase of the tide, the tidal range and mean flow conditions. Then, using LunaTide as described above, we will be able to make predictions of turbulence conditions. These predictions will be compared and validated against field observations.

5.2.3.2 Integration of wind and waves into the model forecast

The integration of wind and waves into the Acadia numerical model or other numerical models of the Bay of Fundy has proven to be difficult and has not been completed. Analysis of data from Grand Passage, Digby Gut and Minas Passage has concluded that waves can have an important impact on the surface flow at these tidal sites during rough seas. However, our efforts to include waves into the Acadia model and to collaborate with others to develop a wave model of the Bay of Fundy have been largely unsuccessful to date. Progress in this area has been slow for two reasons: a lack of data on waves in the Bay of Fundy and difficulties including waves in the FVCOM model with a high-resolution grid and strong tidal currents. Future work to address both problems is continuing.

5.2.3.3 Using hydrodynamic modelling to improve collision risk models

An ongoing challenge for the development of tidal energy sites is understanding the threat to marine life. Considerable effort has been expended to detect the presence and observe the behaviour of marine life at sites before and after the deployment of turbines. In particular, FORCE is continuing to do such work in Grand Passage and Minas Passage.

Using the methods discuss above, we now have the ability to produce accurate predictions of the flow at any location and time Minas Passage. As well, these predictions can incorporate data from field campaigns. By combining this data with the collected data on fish detection from tags and echo sounders, we can better correlate marine life behaviour to the hydrodynamic conditions. Making such a connection could greatly improve the development of collision risk models.

5.3 Bibliography

[1] R. Karsten, D. Greenberg, M. Tarbotton, J. Culina, A. Swan, M. O'Flaherty-Sproul, and A. Corkum (2011), Assessment of the Potential of Tidal Power from Minas Passage and Minas

Basin, final report for OERA funded project, available at https://oera.ca/research/assessment-potential-tidal-power-minas-passage-and-minas-basin
[2] M. O-Flaherty-Sproul and R. Karsten (2013), Southwest Nova Scotia Tidal Energy Resource Assessment Volume 2: Numerical Modelling of Digby Neck Tidal Currents. Part of OERA funded project, available at https://oera.ca/research/southwest-nova-scotia-tidal-energy-resource-assessment
[3] M. Guerra, A. E. Hay, R. A. Cheel, G. Trowse, and R. Karsten, Turbulent flow mapping around a floating in-stream tidal energy platform. Under revision – Extended Abstracts EWTEC 2019
[4] J. Locke, X-Band Marine Radar as a Site Assessment Tool in the Minas Passage, MSc Thesis, Acadia University, defended April 26th, 2019.
[5] Bell, P. S., & Osler, J. C. (2011). Mapping bathymetry using X-band marine radar data recorded from a moving vessel. *Ocean dynamics*, *61*(12), 2141-2156.
[6] J. Culina, J. Locke, R. Karsten, A. Abbasnejad, (2019), "Characterization of an Island Wake at a Tidal Turbine Site Using X-band Marine Radar and Numerical Modelling." *Journal of Ocean Technology*, **14**, 101-114.
[7] McCaffrey, K., Fox-Kemper, B., Hamlington, P. E., & Thomson, J. (2015). Characterization of turbulence anisotropy, coherence, and intermittency at a prospective tidal energy site: Observational data analysis. Renewable Energy, 76, 441-453.

6 Recommendations

In each of the previous sections describing the individual Work Packages, there are specific comments of future work for that part of the project. Here we summarize the recommendations for the entire project.

6.1 Field Work:

1. The project demonstrated mobile, surface measurement devices can be used effectively and efficiently. In particular, in this project, they allowed considerable flexibility in planning field work, allowing the team to work around the operating schedule of the SME turbine deployment and operation (and collaborate with other research projects). As tidal energy in the Bay of Fundy is still in the development and prototyping stage, we recommend the continued exploration of measurement devices that can be flexible/opportunistic to provide the best value to tidal projects.
2. Since waves in the Bay of Fundy are not as large or frequent as in sites in the UK, there has not been considerable effort in measuring or modelling their importance at tidal sites. With a shift to surface deployments and the flow characterization now focussing on turbulence and variation, more research should be focussed on the impact of waves.

6.2 Numerical Modelling:

3. The development of a numerical model capable of simulating an in-situ turbine, in a turbulent-resolved simulated flow at a specific site is a very challenging project. It requires a long-term collaboration of project/site developer and numerical modellers. But the payoff is substantial

and worth the effort. We now have the infrastructure and opportunity to complete such models for the turbine projects in Minas Passage. Such a project should be supported.

4. Numerical modelling requires access to the most advanced computational resources. These are often available to university researchers. Greater effort should be made to build collaboration between project developers and industry to make use of these resources.

6.3 Data Analysis:

5. More and more, data analysis tools are incorporating machine learning methods. These method promise exciting results, but useful development of the tools need collaborations between experts in the field of oceanography/marine energy to work with machine learning experts. Such projects should be supported, in part by making data sets more easily available.
6. Historically, field work has focussed on obtaining long-time data sets, at least one month in duration to allow for harmonic analysis. The results from LunaTide have illustrated that considerable information can be obtained from short time series if combined with other data sets (most importantly an long tide gauge time series) and analysed correctly. We recommend that in field campaigns, especially that aim to produce spatial maps of flow variations, focus on gathering data during different times of the tidal cycles, and at different times in the spring-neap cycle rather than long time series

6.4 Overall:

7. When a project requires considerable reporting, such as this one did, it also requires considerable project management. We recommend that OERA continue to examine how to make project reporting and management more efficient.

9 NRCan Performance measures

9.1 Methodology:

The project had three work packages (WP) to characterizing turbulence in Grand Passage and Minas Passage, two locations where tidal turbines have or will be deployed in flows that display a variety of turbulent features. Work Package 1 used innovative mobile measurement

devices to characterize the spatial variation of turbulence in Grand Passage. Two field experiments were conducted in the vicinity of Sustainable Marine Energy Canada (SME) PLAT-I turbine platform. For both field experiments, measurements of turbulent velocities were collected using stream-following surface drifters with a down-looking turbulence-resolving acoustic Doppler current profiler (ADCP). Data were collected over a range of flow conditions and when the turbines were and were not operating.

Work package 2 (WP2) developed and validated a high-resolution numerical model of the Grand Passage. The numerical simulations were carried out using using EXN/Aero, a GPU based CFD solver being developed at the University of New Brunswick. The research team produced fine grid mesh for Grand Passage with 24 million control-volumes, an average horizontal resolution of $2\ \mathrm{m} \times 2\ \mathrm{m}$, and an innovative smooth transition between the main channel and the shoreline. In the second part of the WP2, numerical models of turbines were embedded into these flow simulations. The researchers developed an innovative methodology based on the actuator line (AL) method and takes advantage of both CPU and GPU processing power to increase computational efficiency. The combined numerical model was used to simulate turbine operation in the realistic, turbulent resolving simulated flow in Grand Passage.

Finally, the third work package further developed data analysis methods and a regional numerical model. On the data analysis side, the research team worked with Luna Ocean Inc. to develop a data analysis tool, LunaTide, that can better predict tidal flow, using a wide range of measurements (ADCPs, drifters, X-band radar, etc.) and numerical simulation data. The process of running the regional model was adapted to run on Compute Canada resources to produce mutli-year datasets of tidal flow

9.2 Key project achievements:

Our projects goal was to contribute to reducing uncertainty and investment risk for TEC devices and advancing the tidal energy industry through a better understanding of turbulent flow at tidal energy sites and how this flow affects turbine performance. Here are the key project achievement in reaching this goal:

1. WP1 demonstrated that surface drifters are an efficient and economical methods for mapping both mean-flow velocities and resolved turbulence in the vicinity of an operating tidal turbine.
2. WP1 generated maps to describe the spatial and temporal variations of mean-flow velocities and turbulence parameters in the studied region of Grand Passage.
3. WP1 mapped out the wake of the SME PLAT-I operating in Grand Passage, identifying the maximum velocity deficit and how farther downstream the wake expands vertically, the velocity deficit decreases, and the wake begins to recover.
4. WP2 demonstrated that the EXN/Aero-UNB numerical model can simulate the multi-dimensional, complicated flow structures of the strong tidal flow in Grand Passage.

5. WP2 simulations were used to illustrate several important the PLAT-I deployments site: the potential interaction with the wake of Peter's Island, the existence of periodic, low-velocity, unsteady flow structures near the platform and the significant variation in velocity profiles between deployment and measurement sites.
6. WP2 demonstrated that a high resolution, realistic model of a tidal turbine could be imbedded into a turbulent resolving simulated flow of a tidal passage, successful implementing the many-to many technique.
7. WP2 simulations successfully produces the wake of the turbine, and illustrated how it can be affected by unsteady tidal flows.
8. WP3 used a high-resolution regional numerical models, to generate multi-year data sets of 3D simulated tidal flow for all tidal passages in the Bay of Fundy.
9. WP3 in collaboration with Luna Oceans demonstrated that LunaTide can predict tidal flow better than traditional harmonic analysis methods, while using shorter and/or intermittent training data sets.
10. WP3, working with FORCE demonstrated that X-Band radar data can be used to predict surface velocities and analyze wakes across the FORCE site.

When the results of all 3 WPs are combined together, the project has produced data sets and data tools that can make maps and forecasts of tidal conditions at a unprecedented level of details and accuracy.

9.3 Benefits to project stakeholders:

The project achievements have led to several benefits for stakeholders in the development of tidal energy in Nova Scotia and throughout Canada. Turbulence is a significant issue at every site being considered for instream tidal energy development. The project has developed or further refined three critical tools for characterizing turbulence and its impacts on turbines. First, an efficient and economical manner to measure the turbulence at a site using drifters. Using this method to map out the turbulence at a deployment site will provide critical information about the site while significantly reduce site assessment costs. Second, the development of a cost-effective and accurate process to develop a numerical model of a turbine *in-situ,* with accurate turbulent flow of the specific site, is critical to designing turbines and turbine arrays for site conditions. Finally, the further development of using X-band radar to map out surface velocities and flow variations will provide improved site assessment at the FORCE site.

In addition to the characterization of turbulence, the further development of data analysis tools, in particular LunaTide, will allow stakeholders to make better use of any field data they have gathered to predict conditions at tidal energy sites. Since LunaTide makes better use of data gathered using cost effective methods--such as surface drifters, radar, drones, transects, etc.--it can be used to reduce the cost of site assessment and continued monitoring of turbine operation. Finally, the project produced a years-long data set of tidal flow in the Bay-of-Fundy

passages that is being and will be used by project developers to make site assessments, plan marine operations, and make power estimates.

The project also produced significant results that will benefit stakeholders outside of the tidal energy field. The developments/advancements in using drifting ADCPs will benefit oceanographer and coastal marine scientists. The advances in using GPU system to produce accurate numerical simulations will benefits scientists and engineers examining a wide range of fluid dynamics problems. The simulated tidal flow data sets are being used in other projects, for example, for site assessment for aquaculture.

9.4 Technology and/or knowledge products generated

There were three significant technology and/or knowledge products generated:

1. The process/technology/software to successfully use drifting ADCPs to analyze flow in a tidal system and around an operating tidal turbine
2. The development of a numerical model based on the EXN/Aero GPU-based CFD solver that can simulate an operating tidal turbine embedded in a turbulence-resolving simulation of a tidal passge.
3. The development with Luna Oceans of the software package LunaTide.

1. Barriers/challenges

The biggest challenge that faced the project was the announcement that OpenHydro had filed for bankruptcy in the summer of 2018. The project was designed to measure/model turbulence in Minas Passage around the operating OpenHydro turbine that was deployed in July 2018. Without the operating turbine, the project had to be adapted and quickly. Fortunately, Sustainable Marine Energy (SME) was planning a test deployment of its PLAT-I in Grand Passage from 2018 to 2020. The project was overhauled to focus on Grand Passage and the PLAT-I. Project goals and timelines had to be adapted to the new site and SME's often dynamic deployment plans. The fact that the project could adapt to this significant change highlighted the flexibility of the mobile field program, which was able to both move to a new location and respond rapidly to changing timelines. The project was also able to build on our previous OERA and NRCan funded projects that competed working on Grand Passage.

The second big challenge was the delay in the purchase of computer hardware to support the project. The GPU system for WP2 was delayed for a year; the CPU for WP3 has still not been purchased. The project adapted by efficiently using the resources that were available and by applying for and receiving additional resources from Compute Canada. This allowed the project to proceed mostly as planned, though the full potential of the numerical simulations will only be realized when used on the dedicated computer systems.

Other smaller challenges in dealing with the unpredictability of doing field work, developing numerical models, analysing data and hiring and funding personnel were overcome with persistence and hard work.

9.5 Knowledge Dissemination

The most significant knowledge dissemination for the project was the Workshop organized by the project leads. The two-day *CFI Connector: Measuring and Modeling Turbulent Tides* workshop provided an opportunity for 23 researchers from institutions across Atlantic Canada and abroad to collaborate with industry and international experts to build on existing research projects and develop new projects related to the measurement and modelling of tidal turbulence. The workshop was held in Pictou, NS and received additional funding from NSERC and Springboard.

As well, R. Karsten was co-organizer of the Pacific Institute of Mathematical Sciences (PIMS) Workshop on Mathematical Sciences and Clean Energy Applications at the University of British Columbia, May 21st-24th, 2019. In particular, he organized the session on Water Energy.

2. Publications and Conference Presentations:

- Baratchi, F. 2018. “Numerical simulation of ducted and non-ducted tidal turbines using actuator line method.” PhD Thesis, defended August, 2018.
- Baratchi, F., T. L. Jeans, and Andrew G. Gerber. 2019 "A modified implementation of actuator line method for simulating ducted tidal turbines." *Ocean Engineering* 193: 106586.
- Baratchi, F., T. L. Jeans, and A. G. Gerber, 2020. "Assessment of blade element actuator disk method for simulations of ducted tidal turbines." *Renewable Energy*.
- Culina, J. J. Locke, R. Karsten, A. Abbasnejad, 2019, “Characterization of an Island Wake at a Tidal Turbine Site Using X-band Marine Radar and Numerical Modelling.” *Journal of Ocean Technology*, **14**, 101-114.
- Guerra, M., A. E. Hay, R. A. Cheel, G. Trowse, and R. Karsten, “Turbulent flow mapping around a floating in-stream tidal energy platform”. *13th European Wave and Tidal Energy Conference*, Naples, Italy, September 1-6, 2019. (Oral presentation by Dr. Guerra Paris)
- Guerra, M., A. E. Hay, R. Karsten, R. A. Cheel, and G. Trowse. “Field measurements of a floating tidal turbine wake”. Pan American Marine Energy Conference, San José, Costa Rica, January 26-28, 2020. (Oral presentation by Dr. Richard Karsten)
- Guerra, M., Hay, A.E., Cheel, R., Trowse, G. and Karsten, R. “Mapping the wake of a full-scale floating tidal turbine platform”, Ocean Sc iences Meeting 2020, San Diego, CA, United States. (Poster presentation by Dr. Guerra Paris)
- Hooper, C., G Trowse, R. Karsten and A. Bharath, “Using LunaTide to produce reliable tidal flow speed predictions with small amounts of training data”, International Network on Offshore Renewable Energies (INORE) North America Symposium, July 9-12, 2019, Victoria. (Poster presentation by C. Hooper)

- Locke, J., X-Band Marine Radar as a Site Assessment Tool in the Minas Passage, MSc Thesis, Acadia University, defended April 26th, 2019.
- Karsten, R., "Large-scale Turbulence in Tidal Channels: Modelling and Measurement", CAIMS 2018, Ryerson University, June 7, 2018. (Oral presentation)
- Karsten, R., G. Trowse, A. Bharath, "Tidal Energy in Grand Passage, Bay of Fundy", EGU 2019, Vienna, April 10, 2019. (Oral presentation by Dr. Richard Karsten)
- Karsten, R., "Taking tidal energy research in the Bay of Fundy to the next level", OERA Webinar series, July 25, 2019. (Oral presentation)
- Karsten, R, G. Trowse, A. Bharath, C. Hooper M. Guerra, A. Creech, F. and Baratchi, "Combining field observations and numerical models into comprehensive maps of tidal currents", energy3 October 18, 2019. (Oral presentation by Dr. Richard Karsten)
- Karsten, R. "Setting the Regional Research Scene: Understanding the Resource, Tidal Energy in Nova Scotia", Pan American Marine Energy Conference, San Jose, Costa Rica, January 26-28, 2020. (Oral presentation)
- Nagel, E., "Environmental Monitoring, Modelling and Forecasting for Instream Tidal Energy Development at the FORCE Test Site", BoFEP 12th Bay of Fundy Science Workshop – 10 May 2018. (Oral presentation)
- Trowse, G, R. Karsten, A. Hay and A. Bharath, "LunaTide: A Phase Learning Method for Predicting Tidal Flow." *In prep*.

The project team was also part of the Data Science room at the Energy3 Conference (October 16-19 2019, Halifax, NS). At this conference examples of field results and numerical simulations were interactively presented to the public.

9.6 Next Five Years

The project will continue to work with in Grand Passage with the SME PLAT-I for at least the coming year. A field campaign is planned for September 2020 to complete a second set of measurements around the SME turbine. During this time the numerical simulations of the SME PLAT-I will be run and validated against field data. Over the next two years, the project team will be extending the use of the field techniques and numerical models at other sites in Minas Passage and Petit Passage in support of projects by SME, Big Moon Power and Nova Innovation. Future work will include a more in-depth look at the effect waves have on surface platforms, an examination of how X-band radar can be better validated with comparison to transect/drifting ADCP data, and research into whether LunaTide can be used to predict turbulence characteristics. Work will continue to provide tidal data to all interested stakeholders.

Although a complete replication of the project is unlikely, we expect that parts of the projects will be replicated in the other tidal passages. The expectation is that most parts of the project will be contributing to site assessment and project design for commercial projects in Minas Passage in 5 years.

9.7 HQP:

Name	Position/degree	Role/ Contribution	Months On Project
Farhad Baratchi	Post Doctoral Fellow	WP2	24
Maricarmen Guerra	Post Doctoral Fellow	WP1	24
Elizabeth Nagel	Recent Graduate	Project Manager	4
Becky Balcom	Undergraduate Student	WP3	1
Coleman Hooper	Undergraduate Student	WP3	4
Aidan Bharath	Post Doctoral Fellow	WP3	1
Jeremy Locke	MSc Student	WP3	2

9.8 NRCan Metrics

	At the end of project	5 yrs after project end (predicted)	In the year 2030 (predicted)	In the year 2050 (predicted)
Annual direct GHG savings (if applicable)/	**NA**			
Annual indirect GHG savings (if applicable)/	**NA**			
Technology readiness level (TRL)/	(change in level over project) NA			
Direct economic impact (if applicable)/	NA			
Indirect economic impact (if applicable)/	NA			
Direct employment full-time equivalent - FTE (male%, female %)/	**FTE – 2 (50% male, 50% female)**	**FTE – 2 (50% male, 50% female)**	**FTE – 4 (50% male, 50% female)**	

Indirect employment full-time equivalent (FTE)/	**FTE – 2 (50% male, 50% female)**	**FTE – 2 (50% male, 50% female)**	**FTE – 4 (50% male, 50% female)**	